# Said in Context: A Coastal Reef Soundscape as a Medium for Acoustic Telemetry

by

Francis M. McQuarrie Jr.

(Under the Direction of C. Brock Woodson, and Catherine R. Edwards)

Abstract

Acoustic telemetry is the passing of information across open ocean using high-frequency transmissions, but the environment between transmitter and receiver can dramatically change signal detection rates. Shallow coastal reef environments vary on predictable time scales, with nocturnal and seasonal snapping shrimp behavior driving background noise. A combination of gliders, moored transceivers, hydrophones, and a surface buoy were used during this 2020 experiment to define the physical and acoustic environment as a medium for telemetry signals to provide context for collected detections. A large portion of the variability in detection efficiency was found to be controlled by background noise levels: the snapping shrimp activity at night and in warmer waters resulted in less successful transmission detections, while efficiency improved during the daytime and during colder months. Wind appeared to have a strong enabling effect, lowering high-frequency noise and increasing detection efficiency, suggesting either a change in noise created (biotic, shrimp behavior) or a change in noise lost (abiotic, attenuation). Snapping shrimp activity was quantified using passive recordings of the benthic e nvironment. Surface bubble loss was calculated to estimate how much noise was lost at the air-sea interface as winds increased, and this loss was often a significant source of attenuation. Snapping shrimp were unaffected by increased winds, but the noise they created was attenuated at the ocean surface. Previous attempts at modeling acoustic propagation were simplistic, prioritizing speed, and did not account for the aforementioned attenuation or background noise. By including estimates of realistic noise and signals strength, the transmission models were improved and are more accurate representations of the reef environment. The wind-driven attenuation of background noise was the largest predictor of detectability. Effects from strong wind lowered detection efficiency when background noise was low and static, but significantly increased detectability in environments where wind lowered the detection threshold. This work can aid acoustic telemetry users working near coastal reefs. Reefs are biologically important habitats, but noise-creating species like snapping shrimp can hinder research efforts. Accounting for variable levels of background noise and signal strength helps temper expectations and add context to collected detection data.

Index words: Marine Acoustics, Acoustic Modeling, Transmission Loss, Biotic Interference, Autonomous Underwater Vehicles, Detection Thresholds

# Said in Context: A Coastal Reef Soundscape as a Medium for Acoustic Telemetry

by

Francis M. McQuarrie Jr.

B.S., Rutgers University, 2016

A Dissertation Submitted to the Graduate Faculty of the
University of Georgia in Partial Fulfillment of the Requirements for the Degree.

Doctor of Philosophy

Athens, Georgia

2025

# Said in Context: A Coastal Reef Soundscape as a Medium for Acoustic Telemetry

by

Francis M. McQuarrie Jr.

Major Professors: C. Brock Woodson
Catherine R. Edwards

Committee: Brian Bledsoe
Renato Castelao
John Schramski
Lauren Freeman

Electronic Version Approved:

Ron Walcott
Dean of the Graduate School
The University of Georgia
August 2025

# Dedication

Dedicated to my wife Anna McQuarrie, and my family. When Anna told me to go back to school she did not know that she would be coming with me. I appreciate all the time, support, patience, and flexibility.

# Acknowledgments

I would like to thank and acknowledge my wife, Anna, my dog, Peaches, and my family for supporting me through this dissertation. I also acknowledge the staff at Gray's Reef National Marine Sanctuary, especially Alison Soss for her map-making and context. Thanks to the Edwards lab: Karen, James, Aiden, and Drew, and the Woodson Lab: Matheus and Yargo. I acknowledge the support and community that the Marine Science Graduate Student Association provided for me and others, well done ocean folk. I acknowledge funding and support from the FACT network, and from the Southeast Coastal Ocean Observing Regional Association (SECOORA). I acknowledge and thank the staff and faculty at the Skidaway Institute of Oceanography, the community is invaluable.

# Contents

# Chapter 1

# Introduction

Acoustic telemetry is a tool used to understand the behavior and residency of animals: instruments attached to animals send signals that can be detected and decoded by local active receivers (Crossin et al., 2017). Uses include (but are not limited to) localization, migration, absence/presence of species, and gatekeeping (tracking the coming and going of animals) in biologically important regions (Ellis et al., 2019; Loher et al., 2017). Telemetry has been used by fisheries to estimate fish stocks and optimize catch efforts (Ellis et al., 2019), and by conservationists to decide what and where to protect (Kendall et al., 2021). Any analysis done on detection data requires knowledge of the environment because every transmission is reliant on the medium as context.

The title of this dissertation refers to that necessary consideration. A related writing tool, "[sic]", is a short-handed way of writing "sic erat scriptum", which translates to "thus it was written." The addition of [sic] is used to note a quote that may appear odd or out of place without the broader context. The irony is that [sic] could erroneously be thought of as an acronym for "said in context", which was not its original intent. Detection data, much like some quotations, should not be viewed in isolation. A common fallacy for telemetry users is that a detection is presence and no detection is absence, when in reality the data is simply heard or not heard. Every time there is a transmission there is a probability that it will be detected by a receiver, and that probability changes with the environment (Edwards et al., 2019; McQuarrie et al., 2021). Researchers must know the reliable range of detections based on environmental conditions to

understand the probability that "no transmissions detected" means "no transmissions to detect." This research seeks to help users define and predict that probability in different scenarios.

Sound propagates differently depending on the medium in which it moves, controlling acoustic detection success (McQuarrie et al., 2021). The physical characteristics of the environment (temperature, density, pressure, etc.) have effects of differing magnitude on the sound speed (Mackenzie, 1981). These physical characteristics vary in the ocean across a wide range of temporal and spatial scales and many of these variations are magnified in shallow coastal waters, making it especially challenging as an environment for acoustic telemetry (Mathies et al., 2014; Matley et al., 2022; O'Brien & Secor, 2021; Simpson et al., 1990). The top and bottom of the water column can be sources of reflection and absorption, and these interactions can dramatically shift detectability (McQuarrie et al., 2025). These boundaries are further context that users should account for when determining variability in real-time, or predicting future detection efficiency (Edwards et al., 2019; McQuarrie et al., 2021; Oliver et al., 2017).

This work centers around a reef structure on the inner coastal shelf of Georgia. Gray's Reef National Marine Sanctuary (GRNMS), a marine protected area, is both a preferred habitat for surrounding ocean life and a challenging acoustic environment, making it a welcome and necessary challenge for researchers needing to gain a better understanding of its inhabitants (ONMS, 2012; Stanley et al., 2021). Over 200 species of animals live at this live-bottom reef including snapping shrimp, a persistent source of noise that hinders active acoustic efforts (McQuarrie et al., 2025; Stanley et al., 2021). Marine protected areas (MPA) are delineated to protect animals and environments but require knowledge of how those animals spend their time, and acoustic telemetry enables better-informed decision-making when creating or refining them (Kendall et al., 2021; Pittman et al., 2014). Time, money, and energy are spent to study these MPAs and their inhabitants (NOAA, 2012) and this work improves the efficiency and accuracy of these studies.

This research aims to understand the factors influencing acoustic telemetry efficiency in shallow coastal environments, and how knowledge of these factors could be leveraged when designing acoustic arrays and analyzing detection data. Chapter 2 includes important background context from previous literature, informing the main objectives of the other chapters and lays out the motivation and foundation for the

research. Chapter 3 revolves around the physical processes affecting detection efficiency on a shallow reef, and the frequency at which these processes are expected to control the telemetry success due to changes in the soundscape and signal to noise ratio. Chapter 4 further examines the effect of increased wind speeds and turbulence on the shallow soundscape, analyzing the reduced high-frequency noise observed while modeling the propagation and transmission loss in a complex, noisy reef. Chapter 5 uses the environmental effects from the previous two chapters to predict detection efficiency in a challenging reef system, modeling sound propagation to measure signal strength and attenuation. Finally, Chapter 6 discusses the broader impacts and implications of the research while exploring possible next steps, concluding this dissertation.

# Chapter 2

# Background Information

## 2.1 Acoustic Telemetry

Acoustic telemetry has been used to study fish movements since its development (Heupel et al., 2006; Kendall et al., 2021), and has grown in popularity and scope as a vast network, tracking everything from migrating whales to octopods (Crossin et al., 2017; Kessel et al., 2014). Telemetry is an efficient and modular way to locate and track animals: not reliant on a boat or diver, active acoustic receivers can be moored, attached to AUVs, or floating on buoys, limited only by the time and energy budgets of the project (Kendall et al., 2021). The efficacy of a receiver is heavily controlled by the surrounding environment, and environmental data provides context for detections due to changes in how the transmissions travel and are received (Cho et al., 2016; Crossin et al., 2017; Edwards et al., 2019; Heupel et al., 2006; Kendall et al., 2021; Oliver et al., 2017; Payne et al., 2010). Predicting the effective range of telemetry instrumentation is essential to understanding collected detection data, because users do not know how far a transmission may have traveled before being detected. That predicted range must account for two main encompassing factors: signal strength upon arrival, calculating or measuring transmission loss and attenuation between transmitter and receiver (Scherrer et al., 2018), and background noise as a possible source of interference (Payne et al., 2010).

Sound attenuates as it propagates through the water column, with energy being lost due to both absorp-

tion and scattering processes (Xiao et al., 2021). On the frequency spectrum this attenuation is asymmetric, with sound attenuation increasing with frequency (UWAPL, 1994). In addition to general attenuation, more acute sources of loss arise from interactions with physical boundaries. These losses include absorption and scattering at the seafloor (Stojanovic & Preisig, 2009), and potential significant losses at the air-sea interface, particularly when surface bubble layers disrupt reflection (UWAPL, 1994). Acoustics in shallow water columns include more interactions with these boundaries, leading to more complex acoustic coverage from tags and transmitters depending on the environment (Swadling et al., 2020).

### 2.1.1 Transmission to Detection

A detection occurs when a receiver successfully hears and decodes a full signal. Acoustic telemetry transmissions are made up of "pings" at set intervals using Innovasea's pulse position modulation (PPM) strategy: 8 separate pings, or pulses of sound at a defined frequency, in 3.2 seconds. The pings (and the spaces between them) are considered a full transmission (Figure 2.1). The transmission can be decoded into a successful detection by a receiver listening for that specific frequency and the space between the pings contains the identity of the transmitter (Scherrer et al., 2018). When mentioning a "transmission" or a "signal" it refers to the entire seconds-long packet of pings and spacing, a "ping" is a single traveling sound-wave, and a "detection" is a successfully detected transmission from a known instrument.

Anything that prevents one ping from being received will eliminate a receiver's ability to successfully identify or detect the transmission. There is a delicate balance of correctly ignoring echoes and interference while deciphering the coded transmissions: too stringent and the instrument misses real detections, too lax and it will be overwhelmed with reflected pings and false detections (Payne et al., 2010; Scherrer et al., 2018). A successful detection includes a timestamp with the unique identity of the tag. The distance between transmitter and receiver is not known, but distance is one of the primary determinants of whether or not a successful detection occurs (McQuarrie et al., 2021; Scherrer et al., 2018). The maximum effective distance can change depending on the environment through which the transmission travels (Edwards

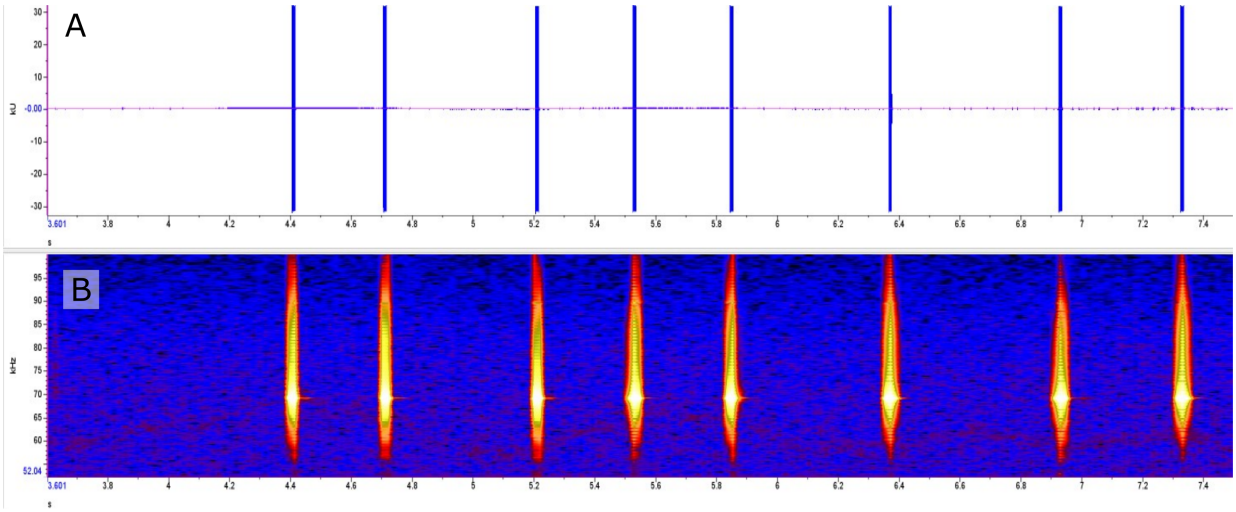


Figure 2.1: An isolated telemetry transmission made up of 8 separate pings: **A** the waveform showing total energy across the entire spectrum (20-100 kHz); **B** a spectrogram showing frequency and intensity of the transmission. Audio file courtesy of Dr. Joseph Iafrate.

et al., 2019; McQuarrie et al., 2021). The longer the distance traveled by the pings, the higher the likelihood of interference and transmission loss (Cho et al., 2016; UWAPL, 1994).

## 2.2 Environmental Context

The South Atlantic Bight (SAB) is a region of the eastern United States coastline between Cape Hatteras, North Carolina and Cape Canaveral, Florida, wider along Georgia's coast and narrower at the edges. The characteristics of the shelf's water column are constantly changing on hourly, daily, and annual frequencies, and these changes may affect telemetry efforts (Cho et al., 2016; Edwards et al., 2019; McQuarrie et al., 2023).

The Gulf Stream forms the eastern boundary of the SAB (Atkinson, 1977). Being shallow and nearshore, the inner coastal shelf is mainly influenced by seasonal river discharge, creating a nearshore coastal frontal zone of significant density gradients (Blanton et al., 2003; Blanton et al., 1994; Blanton & Atkinson, 1983)

in the horizontal and vertical axes that refract and bend sound waves (McQuarrie et al., 2021). On the SAB's inner shelf, mixing from tides usually control these gradients (O'Brien & Secor, 2021; Simpson et al., 1990), complemented by larger seasonal changes in stratification (Blanton et al., 2003; Edwards et al., 2019) and seasonal alongshore winds that drive mixing on the shelf and serve to strengthen or weaken the front through upwelling or downwelling. Gray's Reef National Marine Sanctuary (GRNMS), a shallow reef on the inner coastal shelf of Georgia, is a habitat for hundreds of species of fish and invertebrates that prefer the structured bottom (Kendall et al., 2021; ONMS, 2012), which is why its designated a marine protected area (MPA; Garrison et al., 2016; Kendall et al., 2021). The reef ranges from sparsely to densely colonized live-bottom surrounded by rippled and flat sand (Garrison et al., 2016; ONMS, 2012). The density and porosity of the sea floor will affect how sound travels in shallow systems, and is one of the reasons that reefs such as Gray's Reef are difficult environments for acoustic telemetry (Stanley et al., 2021; Swadling et al., 2020).

The South Atlantic Bight's wind fields act as a circulating force for parts of the inner-shelf that are farther from the Gulf Stream, and is largely responsible for the shelf's seasonal variability (Blanton et al., 2003; Weber & Blanton, 1980). The calendar year can be broken into five seasonal wind regimes with reliable patterns: winter is characterized by strong winds and a colder, largely well-mixed water column (Nov-Feb), and spring brings high levels of freshwater discharge resulting in significant vertical stratification on the inner shelf (Mar-Apr). Summer has the strongest daily stratification driven by longer hotter days and weaker winds (Jun-Jul), followed by fall (Aug) and mariner's fall (Sep-Oct) as transition periods, lowering summer's stratification as winds pick up (Weber & Blanton, 1980). These seasons will be used for this project in lieu of standard calendar definitions of seasons.

Previous research notes different relationships between winds and acoustic telemetry: winds seem to have a beneficial effect on detection efficiency in few scenarios (Cagua et al., 2013), while having negative effects in most others (Edwards et al., 2024; Oliver et al., 2017), possibly due to signal attenuation or turbulent scattering. High wind speeds create turbulence at the surface, crashing waves and bubbles, dominating low frequency noise levels while also mixing the water column (Delory et al., 2014; Prosperetti, 1988;

Revathy & Pillai, 2022). Wind also changes sound attenuation at the air-sea interface, high frequency noise is attenuated at a much faster rate as wind-driven waves create bubble plumes (Table 2.1; Hildebrand et al., 2021; UWAPL, 1994). Consequently, wind has strong direct and indirect effects on the coastal soundscape (the entire acoustic environment), and changes in the soundscape can result in significant swings in detectability (McQuarrie et al., 2025).

Table 2.1: Breakdown of wind's effect on the ocean surface, adapted from the Beaufort scale and Petkovic, 1964.

| Classification | Wind (knots) | Wind (m/s) | Wave Height (m) | Sea Surface Description |
|---|---|---|---|---|
| Light Air | 1–6 | 0.5–3 | 0.1–0.3 | Small wavelets |
| Gentle Breeze | 7–10 | 3–5 | 0.6–1.0 | Whitecaps begin |
| Moderate Breeze | 11–15 | 5–8 | 1.0–1.5 | Numerous whitecaps |
| Fresh Breeze | 16–20 | 8–10 | 2.0–2.5 | Many whitecaps |
| Strong Breeze | 21–26 | 10–13 | 3.0–4.0 | Whitecaps everywhere |
| Near Gale | 27–33 | 13–17 | 4.0–5.5 | Seas heap, foam blown around |

## 2.3 Sound Propagation

The speed at which sound will travel in an environment can be calculated using temperature, salinity, and pressure (Mackenzie, 1981). Pressure is necessary when calculating the sound speed profile (SSP), but in a shallow (<30 m) environment the effect of depth can be considered negligible when compared with the more significant effect of temperature and density differences. Sound refracts and bends away from local sound speed maxima, making the SSPs crucial when modeling high-frequency sound propagation (Godin et al., 2006; McQuarrie et al., 2021). The gradients that affect the sound speed may prevent transmissions from traveling throughout an entire water column, instead bending towards local sound speed minima. Sound propagation modeling (Gul & Zaidi, 2017) can show some disparity between water above and below a thermocline: when transmitters and receivers are on opposite sides, there may be fewer opportunities for successful detections (McQuarrie et al., 2021; O'Brien & Secor, 2021).

Stratification is a product of gradients forming in the ocean, acting as boundaries to slow mixing and

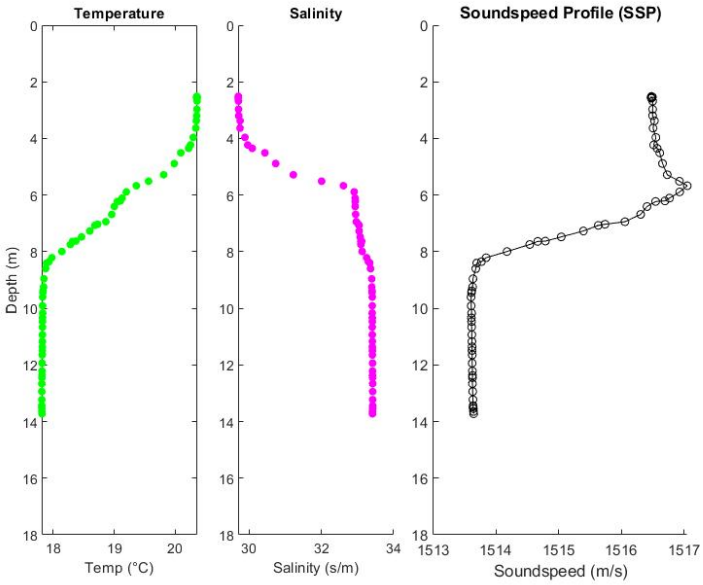


Figure 2.2: Soundspeed profiles (SSPs) calculated using temperature, salinity, and depth (Mackenzie, 1981).

wave propagation (Ivey et al., 2008). These boundaries form where there is a significant difference in temperature (thermocline) or density (pycnocline) with depth, defining their environments and describing how energy will move through them. The difference in sound-wave propagation through mediums is of chief concern to those trying to understand how these transmissions travel and how far away they can be successfully detected (Cimino et al., 2018; O'Brien & Secor, 2021; Oliver et al., 2017).

The signal-to-noise-ratio (SNR) reports the strength of a signal compared to background noise in the same frequency band. Transmissions that have weakened over distance may be detected if the environment is quiet and calm due to the SNR still being high, but elevated background noise would lower the SNR and therefore detection efficiency (McQuarrie et al., 2025). Loud, noisy environments can be thought to have a high "floor" for detections, while quiet environments have a lower "floor." The instrument's physical detection threshold will be the same, a certain SNR is required for detection, but the signal strength that is required can vary considerably (Innovasea, 2021). Background noise is an environmental factor that can lower detection efficiency by lowering the SNR. As SNR drops, the probability of detection also

drops (Innovasea, 2021), and signals that are reliably detected in low-noise environments may go unheard when there are increased levels of interference. If there is a static level of background noise it is relatively easy to compare collected detections, but in environments that have dramatic diurnal swings in noise (Stanley et al., 2021), the number of expected detections should swing as well (Payne et al., 2010). The water column is an acoustic medium, and that medium should be studied before attempting to decipher telemetry data.

## 2.4 Coastal Reefs as Acoustic Environments

Shallow reefs are noisy variable environments compared to deeper, more stable oceanic regions (Kessel et al., 2015; Radford et al., 2010; Radford et al., 2008). A mixture of biotic and abiotic sound sources (Delory et al., 2014) create background noise that can interfere with telemetry efforts by drowning out the active signals. Lower SNRs limit successful detections (McQuarrie et al., 2023; Payne et al., 2010). For the purposes of this research, noise refers solely to background sound that is created, measured, or estimated. Any measurement of "noise" includes the pings that make up acoustic telemetry detections (though these are considered negligible) and any present anthropogenic and biological noise. Snapping shrimp and other benthic invertebrates make broadband noise (0.2-200 kHz) while feeding and communicating (Bohnenstiehl et al., 2016), making the reef a challenging acoustic environment by lowering the SNR, therefore lowering the effective transmitter range and the number of successful detections (Cimino et al., 2018; Oliver et al., 2017; Payne et al., 2010; Radford et al., 2008; Swadling et al., 2020). Below 50 kHz the frequency spectrum is dominated by winds, waves, and animals, and above 100 kHz thermal noise from random molecule motion is primarily responsible for noise levels (Bradley & Stern, 2008). The range of noise that affects acoustic telemetry (50-100 kHz) is in-between those frequency domains and is usually more optimal for active acoustics for that reason: too high on the spectrum to be concerned with waves but attenuates slower than the higher frequencies. Snapping shrimp snaps create broadband noise that encompasses the 50-100 kHz band and can dramatically shift detectability. This work observes,

explains, and predicts that biotic-driven noise interference.

## 2.5 Research Chapters

Range testing of telemetry instruments is expensive and time-consuming, especially in complex live-bottom environments that require spatial and temporal considerations (Payne et al., 2010). Understanding that detection range is dynamic and changing is the first step, but knowing how and why it is changing is critical to improving telemetry strategies and predicting future detection efficiencies.

The next chapters will focus on how the acoustic medium changes on predictable frequencies, and how users can adapt their estimated detection ranges based on expected physical processes and real-time data.

- Chapter 3 details widespread patterns observed in the environment that are echoed in the collected detection data at Gray's Reef. A combination of moored instruments, AUVs, and surface buoy data allow me to define the acoustic medium that transmissions are propagating through. This chapter builds a foundation for the rest of the dissertation and reveals predictable patterns.

- Chapter 4 focuses on defining and explaining an observed relationship between high winds and high detection efficiency that was observed in the previous chapter. I compare snapping shrimp behavior to calculated surface attenuation quantifying the balance between noise created and noise lost during sustained wind events. This chapter's findings identify the mechanism behind the increased detection efficiency, and discuss how to account for it.

- Chapter 5 combines knowledge from the previous two chapters to increase the accuracy of predicted detection ranges. Transmission propagation is modeled through a large variety of coastal soundscapes to isolate the effect of different environmental parameters on signal strength and attenuation. This allows users to accurately predict when and where transmissions will be successfully detected. A generalized additive model (GAM) is created to analyze the effect of different environments on detectability.

# Chapter 3

# Changes in Telemetry Efficiency on Coastal Reefs with High Temporal Variability in Noise Interference

## 3.1 Introduction

Acoustic telemetry, the practice of attaching or implanting small transmitters in fish, whales, and other animals for receivers to detect, is an increasingly popular way to track marine animal movements, understand migration patterns, and discern habitat usage (Ellis et al., 2019; Williams et al., 2019). Estimating the range at which a tagged fish can be reliably detected is an important step in interpreting collected detection data (or lack thereof), but that range changes spatially and temporally (Brownscombe et al., 2020; Kessel et al., 2014; Mathies et al., 2014; McQuarrie et al., 2021; Stocks et al., 2014; Swadling et al., 2020). These transmissions are high-frequency signals made up of 'pings', pulses that are timed so that a receiver can identify the transmitter; if one of those pings is missed or heard twice, a detection cannot occur (Scherrer

et al., 2018). The probability of detecting these active telemetry transmissions, and therefore the viability of deployed instrumentation, is determined by the environment. The distance a transmission can travel varies with environmental conditions, leading to uncertainty when interpreting collected detection data (Goossens et al., 2022; Kessel et al., 2014). Stratification in shallow water columns can refract and bend sound which leads to a heterogeneous distribution of signals in the environment (Edwards et al., 2019; McQuarrie et al., 2021). The level of background noise is another significant factor that decreases the effective range of telemetry transmissions (Innovasea, 2021), decreasing the detection efficiency in noisy environments like coastal reefs (McQuarrie et al., 2023; Pincock, 2008).

The soundscape (acoustic environment) of most live-bottom reefs comprises different sources of sound over a wide range of frequencies: physical sources include crashing waves and turbulence (0.001-0.04 kHz), rain, and popping bubbles (0.8-30 kHz), as well as biological sources that include fish chorusing (0.02-20 kHz) and snapping shrimp (0.05-200 kHz) among other sources (Figure 3.1; Bohnenstiehl et al., 2016; Delory et al., 2014; Potter et al., 1999). Breaking waves in the form of whitecaps, crashing waves, and bubbles make up a large portion of the low-frequency soundscape but create very little high frequency (HF) noise (Delory et al., 2014). Increasing wind magnitude moves the sea surface and increases wave height, causing whitecaps (Petkovic, 1964). Whitecaps and bubbles can form an insulating surface layer that limits reflection and increases acoustic attenuation at the air-sea interface, with HF noise being lost at a much higher rate than low-frequency noise (UWAPL, 1994). Noise attenuation at the surface increases linearly while winds are low, and transitions to a higher power law as white caps start to form ($>$ 6 m/s; Hildebrand et al., 2021). Most active acoustic telemetry efforts are at frequencies above the noise created by winds (Delory et al., 2014) but can be affected by the increased waves and turbulence (Ellis et al., 2019; Jung et al., 2012).

The physical environment affects animal behavior (e.g., animals can be more active nocturnally, less active in colder waters) (Stanley et al., 2021), leading to a combination of physical and biological effects on the soundscape that in turn affect both the propagation and probability of detection of telemetry

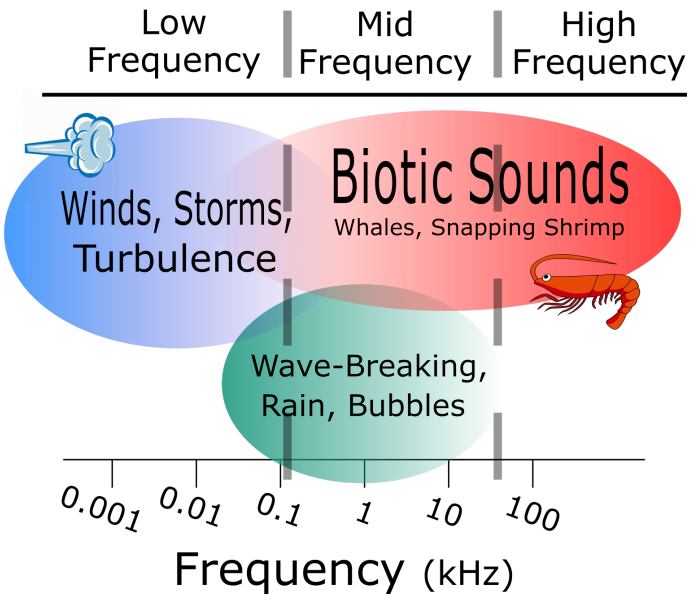


Figure 3.1: Frequency spectrum for some common coastal reef sound sources adapted from Delory et al., 2014, incorporating Stanley et al., 2021. The spectrum has been separated into the described frequency ranges for this experiment (top), to represent the ranges of the SoundTrap 500s (0.2-24 kHz, low/mid) and VR2Tx transceiver (50-90 kHz, high).

signals (Bohnenstiehl et al., 2016; McKenna et al., 2021; Stanley et al., 2021). Shallow coastal reefs are preferred habitats for many fish and invertebrate species that create noise, and are therefore some of the naturally noisiest marine environments (Cagua et al., 2013; ONMS, 2012). Snapping shrimp (*Alpheidae sp.*) create a cavitation bubble that pops, producing a broadband sound wave that reaches much higher frequencies than most other sources of ambient noise (Song et al., 2023) and can interfere with acoustic telemetry where shrimp are numerous (Cagua et al., 2013). The behavior of these shrimp has been studied extensively to better understand the where, when, and why they are snapping. Warmer temperatures increase their snap rate significantly, leading to more noise in summer and fall during their reproductive seasons especially at lower latitudes (Bohnenstiehl et al., 2016). They are generally more active at night and at sunset, leading to higher noise levels during these periods (Cagua et al., 2013; Stanley et al., 2021). Increases in low-frequency background noise can lower the peak frequency of their snaps, possibly due to burrowing behavior or a change in the average size of shrimp snapping (Spiga, 2022). There is also a

hypothesized relationship (Jung et al., 2012) that higher wind speeds affect snapping shrimp activity by showing an inverse relationship between wind speed and high-frequency noise, the majority of which is created by snapping shrimp. The physical processes that affect snapping shrimp behavior will also change the amount of high-frequency background noise (Stanley et al., 2021).

Past research in telemetry has identified detrimental environmental factors in detection efficiency such as nocturnal animal behavior, tidal currents, and stratified water columns (Edwards et al., 2019; Mathies et al., 2014; Payne et al., 2010). Some of these studies had difficulty discerning the effects of physical processes on different timescales (e.g., stratification and noise increasing together, McQuarrie et al., 2023; Oliver et al., 2017); this year-long experiment attempts to target and isolate processes that lead to changes in the efficiency of acoustic telemetry (McQuarrie et al., 2023). In habitats where snapping shrimp are present, they are often the only consistent source of noise at the highest frequencies that overlap transmissions (> 50 kHz; Stanley et al., 2021); certain mammals will make noises in this high frequency range to echolocate but these sounds are far less numerous (Miller & Wahlberg, 2013).

This work focuses on accounting for variable noise interference when using telemetry techniques. This research hypothesizes that noise interference from snapping shrimp changes with seasons, diurnal cycles, and high wind magnitudes, and those changes will be reflected in the acoustic detection data. We expect more transmissions to be detected during periods of lower snapping shrimp activity, with less interfering noise measured and more transmissions detected during daytime versus nighttime. We also predict that detection efficiency will be higher in winter as compared to summer due to differences in background noise created by snapping shrimp. Section 3.2 provides an overview of the region, instruments, and techniques used to analyze the coastal soundscape; sections 3.3.1 and 3.3.2 explore two different timescales and section 3.3.3 introduces a novel relationship between wind and noise. Section 3.4 reviews our findings in context, and reports practical uses and next steps.

## 3.2 Methods

### 3.2.1 Regional Considerations and Acoustic Array

Gray's Reef National Marine Sanctuary (GRNMS) is a live-bottom marine protected area (MPA) and home to a large population of snapping shrimp (ONMS, 2012; Stanley et al., 2021). GRNMS is located on the offshore edge of the inner shelf of the South Atlantic Bight (SAB), the coastal region of the Atlantic Ocean between southern North Carolina and northern Florida (Figure 3.2). The SAB is characterized by a wide continental shelf with low slope and well-defined governing large-scale physical processes. During winter, strong winds and a cold, largely well-mixed water column are expected on the mid shelf (Nov-Feb), and spring brings the highest freshwater discharge creating intense vertical stratification on the inner shelf (Mar-May). Summer is characterized by strong stratification driven by longer hot days with weak winds (Jun-Jul) (Weber & Blanton, 1980). Fall is a shorter transition period into an additional regional season, mariner's fall (Aug; Sep-Oct), which is characterized by some of the year's strongest winds (Weber & Blanton, 1980). Mariner's fall breaks down summer stratification, helping form the winter water environment (Blanton et al., 2003; Blanton & Atkinson, 1983; Weber & Blanton, 1980). These seasonal trends lead to a strong annual signal in temperature over the entire SAB shelf, including Gray's Reef and the inner shelf. These changes in temperature are thought to be important drivers of snapping shrimp behavior and the resulting high-frequency noise levels (Bohnenstiehl et al., 2016; McQuarrie et al., 2023; Stanley et al., 2021).

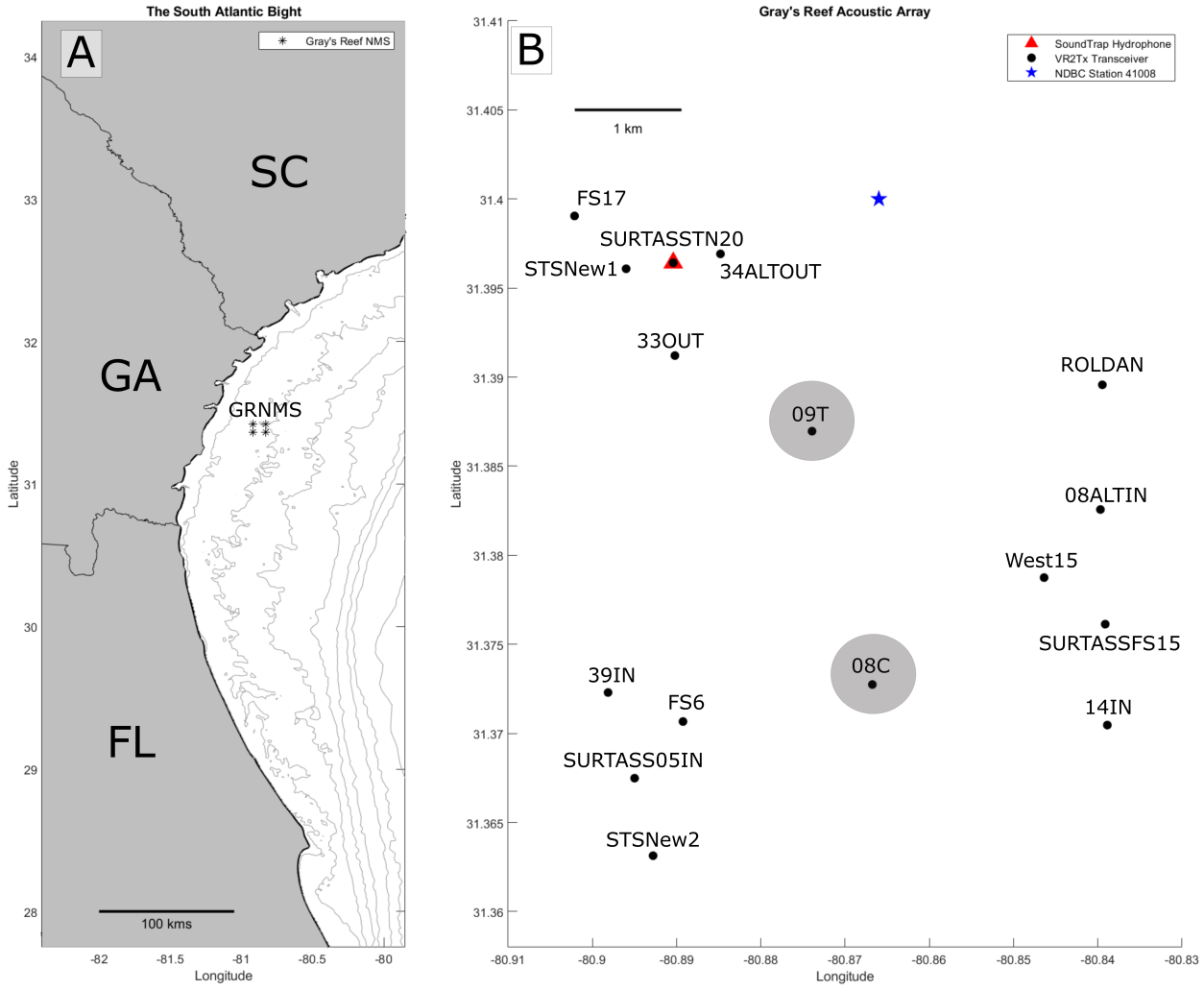


Figure 3.2: **A** Map of the South Atlantic Bight showing the location of Gray's Reef and 10 m isobaths. **B** Gray's Reef National Marine Sanctuary's acoustic array, made up of transceivers, a hydrophone, and surface buoy. 08C and 09T (shaded circles) will not be considered in our analysis due to a scarcity of detections.

Table 3.1: GRNMS's array of moored transceivers, their transmission identity and location. '*' denotes a transceiver that was excluded from analysis due to lack of detections.

| Transceiver Name | Transceiver I.D. | Lat. (°) | Long. (°) | Instrument Depth (m) | Bottom Depth (m) |
|---|---|---|---|---|---|
| SURTASSTN20 | A69-1601-63062 | 31.3964 | -80.8904 | 16.8 | 20.4 |
| SURTASS05IN | A69-1601-63064 | 31.3675 | -80.8950 | 16.8 | 18.2 |
| Roldan | A69-1601-63066 | 31.3896 | -80.8395 | 18.5 | 20.4 |
| 33OUT | A69-1601-63067 | 31.3912 | -80.8902 | 18.0 | 19.8 |
| FS17 | A69-1601-63068 | 31.3991 | -80.9021 | 17.8 | 19.4 |
| 08C* | A69-1601-63070 | 31.3728 | -80.8668 | 18.0 | 19.5 |
| STSNew1 | A69-1601-63073 | 31.3961 | -80.8960 | 13.7 | 15.8 |
| STSNew2 | A69-1601-63074 | 31.3631 | -80.8928 | 16.4 | 18.6 |
| FS6 | A69-1601-63075 | 31.3707 | -80.8893 | 17.7 | 19.8 |
| 08ALTIN | A69-1601-63076 | 31.3826 | -80.8397 | 18.6 | 20.1 |
| 34ALTOUT | A69-1601-63079 | 31.3969 | -80.8848 | 18.4 | 20.5 |
| 09T* | A69-1601-63080 | 31.3870 | -80.8739 | 18.0 | 19.5 |
| 39IN | A69-1601-63081 | 31.3723 | -80.8982 | 15.9 | 17.7 |

From November 20, 2019 to December 22, 2020, an array of 13 Innovasea VR2Tx transceivers, receivers that are equipped with their own transmitters, were attached to moorings at depths between 15-21 meters water depth, 1-3 meters off the bottom and between 400-1500 meters from each other (Figure 3.2; Table 3.1). The instruments transmitted (6x per hour) and received acoustic signals, measured hourly temperature (°C), and averaged high-frequency (50-90 kHz) noise amplitude for the hour. Two transceivers, 09T and 08C, were 1500 meters away from the nearest instrument and heard fewer than 150 detections for the entirety of the deployment ($< 0.1\%$ detected) and will not be considered in this analysis due to data scarcity.

### 3.2.2 High-Frequency Acoustic Transmissions

Each transmission was made up of 8 pings, quick acoustic impulses spread across 3 seconds. The checksum validation system required each ping be collected in order for a detection to occur, and the number and timing of the pings identifies the transmitter (Figure 2.1;Pincock, 2008; Scherrer et al., 2018). The precise timing of the signal makes them vulnerable to noise interference; the manufacturer noted that

ambient high-frequency noise levels over 650 mV make an environment challenging for telemetry, stating that “very few, if any, detections are expected” due to interference (Innovasea, 2021). Environments with between 325-650 mV of background noise are considered moderate: detections should be expected but reliable range may be reduced. An optimal environment is defined as having less than 325 mV of high-frequency background noise. This experiment measured very few hours (70 hours at the quietest part of the reef, $< 0.01\%$) with "optimal" noise levels (Innovasea, 2021), so all hourly HF noise measurements were compared to the "challenging" 650 mV threshold. Detections were binned hourly to align with the temporal scale of the water column data. Data collected before and after the receiver was in place have been identified and removed along with all self-detections (transceivers detecting their own 6 transmissions per hour).

### 3.2.3 Tag Density and Collision Analysis

The pings that make up a single transmission were spaced to identify the transmitter but if two signals occur at similar times a receiver can hear pings from different sources (termed a collision), leading to the receiver failing to identify either transmitter and preventing a successful detection (or worse, creating a false detection). There is a blanking period to limit this interference but it is still a concern for areas with a high number of transmitting instruments (tags, moorings, etc.; Scherrer et al., 2018).

The probability of collisions was calculated using the transmit delay (timing of signals), burst duration (length of signals), and number of transmitters in detection range using a method detailed in Binder et al., 2016. The bulk ($>90\%$) of tag-detections came from six tagged black sea bass that transmitted a 69 kHz signal every 110-190 seconds, staggered to avoid collisions, with a duration of 3 seconds. The VR2Tx transceivers transmitted far less, once every 540-660 seconds for the same 3-second duration. This was a relatively low number of signals to detect for the majority of our array resulting in a low probability of collisions (Table 3.2). Only one transceiver had more than 3% of their total detections originate from fish tags (`SURTASS05IN` accounted for 99% of tag-detections across all transceivers during this experiment),

Table 3.2: Results of running 10,000 iterations of a collision analysis Binder et al., 2016. The worst-case scenario (*) with the highest transmission-density was never observed.

| Equipment | Collision Probability | Predicted / Total Detections | Efficiency |
|---|---|---|---|
| **VR2Tx Transceiver** ~540–660 sec. delay, 3.2 sec. burst | | | |
| 1 Transceiver | 0.00 | 6 / 6 | 100% |
| 2 Transceivers | 0.009 | 12 / 12 | 100% |
| 3 Transceivers | 0.02 | 18 / 18 | 100% |
| 4 Transceivers | 0.03 | 23 / 24 | 96% |
| **V9-2x Fish Tags** ~110–190 sec. delay, 3.2 sec. burst | | | |
| 1 Tagged Fish | 0.00 | 24 / 24 | 100% |
| 2 Tagged Fish | 0.04 | 45 / 48 | 94% |
| 4 Tagged Fish | 0.115 | 83 / 96 | 86% |
| *6 Tagged Fish | 0.18 | 115 / 144 | 80% |
| **Cho et al. 2016** ~35–55 sec. delay, 5 sec. burst | | | |
| 1 Transmitter | 0.00 | 72 / 72 | 100% |
| 4 Transmitters | 0.49 | 144 / 288 | 50% |
| 7 Transmitters | 0.75 | 128 / 502 | 25% |
| 10 Transmitters | 0.87 | 93 / 718 | 13% |

with the vast majority of detections being other moored VR2Tx transceivers (Table 3.1). In Table 3.2, 6 fish tags are included but no more than 3 were ever heard during the same hour.

### 3.2.4 Environmental Context

Wind velocities, surface temperature, and wave height were collected by National Data Buoy Center's (NDBC) Station 41008 located within the GRNMS (Figure 3.2). The temperature collected by the moored VR2Tx transceivers was subtracted from the NDBC buoy's surface temperature to estimate bulk thermal stratification. Wind speed was binned using the Beaufort wind scale to help define the sea state at the air-sea boundary (Petkovic, 1964).

The hourly noise reported by the transceivers was defined as the high-frequency (50-90 kHz) noise level estimated by averaging measurements taken once per minute, the root-mean-square (RMS) amplitude

of the frequency band. Low-frequency noise data was measured by deployed hydrophones, SoundTrap 500 STDs, which were moored at GRNMS in support of NOAA's Sanctuary Sound project. These hydrophones continuously recorded a wide frequency range during a series of deployments between 2019-2021. The noise measured by these hydrophones was broken down into octave levels defined by frequency bands (ONMS, 2020). Three levels have been selected for this analysis: low-frequency (0.17-0.35 kHz) is dominated by sounds from storms and plunging waves; mid-frequency (11-22 kHz) measurements contain a mix of rain, bubbles popping, and biological sources; high frequency (50-90 kHz) noise is expected to include snapping shrimp as the primary source of noise and the transmissions themselves (Figure 3.1; Table 3.3; ONMS, 2012; Stanley et al., 2021).

### 3.2.5 Noise Measurements

The background noise collected by the VR2Tx transceivers were reported in mV instead of relative decibels or sound pressure levels. The broadband nature of the measurements makes converting them to a relative unit (such as dB re 1 µPa) complex, it would add large amounts of uncertainty and the data would still not be comparable to the hydrophone-based measurements. The VR2Tx millivolts were designed to give the user insight into the acoustic environment while deployed and are used accordingly.

Table 3.3: Breakdown of analyzed noise data and this work's defined frequency bands.

| | **Frequency Band (kHz)** | **Instrument** | **Unit** |
|---|---|---|---|
| Low-Frequency | 0.17–0.35 | SoundTrap 500 | dB re 1 µPa |
| Mid-Frequency | 11–22 | SoundTrap 500 | dB re 1 µPa |
| High-Frequency | 50–90 | VR2Tx Transceiver | mV |

### 3.2.6 Statistical Analysis

A correlation analysis was applied to the detection and environmental data to quantify the acoustic environment and its relationship to telemetry efficiency. The data was normalized by subtracting the mean

Table 3.4: Monthly averages with 95% confidence interval at SURTASSTN20. January's total is not included, only 55 hours were analyzed.

| **Month 2020** | **Temp** (°C) | **HF Noise** (mV) | **Wind Speed** (m/s) | **Total Detections** | **Average Dets/Hr** |
|---|---|---|---|---|---|
| January | 13.4±0.1 | 610±37 | 9.7±2.0 | – | – |
| February | 14.0±0.5 | 654±49 | 6.4±3.0 | 1874 | 2.69±4.2 |
| March | 15.4±1.4 | 697±44 | 4.9±2.6 | 717 | 0.96±1.70 |
| April | 19.8±0.9 | 745±30 | 5.6±2.6 | 295 | 0.41±1.13 |
| May | 22.4±1.0 | 760±26 | 5.0±2.2 | 217 | 0.29±0.86 |
| June | 25.6±0.5 | 775±21 | 5.4±2.2 | 241 | 0.33±0.91 |
| July | 28.1±1.0 | 774±24 | 5.0±2.0 | 292 | 0.39±0.88 |
| August | 29.2±0.1 | 789±22 | 5.1±2.3 | 32 | 0.04±0.32 |
| September | 28.0±1.6 | 788±32 | 6.7±3.4 | 46 | 0.06±0.41 |
| October | 24.7±0.4 | 781±27 | 6.1±2.9 | 35 | 0.04±0.34 |
| November | 21.9±1.0 | 762±31 | 6.5±2.8 | 38 | 0.05±0.35 |
| December | 17.7±1.0 | 697±43 | 6.1±3.7 | 162 | 0.04±0.99 |

and dividing by the standard deviation, then the Pearson correlation coefficient and p-value are calculated between variables assuming linear relationships. Statistical significance will be defined as having a p-value below 0.05, and the strength of the relationship will range from -1 being the strongest negative to 1 being the strongest positive relationship.

## 3.3 Results

### 3.3.1 Seasonal Variability

Seasonal differences represented the longest timescale analyzed in this experiment (370 days), which allowed for the capture of expected variations in benthic activity (and resulting background noise) due to changes in the water temperature (Table 3.4; Figure 3.3). SURTASSTN20 was in a dense part of the reef and measured large shifts in HF noise, winter was the only season with average noise levels deemed moderate (Jan: 610±37 mV), while spring (Mar: 697±45 mV) summer (July: 774±24 mV), fall (Aug: 789±22 mV),

and mariner's fall (Oct: 780±27 mV) all had challenging averages (Figure 3.3). The percentage of time spent with noise below the challenging threshold (>650 mV) at SURTASSTN20's dense live-bottom varied by season: winter, 20.2%; spring, 4.6%, and summer, fall, and mariner's fall all had 0 hours below the threshold. At the other end of the acoustic spectrum, FS17 (a transceiver in a sunken part of the reef) measured the least amount of noise, only 11% of hours were considered "challenging".

All 11 transceivers recorded fewer detections during seasons with warmer bottom temperatures and higher background noise (Table 3.4; Figure 3.3). The contrast is highest at SURTASS05IN where there were more transmissions to detect from tagged fish: the same fish were detected, but February had an average bottom temperature of 14.1 °C and 48.8±17 detections, while August had a 29.2 °C bottom temp and collected an average of 24.5±11 detections per hour. Bottom temperature and hourly detections at SURTASS05IN had a significantly negative relationship ($R^2$=0.25, p-val<0.01), while bottom temperature and HF noise's relationship was significantly positive ($R^2$=0.53, p-val<0.01).

### 3.3.2 Diurnal Time Scales

High-frequency noise increased at sunset and remained elevated for most of the night (Figure 3.4). This diurnal pattern is amplified during summer and fall (Bohnenstiehl et al., 2016; Stanley et al., 2021; Figure3.5). Average detection efficiency at SURTASSTN20 was higher during the day when noise was low compared to night-time detection efficiencies ($R^2$=0.26, p-val<0.01)(Figures 3.4, 3.5). There is significantly (p-val<0.01) more noise at night than during the day throughout the year corresponding to reduced detections (Figure 3.5).

### 3.3.3 Synoptic Wind Forcing

Increasing wind speeds led to higher significant wave height ($R^2$=0.45, p-val<0.01) and lower bulk thermal stratification ($R^2$=0.06, p-val<0.01; Figure 3.7). Paired with this mixing was increased low-frequency noise, presumably from crashing waves and popping bubbles, and decreased high-frequency noise ( Figure

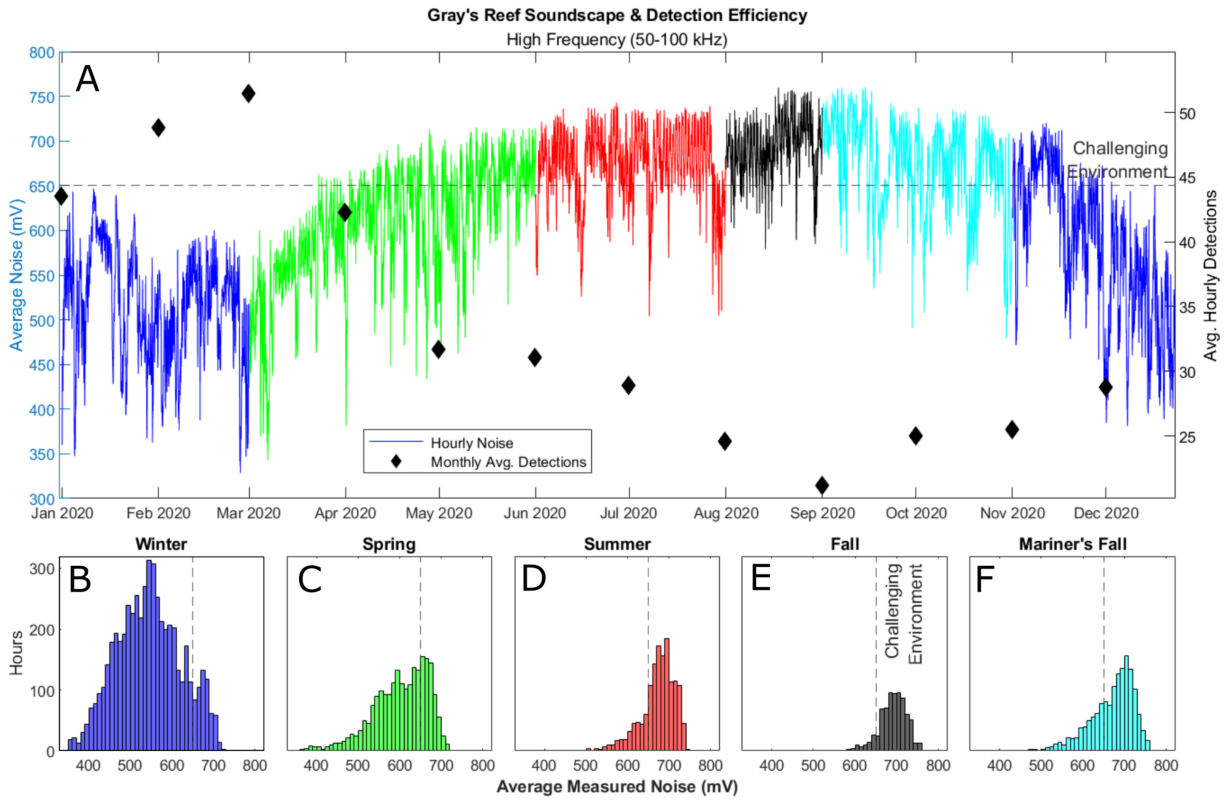


Figure 3.3: Time series of high frequency noise from `SURTASS05IN` at Gray's Reef colored by season: winter (blue), spring (green), summer (red), fall ( black), and mariner's fall (teal). **A** Hourly HF noise (line) compared to the average hourly detections (diamonds) collected that month, with (–) denoting a challenging acoustic environment. **B-F** histograms of hourly average noise for each season.

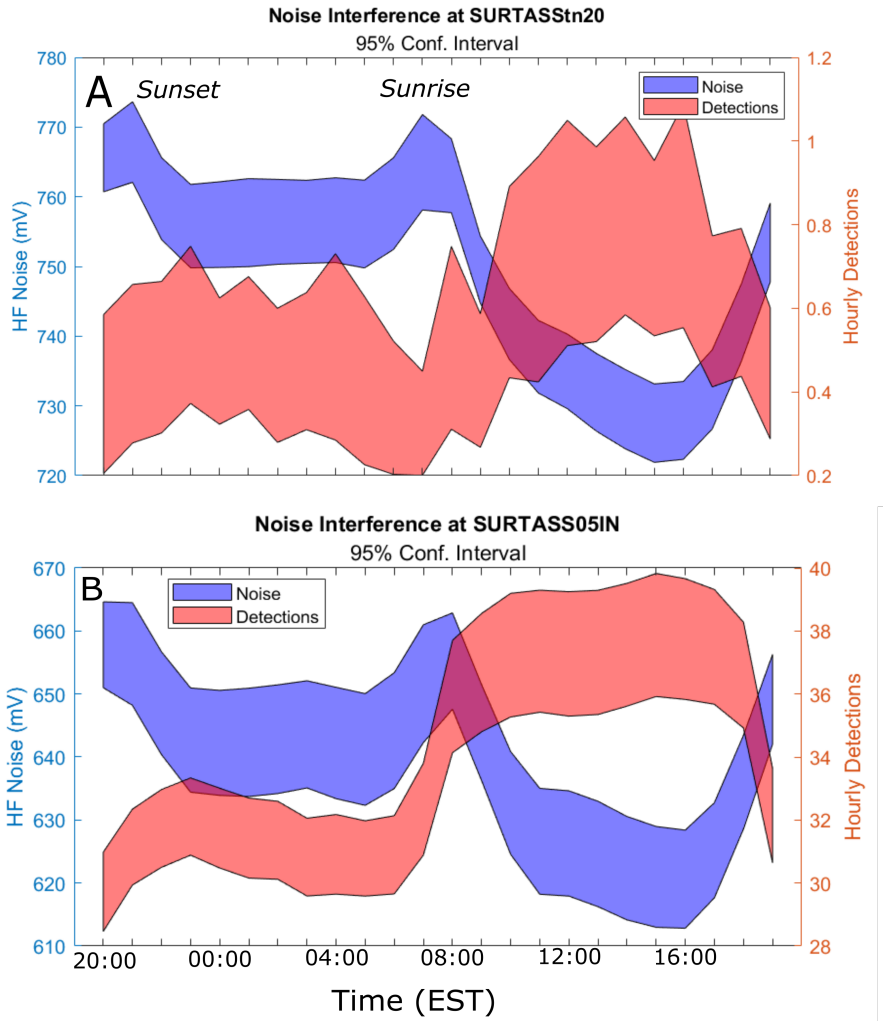


Figure 3.4: Average noise (blue) and detections (red) from two VR2Tx transceivers, one moored at **A** SURTASSTN20, and the other at **B** SURTASS05IN. 95% confidence interval is shaded. Times in EST.

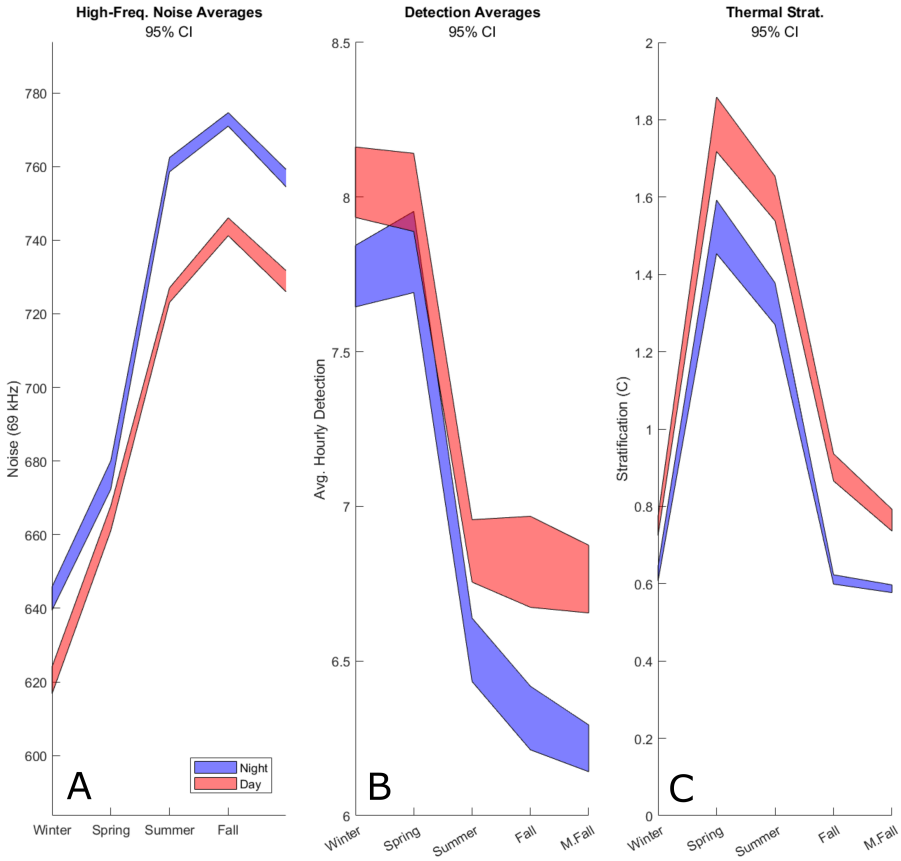


Figure 3.5: Hourly environmental data separated by time of day and season: **A** measured high-frequency noise, **B** detections, and **C** bulk thermal stratification with 95% confidence interval shaded.

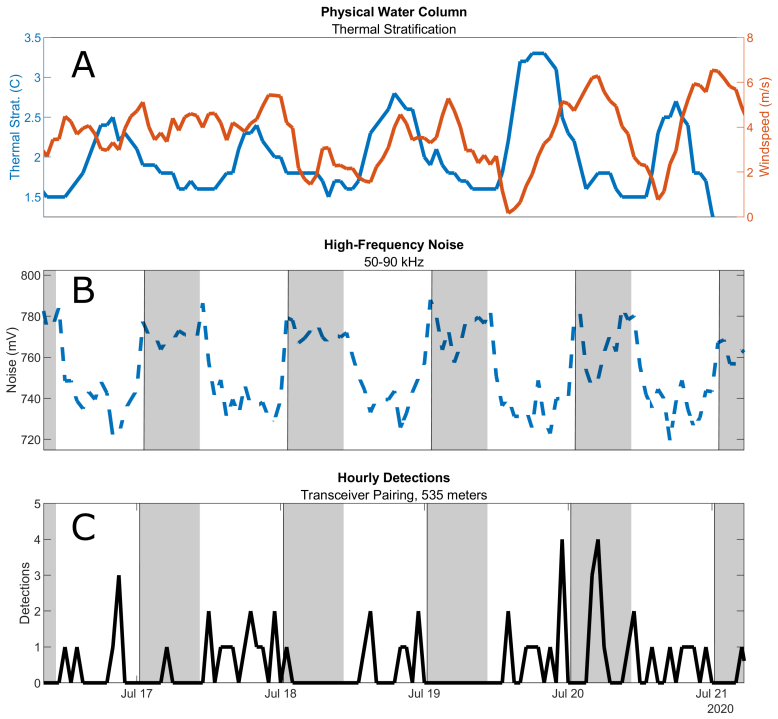


Figure 3.6: Time series of **A** bulk thermal stratification and wind magnitude, **B** high-frequency noise from SURTASSTN20, and **C** isolated detections from STSNew1 to SURTASSTN20, two VR2Tx transceivers that were 535 meters apart. Night is shaded in **B** and **C**.

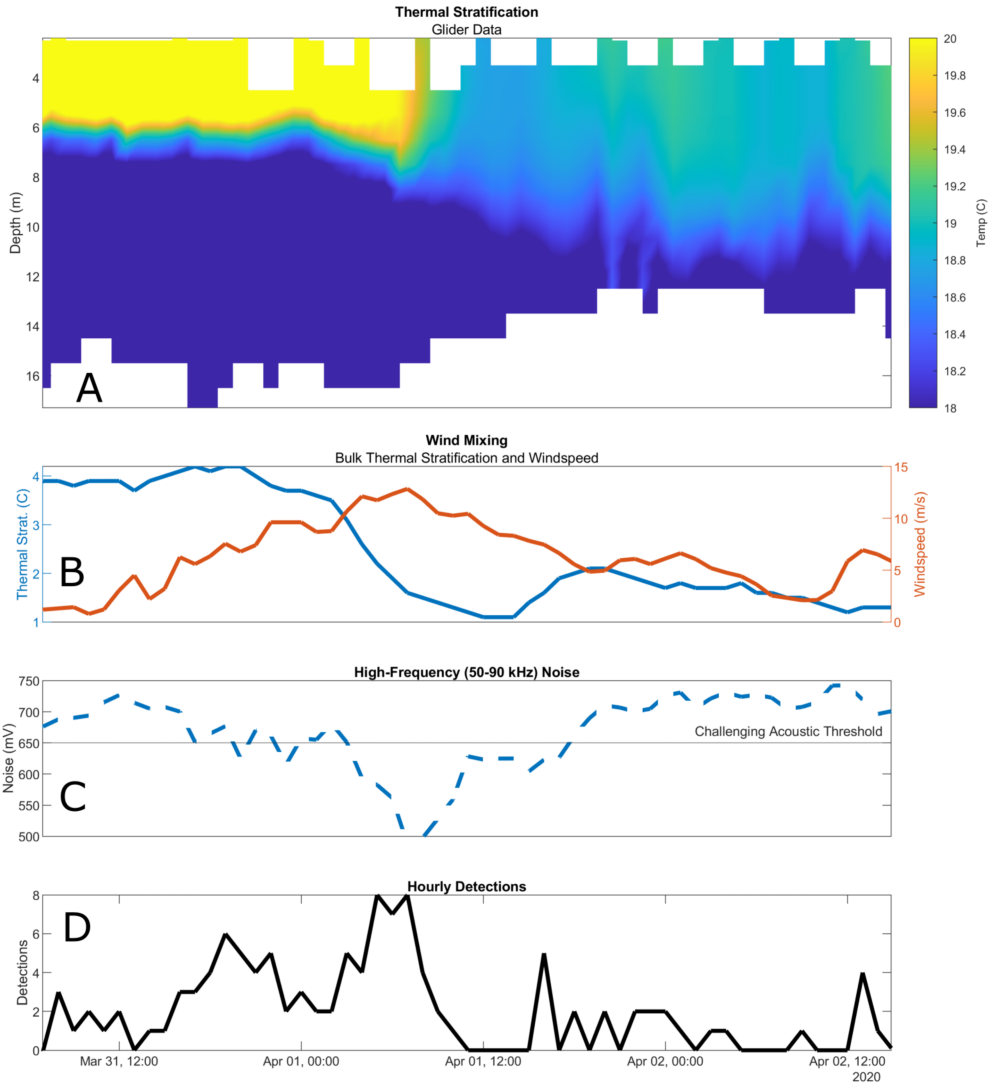


Figure 3.7: Time series at Gray's Reef for 3 days in spring 2020: **A** AUV-collected thermal (color) water column profile collected, **B** wind magnitude (orange line) and bulk thermal stratification (blue line), **C** high-frequency (50-90 kHz) noise (blue, —), and **D** hourly detections (black) collected by `SURTASSTN20`.

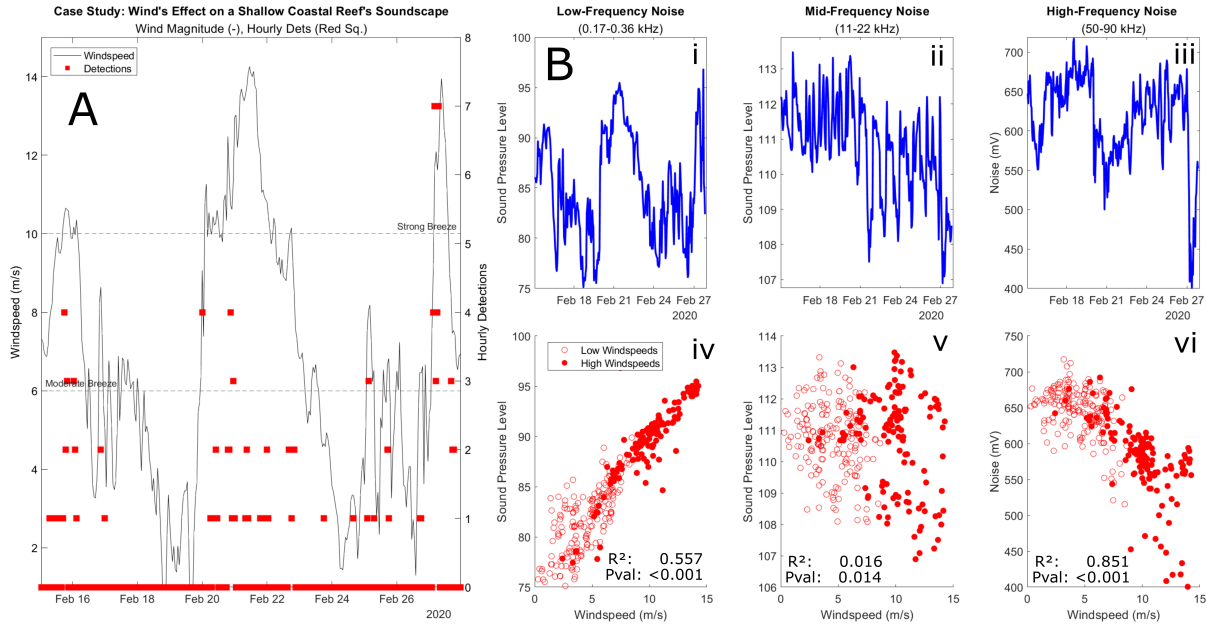


Figure 3.8: Example of a high wind event: **A** wind magnitude (m/s, black) and hourly detections (red) collected by SURTASSTN20, with moderate and strong breeze thresholds denoted (–); subsets **Bi-iii** low and mid frequency noise (blue) from the SoundTrap hydrophones, and high frequency noise from the VR2Tx transceiver, both moored at SURTASSTN20; **Biv-vi** wind magnitude versus the sound pressure level (red) with correlation values.

3.8; Prosperetti, 1988). Background noise decreased as wind increased (p-val<0.01), leading to a less challenging acoustic environment: every season showed significant (p-val<0.01) decrease in HF noise with increasing wind speeds. (Table 3.4; Figure 3.9). Out of the 11 transceivers analyzed, 10 were more successful at detecting transmissions during high (8-12 m/s) winds versus the same environments in low (< 4 m/s) wind conditions, average detection rate increased and high-frequency noise dropped (McQuarrie et al., 2023; Figure 3.10).

One transceiver (FS17) was located at comparable depths as the other moorings (19 meters) but in a sunken, protected part of the reef. FS17 had the least high-frequency noise (average HF noise was 553 mV, 22% less than the closest transceiver; Figure 3.11). Background noise levels at this location were not significantly affected by the wind ($p = 0.9678$ between noise and wind speed, compared to $p < 0.01$ for

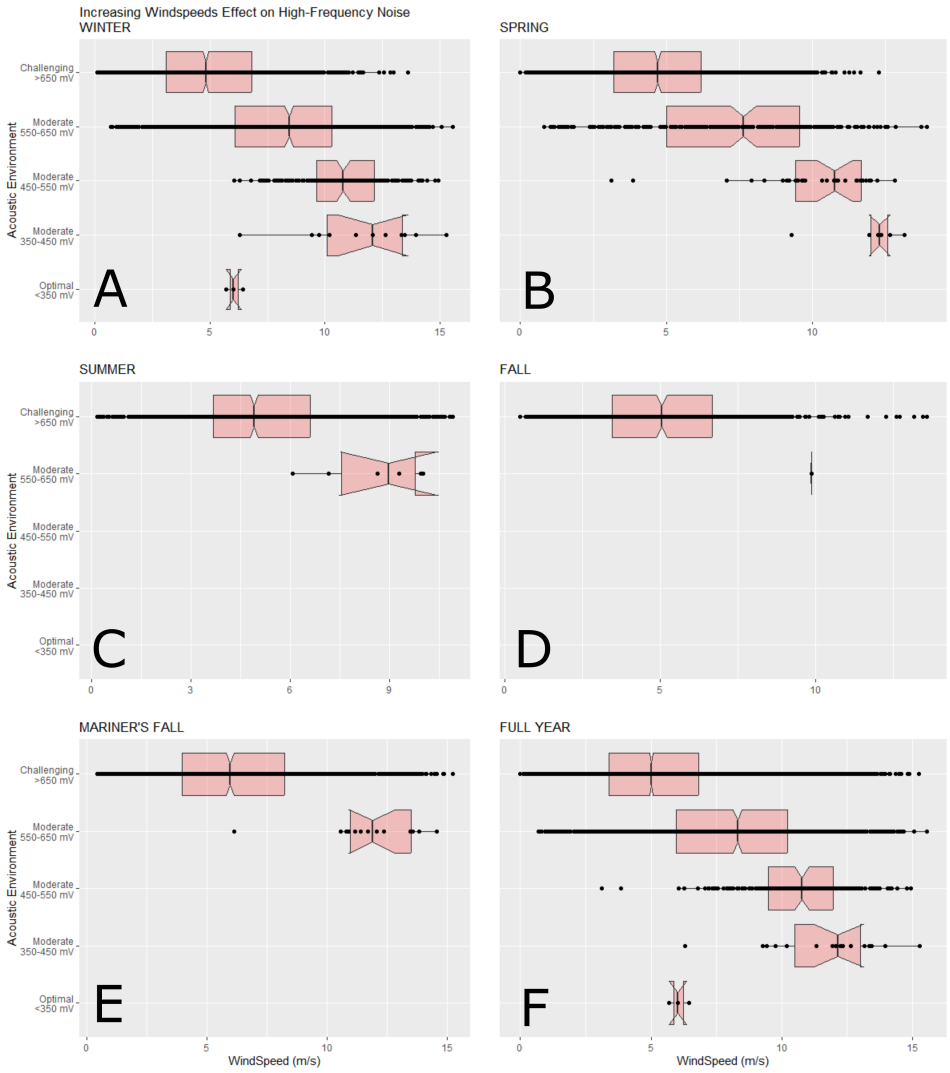


Figure 3.9: Distribution of measured HF background noise (red) at SURTASSTN20, binned by wind magnitude. Box plots show mean and 95% confidence interval for each season. The percentage of hours considered acoustically challenging: **A** winter (61%), **B** spring (85.7%), **C** summer (> 99%), **D** fall (> 99%), **E** mariner's fall (> 99%), and **F** the entire year (81%).

all other transceivers). At times this instrument recorded fewer detections when the winds were 8+ m/s, pointing to other possible effects of wind. Seasonal temperatures still drove high-frequency noise levels in FS17's quieter environment ($R^2$ = 0.80, $p < 0.1$; Table 3.4).

## 3.4 Discussion

Acoustic detections occurred more frequently when background noise dropped. Seasonal warming of the water column is correlated with increased high-frequency noise and reduced detections (Table 3.4; Figure 3.3). Nocturnal behavior of snapping shrimp raises the level of high-frequency background noise after sunset and limits detection efficiency (Figure 3.4); this increase in noise is dampened during high wind conditions (Figure 3.6). High-frequency noise is lost to the surface at a much higher rate than low-frequency noise, making storms and high-wind events optimal environments for acoustic telemetry. The difference between low frequency and high frequency noise attenuation is an important result for estimating an effective detection range in live-bottom environments where high-frequency noise interference is pervasive (Payne et al., 2010; Stanley et al., 2021).

### 3.4.1 Decreasing Background Noise Increases Detection Success

Many transceivers that heard nothing for days (missing a minimum of 144 possible detections per day) suddenly heard several transmissions per hour when winds increased and HF noise decreased. Snapping shrimp are the primary source of reef noise at these frequencies (Delory et al., 2014; Innovasea, 2021). This increase in efficiency could be due to a more homogeneous environment because it provides more physical sound paths between transmitters and receivers, reducing refraction, however the observed detections at high wind speeds occurred both in stratified and mixed environments (Figure 3.6) and some of the highest detection efficiency occurred during the stratified spring season (Figure 3.5). Further, when the winds

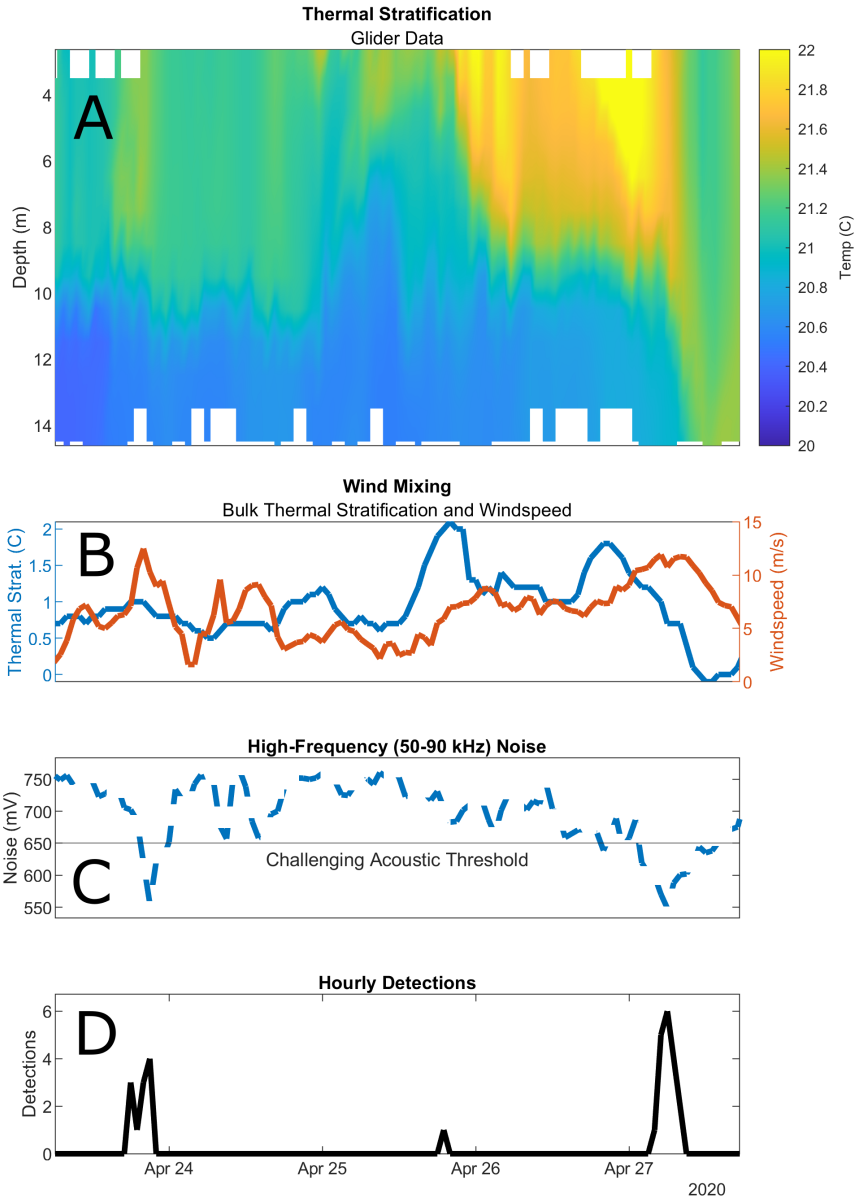


Figure 3.10: Time series data from SURTASSTN20's VR2Tx transceiver: **A** glider temperature data shown over depth (color); **B** bulk thermal stratification (blue) and wind speed (orange); **C** high-frequency noise (blue, –); and **D** hourly detections (black) of the nearest transceiver, STSNew1.

decreased, the water column remained mixed but noise rebounded and the efficiency fell back to previous levels (Figure 3.7). Although the difference in detection efficiency was expected to be most significant when noise levels dropped below the 'challenging' threshold, large decreases in noise were accompanied with more detections even when noise remained above this threshold (for example: 780 dropping to 690 mV).

Snapping shrimp are one of the few consistent sources of coastal reef noise over 50 kHz (Figure 3.1), and the recorded high frequency noise mirrors their nocturnal and seasonal patterns, becoming louder and interfering with telemetry at night (Figure 3.4) and in warmer times of year (Table 3.4; Figure 3.3) (Bohnenstiehl et al., 2016; Lillis & Mooney, 2018; Song et al., 2023). Although a transceiver's single hourly noise measurement makes it impossible to discern individual sound sources the noise response seen on nocturnal and seasonal frequencies corroborate that this biotic element is a large percentage of overall noise (Bohnenstiehl et al., 2016; Jung et al., 2012).

During periods with high wind speeds, successful detections occurred more frequently than periods with low winds. The winds had a clear and significant effect on the soundscape (Figure 3.8). The effect of wind at lower frequencies is direct: higher wind speeds equate to more white-capping and higher turbulence lead to increased low-frequency noise (Delory et al., 2014; Prosperetti, 1988). At higher frequencies, there are a few different possible relationships between wind and noise to be considered beginning with the sound source, snapping shrimp. Previous experiments have shown that low-frequency noise has reduced the peak frequency of snapping shrimp snaps; this drop in peak frequency is hypothesized to be caused by the shrimp burrowing into their habitats, attenuating the noise of their snaps and snapping less, and/or limiting the snaps from female and smaller shrimp leading to a lower peak frequency from the larger males (Jung et al., 2012). Before winds reach 5 m/s the high-frequency noise is mostly unaffected, but once white-caps start forming the noise levels dropped sharply with increased wind magnitude (Figure 3.7; McQuarrie et al., 2023; Petkovic, 1964). In an experiment where a speaker was playing low-frequency noise, snapping shrimp activity and peak frequency quickly rose back to normal immediately after the speaker was turned off (Spiga, 2022). High-frequency noise and detection rates respond quickly to changes in the wind even

when the water remains physically homogeneous (Figure 3.7).

### 3.4.2 Sound Attenuation Due to Bubbles

An indirect effect of wind on the high-frequency soundscape is the change in the surface boundary layer. As whitecaps form, a turbulent layer of bubbles at the surface is responsible for attenuating high-frequency sound at a much higher rate than low-frequency sound (Hildebrand et al., 2021; UWAPL, 1994). This change in the air-sea interface is another possible reason why the water column is quieter (with respect to high-frequencies) during high wind events, as surface layer bubble plumes can dampen the sounds that are already present as opposed to changing shrimp behavior. The turbulent surface texture also reduces the likelihood and intensity of reflected sounds, limiting possible pathways leading to even less noise propagating through the system (Hildebrand et al., 2021). It is unclear what effect from wind enables acoustic telemetry, less noise being created by shrimp (Jung et al., 2012) or higher attenuation at the surface (ONR, Published 1999/Updated 3/2023; UWAPL, 1994), but it is likely a combination of these biotic and abiotic factors. Measures of benthic activity would help track the shrimp snaps themselves, not just the created noise, and the next chapter explores this balance.

### 3.4.3 Different Pattern: Quieter Environments

Breaking surface waves create plumes of bubbles and turbulence, limiting reflection of sound waves that may otherwise lead to detections (Gimbert & Tsai, 2015). This change in possible transmission pathways may explain the differences between the quietest transceiver on the reef (FS17) in a sunken lagoon and the other transceivers (Figure 3.11). SURTASSTN20's noise had a significant (p-val$<$0.01) relationship with wind, while FS17 showed no significance (p-val=0.97). The transceiver that was closest to FS17 also had the steepest path between receiver and transmitter with a depth difference of 4.1 meters. This mooring measured lower noise levels than every other transceiver and had lower detection efficiency during hours

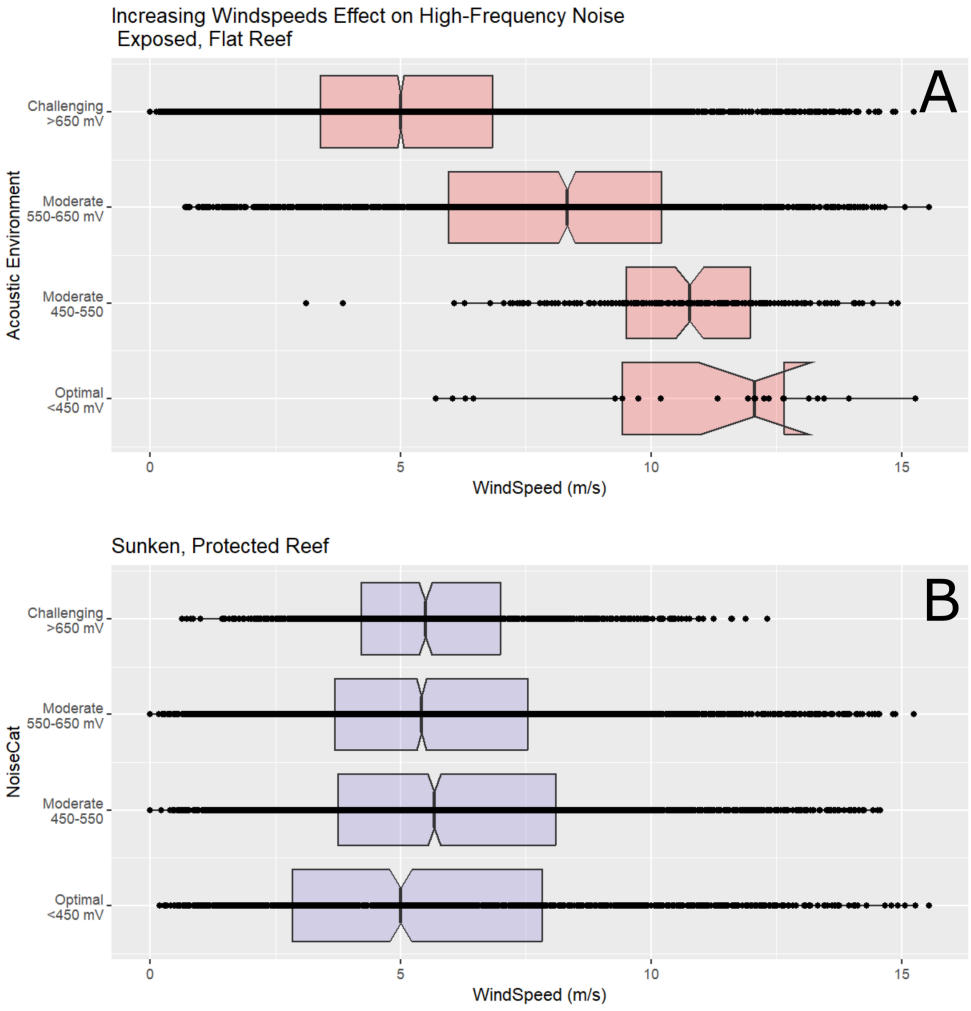


Figure 3.11: High-frequency (50-90 kHz) noise binned by wind speed for two different VR2Tx transceivers: **A** `SURTASSTN20` (red) and **B** `FS17` (blue). Challenging, moderate, and optimal background noise levels are defined by Innovasea, 2021, but moderate is broken down further for clarity.

with increased winds: the transmitting instrument in this case is the instrument closest to the surface at 13 meters, 2 meters above the 15 meter bottom. Currents created by wind may limit the pathways between the transceivers at different depths by restricting reflections and tilting the instrument away from the sunken portion. The same bubble plumes that increase attenuation and lower background noise may also prevent detections that require the air-sea interface to act as a reflective surface. This specific transceiver's environment is representative of telemetry efforts in more optimal, quieter acoustic environments, acting as further proof that knowledge of the medium is crucial to successfully collecting and analyzing detection data.

Recent work in the Netherlands (Edwards et al., 2024) found that high wind speeds had a strong detrimental influence on acoustic telemetry detection success in a much different environment, an intertidal zone within the North Sea. This region of the western Dutch Wadden Sea was significantly colder (temp. 12.1° C, compared to our 21.5 ° C), shallower (8.8 m, compared to our 19.22 m), and quieter (HF noise 399 mV, compared to our 705.8 mV, collected by the same model VR2Tx transceivers) (Edwards et al., 2024). Without high levels of HF background noise, and with some transceivers within 2 m of the surface, wind-driven waves and turbulence at the surface may prevent detections (Hildebrand et al., 2021). The comparison between these two environments helps shed light on how the soundscape affects acoustic telemetry and prompts further studies on why the winds have such a positive effect on detection efficiency in live-bottom, noisy environments.

These results are likely to be applicable to live-bottom reefs where snapping shrimp are present, accounting for large swings in the background noise levels. This study accounted for proximity to denser parts of the reef, but variation in bottom composition may change the relationship with wind as it may affect a sandy bottom boundary layer differently than a rigid reef. Targeted experiments that measure noise at higher frequencies during wind events would give a better explanation for why high-frequency noise levels decrease, discerning whether there is less noise being created, more noise being lost, or a combination of the two.

## 3.5 Conclusion

Acoustic telemetry efficiency is dependent on the medium through which sound travels, and to use it in challenging environments like coastal reefs requires understanding and adapting to the spatial and temporal variability in the soundscape. Physical processes that drive snapping shrimp behavior affect the likelihood of detecting high-frequency transmissions at known frequencies: seasonal warming increases shrimp behavior while limiting detections, and nighttime benthic activity creates more noise and leads to higher transmission loss. The relationship between wind and telemetry efficiency will be explored further in the next chapter, separating the biotic sound creation from the abiotic surface attenuation.

Moving forward, users attempting to study environments with snapping shrimp should consider these findings: at sunset and during nighttime, telemetry users should narrow their expected detection ranges due to the limited detection efficiency. Similar adaptations should be made in high wind conditions, expecting less high-frequency noise and thus a larger detection range. Array designs in live-bottom reefs need to account for a warmer summer water column having a smaller reliable detection range, especially at night, while also expecting far greater transmission efficiency in winter. A successful design may incorporate flexible instrument positioning (extra moorings, variable instrument density, etc.) to handle expected low and high-detection range scenarios (Ellis et al., 2019). Range-testing in only one season may not be adequate if the experiment requires a prolonged deployment or long-term monitoring, or if the experiment is started months later when the acoustic soundscape has changed. The goals of the experiment (home-ranging, migration tracking, etc.) need to inform the receiver deployment strategy, and that strategy must take into account to changes in the soundscape.

# Chapter 4

# A Reef's High-Frequency Soundscape and the Effect on Telemetry Efforts: a Biotic and Abiotic Balance

## 4.1 Introduction

Acoustic telemetry is a popular research tool for tracking marine animals, but the probability of detecting these signals heavily depends on the environment, as explored in Chapter 2 (Edwards et al., 2019; McQuarrie et al., 2023; Payne et al., 2010). A lack of detections can mistakenly be considered absence of transmissions to detect, when in reality a transmission may have been present but the receiver failed to detect it (Cho et al., 2016; Edwards et al., 2019; Payne et al., 2010). Acoustic telemetry detection efficiency is expected to decrease with distance (Gjelland & Hedger, 2013), especially in shallow coastal environments (McQuarrie et al., 2021), but changes in the physical environment can also directly influence transmission detection (Edwards et al., 2019; Huveneers et al., 2016; Oliver et al., 2017). Consequently, environment-

specific range testing is an important part of estimating dynamic detection probability and range (Kendall et al., 2021). Understanding the processes that determine how far transmissions travel is a fundamental part of the design of acoustic arrays (Ellis et al., 2019).

Shallow coastal waters affect how sounds travel, and these environments are often characterized by strong spatial and temporal variability of water column properties (Blanton et al., 1994) that can change detection efficiency (McQuarrie et al., 2021). The speed of sound is dependent on the physical properties of the water column (temperature, salinity, pressure) and the sound speed profile (SSP) dictates how signals travel (Mackenzie, 1981); these profiles can vary rapidly in shallow water columns affected by both top and bottom boundary layers (McQuarrie et al., 2021). The rate at which sound travels and attenuates depends on the sound frequency and environmental conditions (Stojanovic & Preisig, 2009). Sound bends and refracts away from local sound speed maxima which depend on temperature and salinity, so stratified environments often result in more heterogeneous soundscapes (Mackenzie, 1981; McQuarrie et al., 2021). Most of the attenuation in shallow (<20 m) environments involves at least one boundary layer and winds increase sound attenuation at the air-sea interface (UWAPL, 1994). Wind-driven white caps and waves create turbulence and bubble plumes that result in an asymmetric effect on background noise at different frequencies: the wind creates large amounts of low-frequency noise through wave breaking and turbulence (Hildebrand et al., 2021; Huang et al., 2024), while attenuating high-frequency noise at a higher rate and limiting surface reflectance (Pelaez-Zapata et al., 2024; Prosperetti, 1988).

One of the most important factors in telemetry efficiency is local background noise, sounds at similar frequencies can interfere with detections by masking the transmissions (Payne et al., 2010; Swadling et al., 2020). Live-bottom coastal reefs are expected to be acoustically challenging soundscapes due to both abiotic (wind, waves, bubbles) and biotic (fish, snapping shrimp, etc.) sources of background noise (Delory et al., 2014; Stanley et al., 2021). Waves, storms, and bubbles create low-frequency (<20 kHz) noise (Prosperetti, 1988), with very little overlap with the frequencies commonly used in acoustic telemetry (50-90 kHz) (Pincock, 2008). Snapping shrimp are of specific concern for interference due to the broadband (0.2-200 kHz) nature of their snaps, made when their claws form and pop a cavitation bubble that

creates a powerful and consistent sound that is one of the few common biotic sources of noise at higher frequencies (> 50 kHz) (Bohnenstiehl et al., 2016; Song et al., 2023). The rate of snapping varies over predictable time scales: seasonal signals in which warming increases snaps (Stanley et al., 2021), and diel cycles over which shrimp are expected to be more active at sunset and during the night (Bohnenstiehl et al., 2016).

Ambient noise near the transmission frequency band can limit detection efficiency (Payne et al., 2010), so snapping shrimp activity should concern researchers using telemetry techniques. Studying environments where snapping shrimp are present requires accounting for their behavior: more detections are expected when snapping shrimp are less active due to decreased noise interference (McQuarrie et al., 2023), an issue cited by the manufacturer (Innovasea, 2021). Estimation of background noise and telemetry efficiency could be critical for providing context and interpretation for collected detection data (McQuarrie et al., 2023).

This research explores a previously noted positive relationship between wind speed and detection efficiency on a shallow, noisy reef (McQuarrie et al., 2023), for which the underlying mechanism was not identified. A biotic explanation would be that snapping shrimp are less active during high winds, creating less noise and lowering interference, increasing the number of successful detections (Figure 4.1A; Jung et al., 2012). A competing abiotic explanation is that benthic activity is not affected by the increased winds and the same amount of noise is being created, but increased surface attenuation enables telemetry efforts by lowering background noise (Figure 4.1B; UWAPL, 1994). Wind appears to be an important factor in telemetry efficiency in a variety of environments (Edwards et al., 2024; McQuarrie et al., 2023; Pelaez-Zapata et al., 2024), and understanding the mechanism would add context to collected detection data.

We hypothesize that high winds result in less noise created by lowering shrimp activity and increasing surface attenuation, both contributing to a quieter, more optimal environment for acoustic telemetry that results in higher detection efficiency. We expect decreased snap rates during periods of high winds, and a higher rate of noise attenuated at the surface, accounting for both biotic and abiotic factors in the

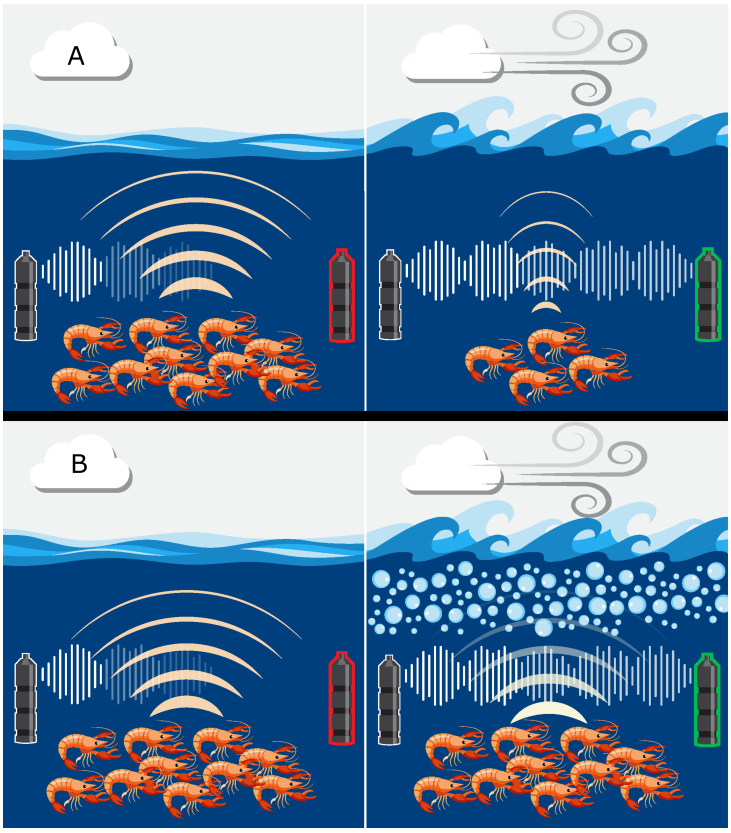


Figure 4.1: Schematic detailing the hypothesized relationships between wind and detection efficiency. **A** The biotic hypothesis, as winds increase snapping shrimp are less active leading to less noise being created and higher detection efficiency of transmissions. **B** The abiotic hypothesis, as winds increase, snapping shrimp are unaffected and create the same amount of noise, but there is significant sound attenuation due to surface bubble loss (SBL). Illustration by Lee Ann DeLeo (SkIO/UGA).

soundscape variability. If defined, this relationship would be a practical way to use atmospheric and buoy wave data to inform acoustic studies and detection ranges in these biologically important but acoustically challenging environments.

The following research tests our hypothesis for why telemetry efforts are more successful as winds increase (changes in snapping shrimp behavior and increased surface attenuation). Section 4.2.1 describes the experimental region and data collection methods, detailing the instruments and data formats. Section 4.2.3 explains how snapping shrimp behavior is estimated from passive acoustic data to quantify high-frequency noise creation, and Section 4.2.4 describes the method for quantifying noise attenuation by calculating surface bubble loss. In Section 4.3, detection data from moored transceivers is compared to the noise created and noise lost during high winds to explore the mechanism behind the increased detection success. Section 4.4 breaks down the findings and significance of the outcomes, and present some ways to account for this relationship.

## 4.2 Methods

### 4.2.1 Environmental Context

Gray's Reef National Marine Sanctuary (GRNMS) is a live-bottom reef off the coast of the southeastern United States on the South Atlantic Bight (SAB), which is a broad shelf influenced by the Gulf Stream and the discharge of freshwater rivers closer to shore (Figure 4.2) (Blanton et al., 1994). GRNMS lies along the 20 m isobath and provides habitat for more than 200 species of fish and invertebrates including snapping shrimp (ONMS, 2012; Stanley et al., 2021).

National Data Buoy Center (NDBC) Station 41008 measures significant wave height (m, highest one-third all the waves during 20-minute sampling), sea surface temperature (SST, C°, 2 m below the surface), and wind speed (m/s, averaged over an 8 minute period) at GRNMS (31°24'0" N, 80°51'59" W)(Table 4.1). Missing data (115 hours out of 8784, <2%), none of which were subsequent, were linearly interpolated

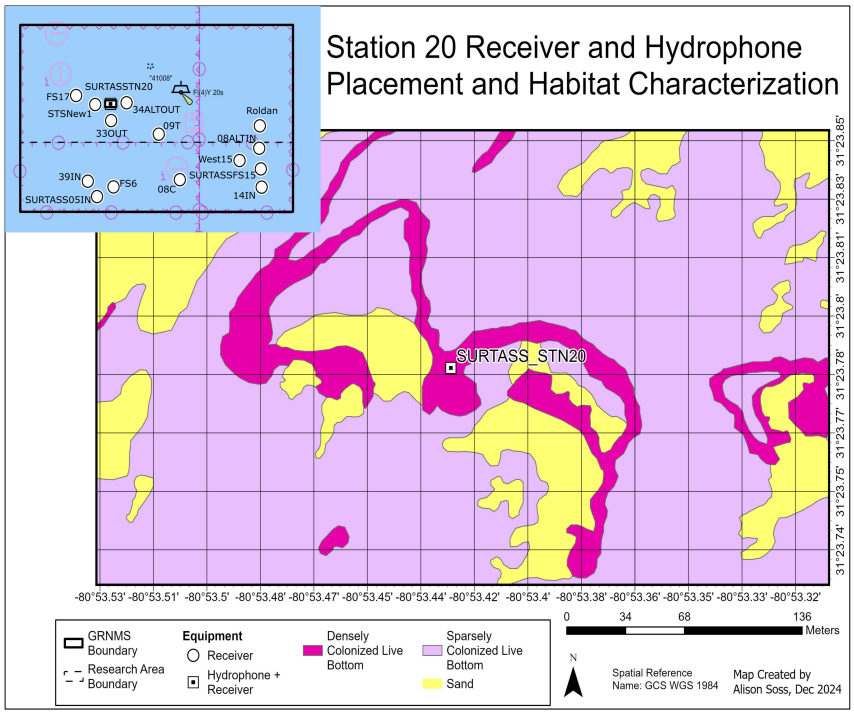


Figure 4.2: Habitat characterization for SURTASSTN20 at GRNMS. Colors denote bottom composition. Map credit: Alison Soss (NOAA/GRNMS).

in time. Wind events were defined as periods with 2 or more days of sustained strong (>8 m/s) winds, including several hours before and after to isolate the possible effects of the wind event. We assume that horizontal stratification, which changes seasonally on the inner shelf near GRNMS (Blanton & Atkinson, 1983), was small within Gray's Reef itself. For the purposes of this research, we assume that data collected at the sea surface was representative of the entire sanctuary.

During the evaluation period, autonomous underwater vehicles (AUVs, gliders) were deployed to profile the water column for three separate missions totaling 88 days measuring conductivity, temperature, and pressure with a Seabird Electronics pumped GPCTD as it dived and climbed at a 26° angle to support the SURTASS Soundscapes program, designed to create best practices in acoustic monitoring programs for marine-protected areas (Table 4.1) (Stanley et al., 2021). Data were processed to remove data points before and after deployment, then bin-averaged to 1-hour and 1-meter resolutions. Bulk thermal and density stratification measurements are estimated as the differences between the minimum and maximum from each binned hour to quantify vertical changes.

Table 4.1: Overview of instrumentation and data. Bottom temperature, detections, noise, and snap rate ranges are from `SURTASSTN20`.

| Variable | Units | Source | Range | Usage |
|---|---|---|---|---|
| Bottom Temp. | C° | VR2Tx | 13.5–21.5 | Env. context |
| Detections | detections/hr | VR2Tx | 0–8 | Telemetry efficiency |
| High-Freq. Noise | mV | VR2Tx | 400–769 | Interference (50–90 kHz) |
| Snaps | snaps/hr | SoundTrap 500 | 171–6758 | Noise Creation |
| SST | C° | NDBC Station 41008 | 12.6–23.7 | Env. context |
| Surface Bubble Loss (SBL) | dB | Calculated | 0.2–15 | Noise attenuation |
| Thermal Stratification | Δ C° | VR2Tx, NDBC | 0–6.5 | Env. context |
| Wave Height | m | NDBC Station 41008 | 0–2.87 | Env. context |
| Wind Speed | m/s | NDBC Station 41008 | 0.2–14.3 | Env. context |

### 4.2.2 Telemetry Detections and Acoustic Measurements

Thirteen Innovasea VR2Tx transceivers were moored at GRNMS between November 2019 and December 2020, with water depths ranging from 14-21 m and spread apart so that the nearest receiver was between

400-1400 m away (Figure 4.2). Each transceiver sent and received low-power (142 dB) transmissions, and reported background noise (50-90 kHz, measured 6 times per hour then averaged as an hourly value) and temperature (C°, once per hour). The transmissions themselves are a short (3 second) series of 8-10 high-frequency (69 kHz) pings, with the timing between pings identifying the unique transmitter (Scherrer et al., 2018). The transmitter IDs for the transceivers moored at GRNMS (Figure 4.2) were known a priori, as were the serial numbers implanted in six black sea bass tagged by GRNMS partners in 2019; unknown tags were assumed to come from fish tagged outside Gray's Reef. The majority (>98%) of total detections in the array were from the identified VR2Tx transceivers, with a small number of detections originated from tagged fish. The transceivers were programmed to transmit once every 540-660 seconds, offset from each other to avoid collisions. Six transceiver detections per hour is considered 100% efficiency between two specific VR2Tx instruments, but some transceivers may receive more due to the offset. Reported detection efficiency was calculated between two instruments assuming a maximum of 6 detections per hour.

Acoustic data analyzed for this research were collected and quantified from two different data sets: high-frequency noise measured by VR2Tx transceivers, and continuous low-frequency hydrophone recordings (Table 4.1). High-frequency noise measured in the 50-90 kHz band by VR2Tx transceivers was an hourly average of the background noise measured (in millivolts, mV) once per minute across a relatively broad frequency band. This measurement was designed so that telemetry users could estimate possible noise interference in the transmission frequency band. Converting the VR2Tx transceiver's millivolt measurements to a unit like sound pressure levels (e.g., dB re 1 $\mu Pa$) would inject large amounts of uncertainty due to the broad frequency band (pers. comm. with Innovasea), so we choose to use the manufacturer's measurement in mV as prescribed. The transmissions were included in the transceiver's noise measurements but were considered negligible with respect to external sources. Low-frequency (0.2-24 kHz) sound recordings were collected by a SoundTrap 500 hydrophone moored 1 meter off the live-bottom reef structure at Station `SURTASSTN20` (Figure 4.2) in support of the Sanctuary Sound project (Stanley et al., 2021). The recordings included a range of biotic and abiotic sound sources (Stanley et al., 2021) but the mid-frequency

band (1.5-20 kHz) was expected to be primarily snapping shrimp (Bohnenstiehl et al., 2016; Stanley et al., 2021). The low- and high-frequency noise measurements are collected and analyzed independently, and though they cannot be directly compared, both contribute to define the acoustic environment.

Two stations were chosen as representative of the array: SURTASSTN20, a high-noise environment that mostly detected a nearby transceiver, and SURTASS05IN, a quieter environment with a higher number of transmissions to detect. The SURTASSTN20 mooring (31°23'47" N 80°53'25" W; Figure 4.2) was located within a densely colonized portion of the reef. SURTASSTN20 contained both a VR2Tx transceiver measuring high-frequency noise and a SoundTrap 500 hydrophone measuring low-frequency noise. The majority (>70%) of detections collected by SURTASSTN20 were from a transceiver 440 m away (STSNew1), and of the detections of actual fish, 1242 of the 1277 (97%) tagged fish detections collected by SURTASSTN20 originated from a single tagged sea bass between in just 13 days (January 29 - February 10th, 2020, Table 4.2). Collision analysis, following (Binder et al., 2016), suggests a very low (<5%) probability of transmission collision for SURTASSTN20 due to the low number of short transmissions.

A second station, SURTASS05IN, was located farther to the southwest ( 31°22'2.96" N 80°53'42.00" W) in a live-bottom habitat and was observed to be significantly quieter than SURTASSTN20, with 14% less average HF noise (p-val<0.01, Table 4.2). The SURTASS05IN mooring did not have a low-frequency hydrophone during this period, so snap rates from SURTASSTN20 were considered representative of the snapping shrimp population. The VR2Tx transceiver detected an order of magnitude more signals than the instrument at SURTASSTN20 (Table 4.2) due to tagged fish residing nearby and transmitting at a higher rate. It was a relatively high-transmission density environment with many signals to detect which meant collisions were more likely (10-20% chance of collision, following (Binder et al., 2016)). This difference in transmission density makes it difficult to directly compare detection efficiency of the two transceivers (SURTASSTN20 and SURTASS05IN), but both are useful given their environmental context as telemetry instrumentation in moderate to challenging acoustic environments.

Table 4.2: Mooring data summary for SURTASSTN20 and SURTASS05IN.

| Mooring | Avg. HF Noise (mV) | Total Detections | Transceiver Detections | Tagged Fish Detections |
|---|---|---|---|---|
| SURTASSTN20 | 749±54 | 4,398 | 3,121 (71%) | 1,277 (29%) |
| SURTASS05IN | 642±83 | 312,101 | 19,492 (6%) | 292,609 (94%) |

### 4.2.3 Measuring Biotic Influence: Snap Rates

Snapping shrimp behavior was quantified using continuous recordings from a SoundTrap 500 hydrophone at SURTASSTN20. Recordings were sampled at 48 kHz then bandpass-filtered (Kaiser window with a default transition bandwidth of 0.02 times the Nyquist frequency, 1.5-20 kHz) to isolate snapping shrimp influence (Bohnenstiehl et al., 2016), providing a sharp frequency cutoff and preventing any phase distortion. Snap rate was estimated using an amplitude threshold detector in Raven Pro 1.6 (an acoustic analysis software built to discern auditory signals; K. Lisa Yang Center, 2024), detecting spikes in waveform intensity in the filtered recordings (Figure 4.3). An amplitude of 1000 units (1 kU) was chosen as a reasonable intensity threshold to count as a snap, where the dimensionless units are the root-mean-square (RMS) amplitude over the entire selected frequency band, an "effective amplitude" for sound processing ((K. Lisa Yang Center, 2024)). This snap detection algorithm was automated and verified by random selection of 10 10-second intervals, each of which properly captured only the snaps exceeding the chosen threshold and correctly disregarded quieter snaps. The reported snap rate is the number of snaps that met the intensity threshold in an hour, used as a proxy for the noise created. The snap rate was calculated for data spanning several months in 2020 and 2021, and here is separated into spring (January 30th - May 4th, 2020) and fall/winter (September 29, 2020 - December 31st, 2020) deployments for a total of 4515 hours analyzed. Measured snap rate variability (noise created) is then compared with calculated noise lost at the surface.

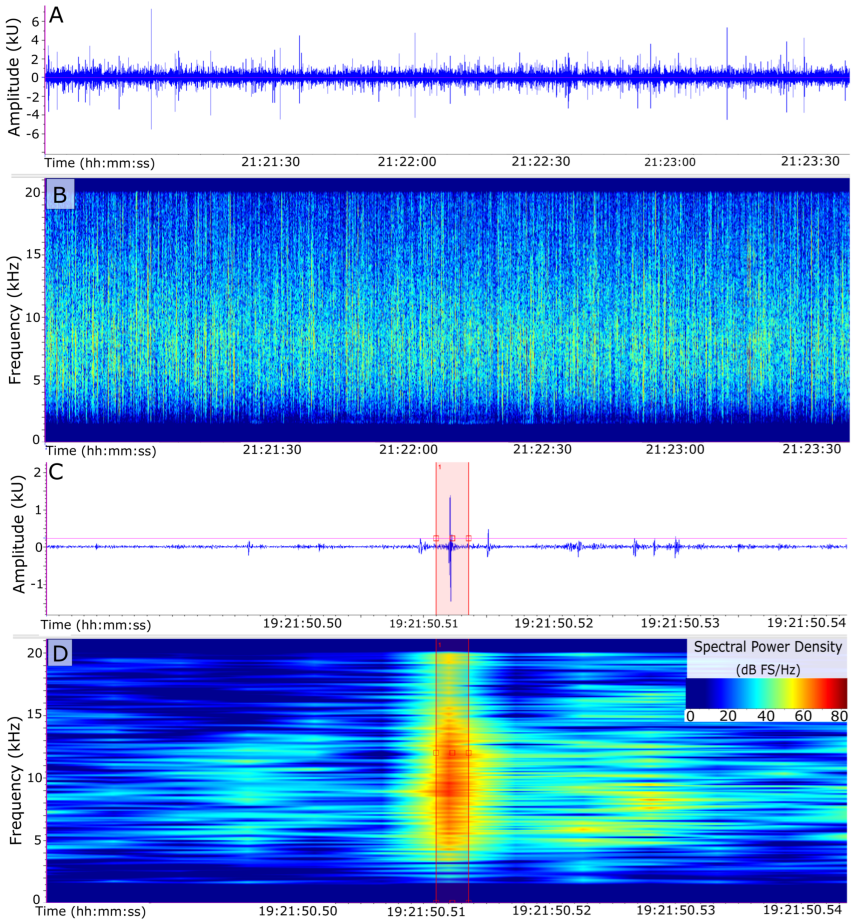


Figure 4.3: SoundTrap 500 recordings were bandpass-filtered (1.5-20 kHz), visualized in Raven Pro as **A** a full-spectrum waveform with RMS amplitude (blue) and **B** spectrogram, plotting intensity (dB FS/Hz) normalized to 1 Hz bandwidth. **C** Example waveform amplitude (blue line) identifying single snap exceeding the 1000 U threshold (shaded in red); **D** spectrogram from the same time (snap shaded in red).

### 4.2.4 Calculating Abiotic Influence: Surface Bubble Loss

Wind-driven waves generate whitecaps and turbulence that can create a layer of bubbles at the surface (ONR, Published 1999/Updated 3/2023; Prosperetti, 1988). This bubble layer dampens propagation, limits reflection, and increases absorption of sound (Hildebrand et al., 2021; ONR, Published 1999/Updated 3/2023). Wind and wave height data from NDBC Station 41008 were used to calculate noise attenuation through surface bubble loss (SBL) as (UWAPL, 1994):

$$SBL\ (dB) = \frac{1.26 \times 10^{-3}}{sin\theta} U^{1.57} f^{0.85}, \qquad U\ \geq 6\ m/s$$

and

$$SBL\ (dB) = SBL(U = 6\ m/s)e^{1.2(U-6)}, \qquad U\ < 6\ m/s$$

where U is the wind speed, f is the transmission frequency (69 kHz), and $\theta$ is the angle at which the signal meets the surface (UWAPL, 1994), with a 6 m/s wind speed threshold to account for the difference in sea state once white caps form (Figure 4.4). The SBL was capped at a maximum of 15 dB to reflect measured limits on sound attenuation as bubbles entrain together and scatter noise at the surface (Prosperetti, 1988; UWAPL, 1994). Snapping shrimp are ubiquitous in the densely colonized parts of Gray's Reef (ONMS, 2012), so snapping shrimp are considered sound sources over the entire domain instead of sporadic point sources. Attenuation was calculated with the most conservative reasonable estimate of angle of incidence ($\theta$) at 10° to estimate the higher attenuation loss expected at low incident angles (Figure 4.4).

### 4.2.5 Filtering & Statistical Analysis

A 4th-order low pass recursive Butterworth filter was used to isolate the low-frequency variability (>40 hours). The time series data contained variability on multiple concurrent timescales, and this filter protected trends while removing the higher-frequency components. To reduce autocorrelation, the filtered data was sub-

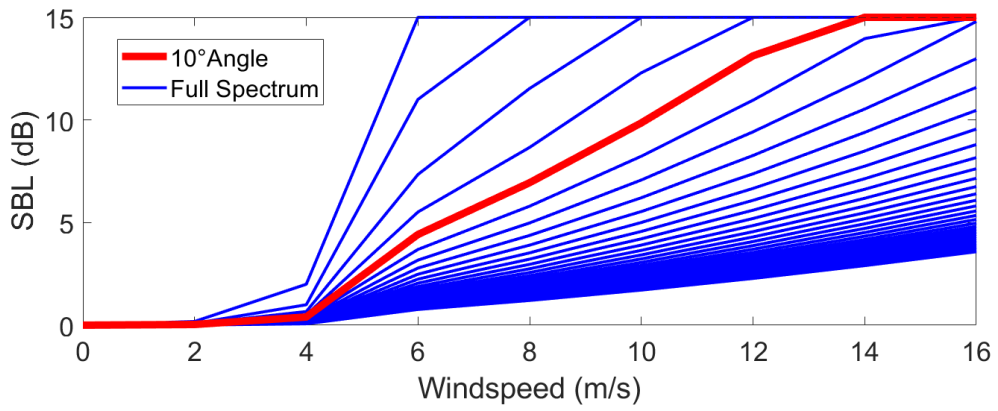


Figure 4.4: Surface Bubble Loss (SBL) calculated at 69 kHz, the transmission frequency and center of the HF noise measurement (50-90 kHz). A range of angles from 2-90° are plotted with 10° bolded to highlight the angle chosen for this analysis. Lower angles and higher frequencies increase SBL attenuation.

sampled at a 40-hour window for statistical analysis. Data were then normalized by subtracting the mean and dividing by the standard deviation, with significant outliers removed. The Pearson correlation coefficients and associated statistical significance (p-value) were calculated for both the raw and filtered data to quantify the relationship between environmental variables (temperature, wind speed, noise), assuming linear relationships. The $R^2$ value represents the correlation coefficient between the two variables, measuring the variance, and they are paired with p-values lower than 0.01 unless otherwise noted. The Spearman correlation coefficients were chosen for snap rate and detection data to account for non-normality, the sporadic detection patterns, and the discrete nature of hourly count data assuming monotonic (but not necessarily linear) relationships between them and environmental variables. Detection data and snap rates are not expected to be (and are not) normally distributed. Spearman's rank correlation converts them to a ranking and computes the Pearson correlation on those ranks as a way to measure variability without assuming linearity or normality. Reported $R^2$ values still measured the variance and were paired with p-values lower than 0.01.

## 4.3 Results

In this section, we evaluate the relative influence of biotic and abiotic variability in the soundscape by comparing the estimated noise creation by snapping shrimp and the estimated SBL attenuation to measured HF noise levels. Shrimp snapping was compared to predictable environmental variability and these behavior patterns were analyzed as a proxy for noise interference. Wind speed and SBL were compared with shrimp snaps, measured noise, and telemetry detections to isolate the effect of increasing winds and wave height. The balance between noise created and noise lost was tested during high-wind events.

### 4.3.1 Variability in Snapping Shrimp Behavior

Bottom temperature appears to be the strongest driver of snapping shrimp behavior (n=2268 hrs, $R^2$=0.93, p-val $<$ 0.01) and resulting HF noise ($R^2$=0.66, p-val $<$ 0.01), as reflected in observed seasonal trends (Figure 4.5; Table 4.3). Warming spring temperatures are associated with increased snapping shrimp activity (Figure 4.5A), while cooling fall waters are associated with decreased snapping activity (Figure 4.5B). This seasonal increase in background noise interference was inversely related to detection efficiency data, the VR2Tx acoustic telemetry transceiver at `SURTASSTN20` detected transmissions from the nearest transceiver (`STSNew1`) more often in winter, with the average (mean) efficiency dropping lower in summer: Feb, 13%; Mar, 9%; Apr, 4%; May, 3%; Jun, 3%; Jul, 4%; Aug, 0.5%; Sep, 0.8%; Oct, 0.8%; Nov, 0.9%; Dec, 6% (Table 4.3).

Diurnal and crepuscular behavior patterns emerged from the data measured at `SURTASSTN20` (Figure 4.5C), with peak shrimp behavior detected at sunset and sunrise followed by low activity levels during the day. When averaged over a canonical day in Figure 4.6, the highest average number of snaps per hour occurred at sunset (95% confidence interval: 19:00 average, 2960-3459 snaps per hour), followed by sunrise (06:00 average, 2709-3366 snaps per hour). There were relatively high activity levels at sunrise compared with low snap rates mid-day (13:00 average, 1665-2039 snaps per hour) (Figure 4.6), an average difference

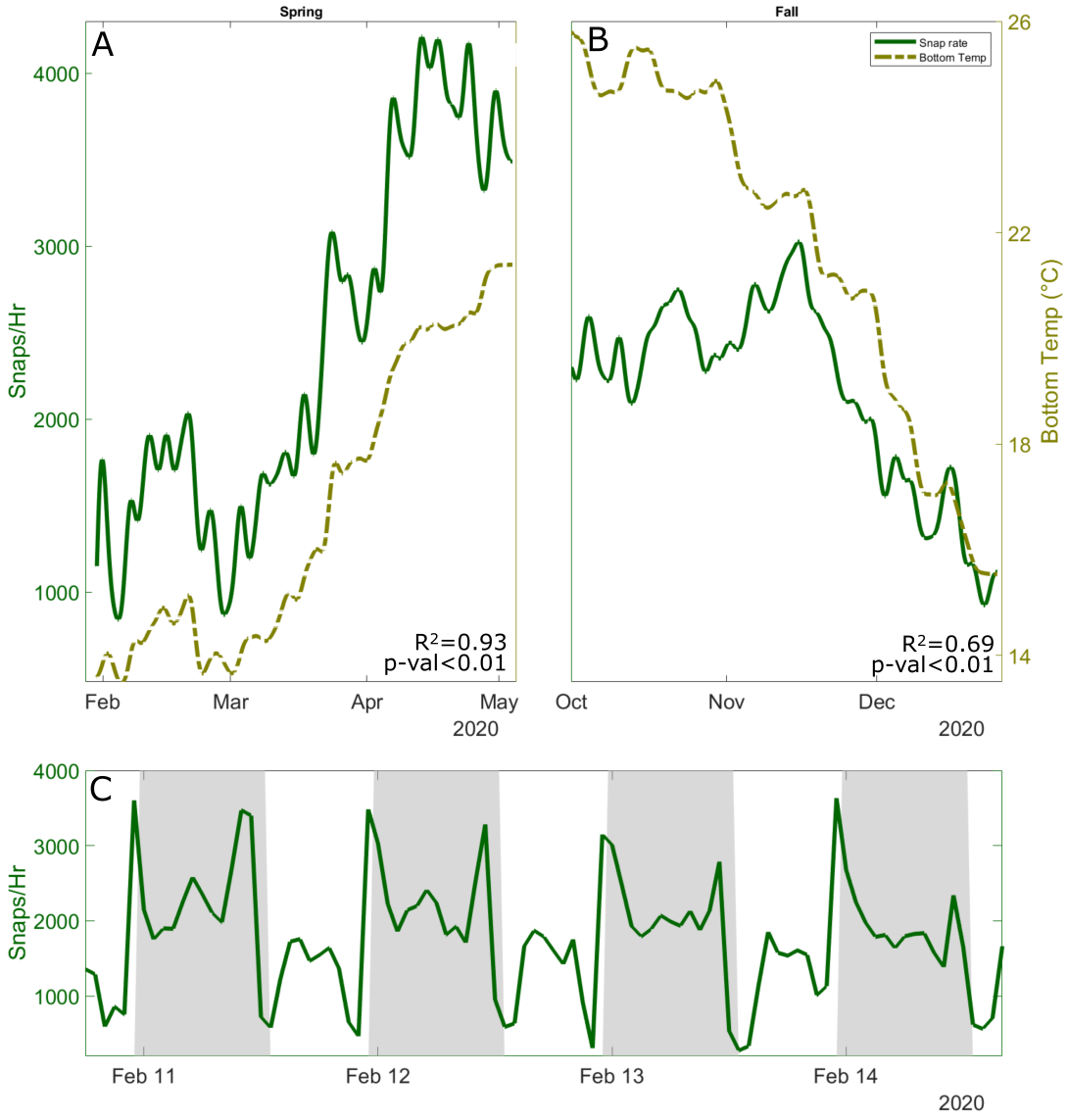


Figure 4.5: Temporal variability at SURTASSTN20. **A** Low pass-filtered bottom temperature (light green, dashed) and snapping shrimp snap rate (dark green, solid) in **A** spring and **B** fall. **C** Snap rate (green) are plotted with night time shaded to highlight crepuscular and diurnal behavior patterns. Times in UTC.

Table 4.3: Monthly mean averages for GRNMS. Bottom temperature and noise (50–90 kHz) were collected by transceiver at SURTASSTN20; wind speed (m/s) and SST (C°) are measured by NDBC Station 41008.

| **Month** | **Bottom Temp** (C°) | **Wind Speed** (m/s) | **Hourly Snaps** | **HF Noise** (mV) | **Avg. Detections** |
|---|---|---|---|---|---|
| Feb. 2020 | 14.0±0.5 | 6.45±3.03 | 1,479±736 | 655±49 | 2.7±4.2 |
| Mar. 2020 | 15.4±1.3 | 4.92±2.57 | 2,012±886 | 697±45 | 1.0±1.7 |
| Apr. 2020 | 19.8±0.9 | 5.64±2.64 | 3,664±897 | 746±30 | 0.4±1.1 |
| May 2020 | 22.4±0.9 | 4.97±2.26 | 3,604±1,105 | 760±25 | 0.3±0.9 |
| Oct. 2020 | 24.7±0.4 | 6.12±2.88 | 2,427±767 | 781±27 | 0.04±0.3 |
| Nov. 2020 | 21.8±1.0 | 6.54±2.77 | 2,503±783 | 762±30 | 0.05±0.4 |
| Dec. 2020 | 17.6±1.2 | 6.14±3.43 | 1,294±623 | 697±42 | 0.40±1.0 |

of 73% more snaps at sunrise versus midday. Snap rate rose sharply at night and dropped during the day, with a positive (but variable) snap rate increase from day to night, quantified monthly: February 2020, 53.8%; March, 25.1%; April, 13.1%; October, 46.8%; November, 20.2%; December, 59.6%) (Figures 4.5C, 4.6; Table 4.3). Snap rate and transmission detection had a statistically significant relationship (p-val $<$ 0.01), and there were far more detections when there were fewer snaps, 22.2% more detections at midday when the acoustic environment was more optimal versus sunset when average noise was highest (Figure 4.6).

There was no observed correlation between wind speed and snap rate (filtered p-value=0.07; raw p-value = 0.53), SBL and snap rate (filtered p-value=0.04; raw p-value = 0.27), or between significant wave height and snap rate (filtered p-value=0.37; raw p-value =0.51).

### 4.3.2 The Effect of Wind-Driven Attenuation on the Soundscape

During the spring deployment at SURTASSTN20 (2268 hours analyzed), wind speeds ranged between 0.2 - 14.3 m/s (average of 5.7 m/s); calculations of SBL with these values represent the full measured spectrum of SBL attenuation (0-15 dB). The relationship between HF noise and wind speed is statisti-

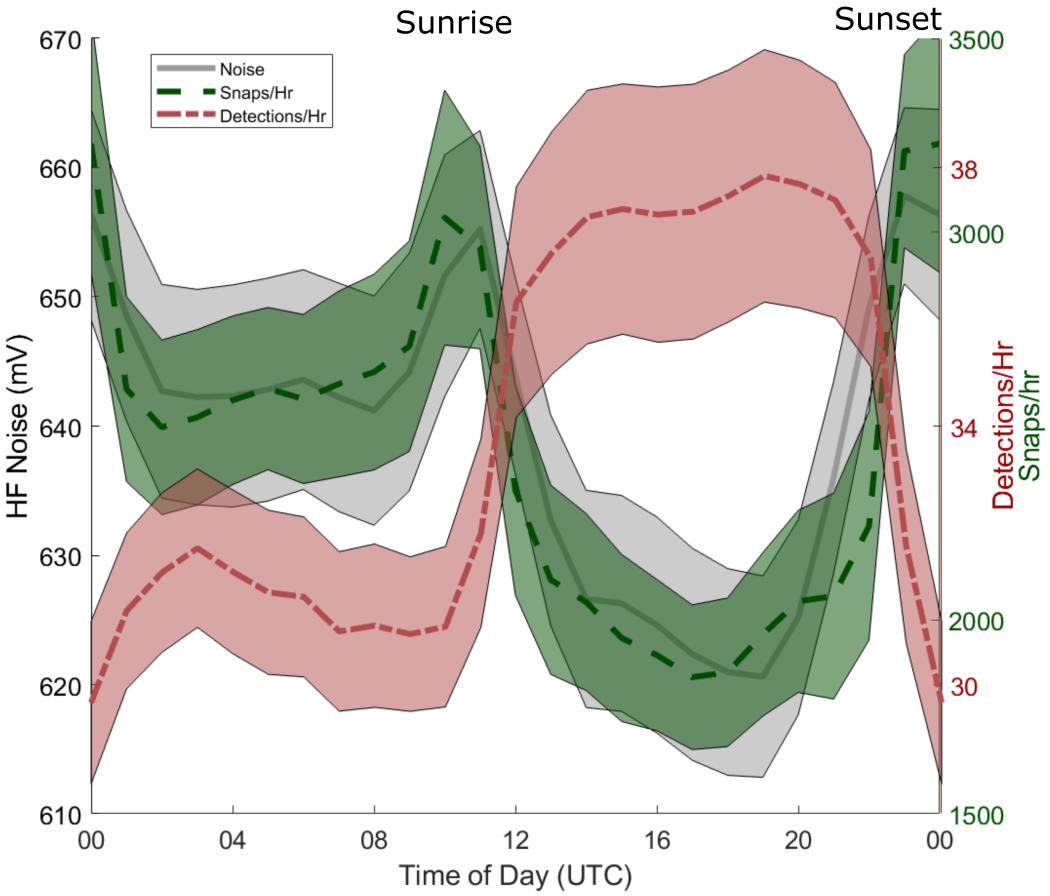


Figure 4.6: Canonical day averages: HF noise (gray), shrimp snap rate (green), and hourly detections (red). HF noise and transmission detections are from `SURTASS05IN`.

cally significant ($R^2$=0.30, p-val <0.01), as is the relationship between HF noise and SBL attenuation ($R^2$=0.32, p-val <0.01). Low-frequency (0.17-0.36 kHz) noise increased with wind speed, and stayed relatively constant after whitecaps and the surface bubble layer formed (Figure 4.7A.) In contrast, high-frequency noise (50-90 kHz) dropped quickly with wind speeds greater than 6 m/s; detection efficiency between `SURTASSTN20` and `STSNew1` rose sharply over this period as potential noise interference dropped ($R^2$=0.90, p-val <0.01) (Figure 4.7B). During specific wind events, the increase in low-frequency noise and decrease in high-frequency noise were both clear, even during nighttime when snapping shrimp were expected to be most active (Figure 4.8). Snapping shrimp behavior appeared unaffected by increased winds (Figures 4.9, 4.10), suggesting that the same amount of noise is created during periods of high winds but the surface attenuation at the bubble layer lowers HF noise interference (Figure 4.9).

A stronger pattern between attenuation and noise emerges when isolating high wind events (average length of 4.5 days): when short-term variability in winds is removed (40 hr cutoff), SBL is highly correlated with high-frequency noise ($R^2$=0.87-0.97, p-vals <0.01) (Table 4.4; Figures 4.10, 4.11). Figure 4.10 shows that snapping shrimp activity is responsible for the majority of HF noise creation (Figure 4.10A) and SBL and HF noise were inversely correlated (Figure 4.10C) but snapping shrimp activity changed very little with high winds (Figure 4.10E). After low pass filtering, wind events appeared as large changes in HF noise (Figure 4.10D), while snap rates were mostly unaffected (Figure 4.10B,F). Figure 4.11 isolates a single wind event to highlight these interactions, showing a strong statistical relationship between SBL and HF noise (4.11A,B), SBL and detection efficiency (4.11C,D), but no correlation between SBL and snapping behavior (4.11E,F).

Figure 4.12 highlights a case study: SBL attenuation is correlated with detection efficiency (p-val<0.01), very few (if any) transmissions are detected for days, but efficiency grows to 60-100% when winds are highest. Figure 4.12A,C includes AUV collected density data for added context. High SBL and the resulting decrease in HF noise were closely tied to sporadic spikes in detection efficiency while stratification appeared unrelated, and snapping behavior continued on crepuscular and diurnal patterns regardless of the wind events (Figure 4.12D; see Supplementary Figures 1 and 2).

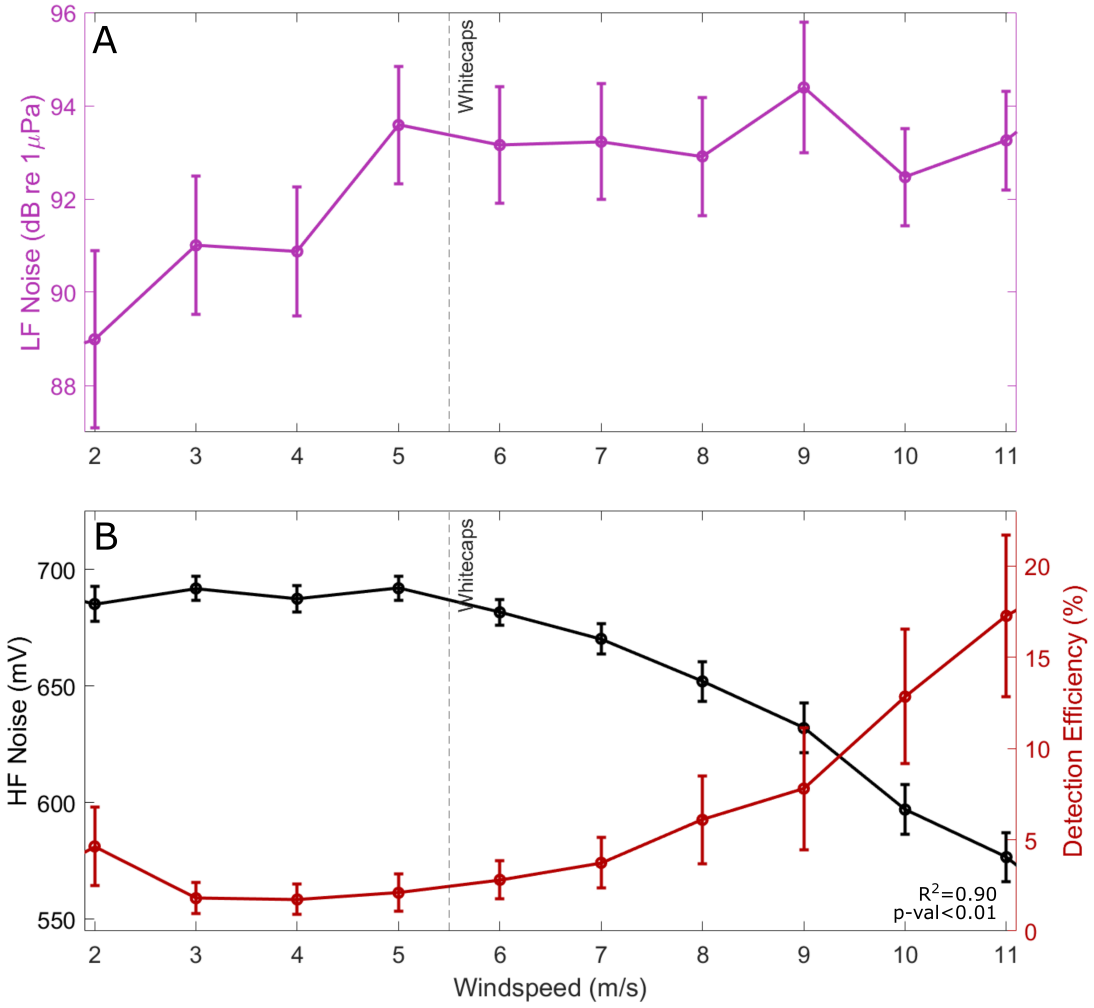


Figure 4.7: Binned averaging from the Spring deployment at SURTASSTN20. **A** Low-frequency (0.17-0.36 kHz) noise measured by SoundTrap 500 hydrophone; **B** High-frequency (50-90 kHz) noise measured by VR2Tx transceiver, and detection efficiency between SURTASSTN20 and STSNew1. Formation of whitecaps is noted vertically (–).

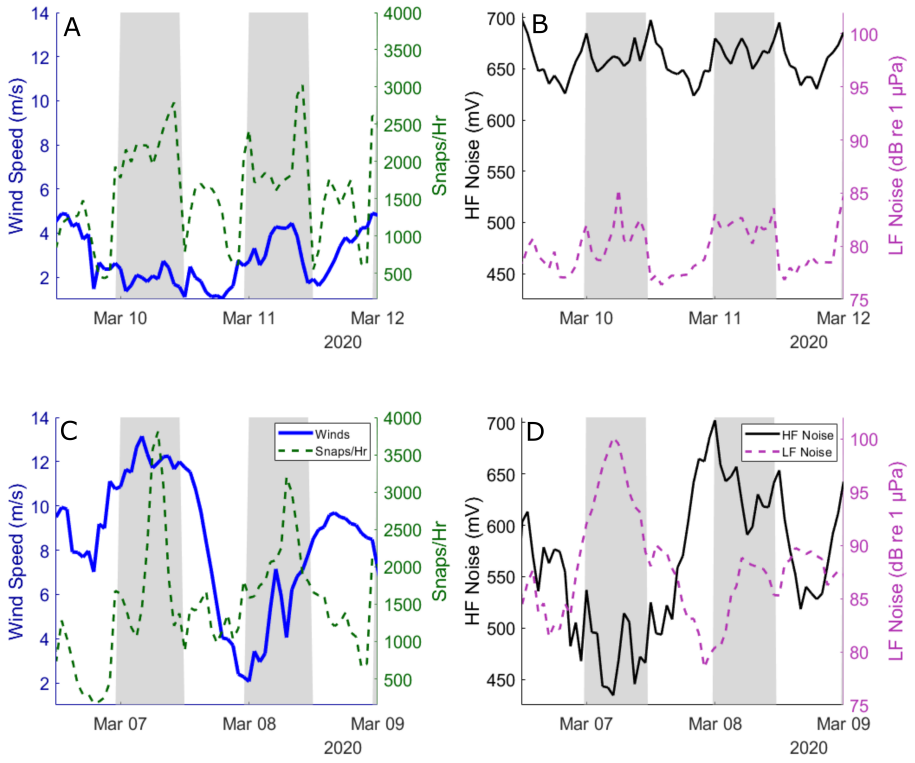


Figure 4.8: Comparison between **A,B** calm and **C,D** high wind scenarios. Low-frequency (0.17-0.36 kHz) noise is measured by SoundTrap 500 hydrophone; high-frequency (50-90 kHz) noise is measured by VR2Tx transceiver. Nighttime is shaded.

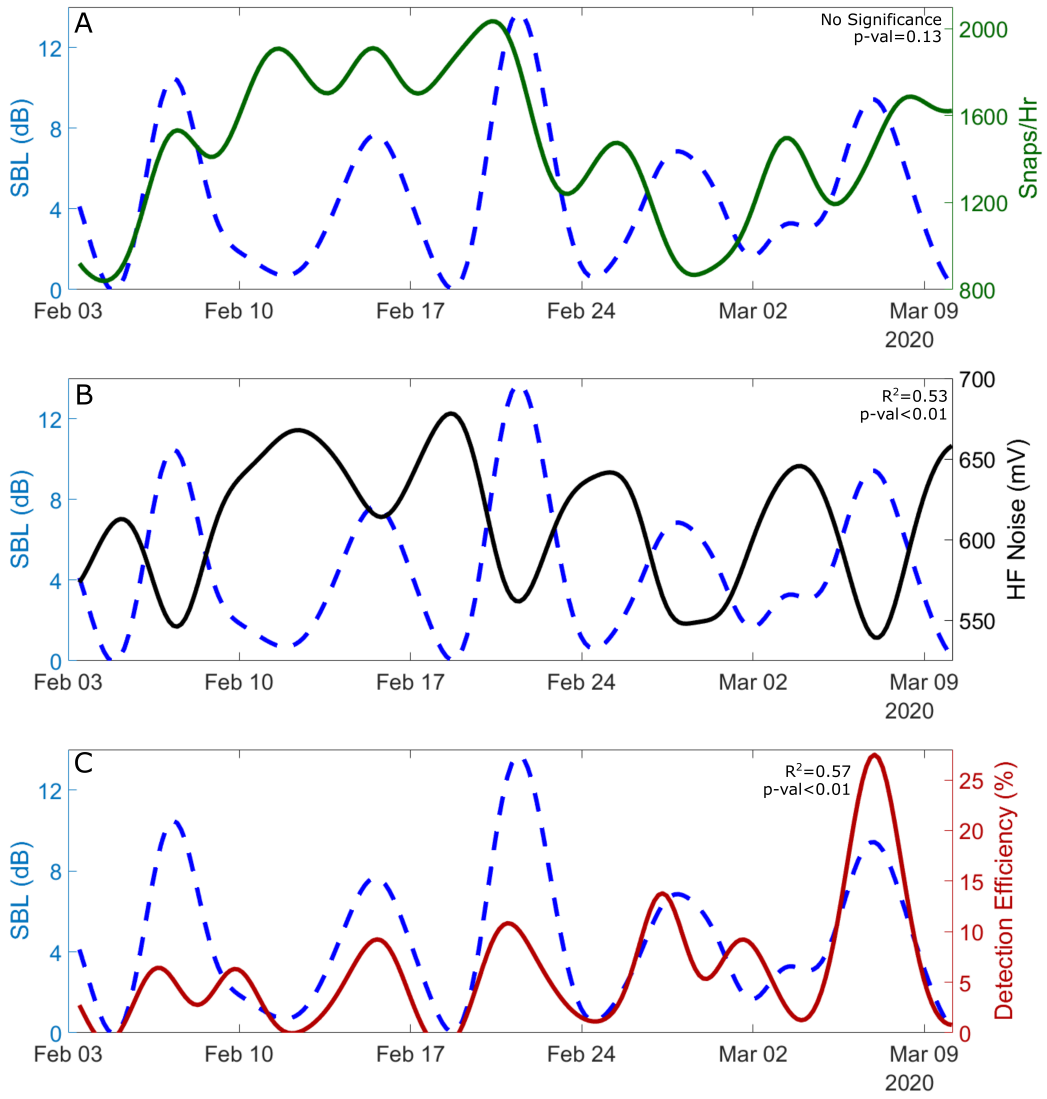


Figure 4.9: Data from SURTASSTN20 in Spring 2020. Calculated SBL (blue dashed) versus **A** snapping shrimp activity (green), **B** HF noise (black), and **C** detection efficiency (red) between SURTASSTN20 and STSNew1, 440m away.

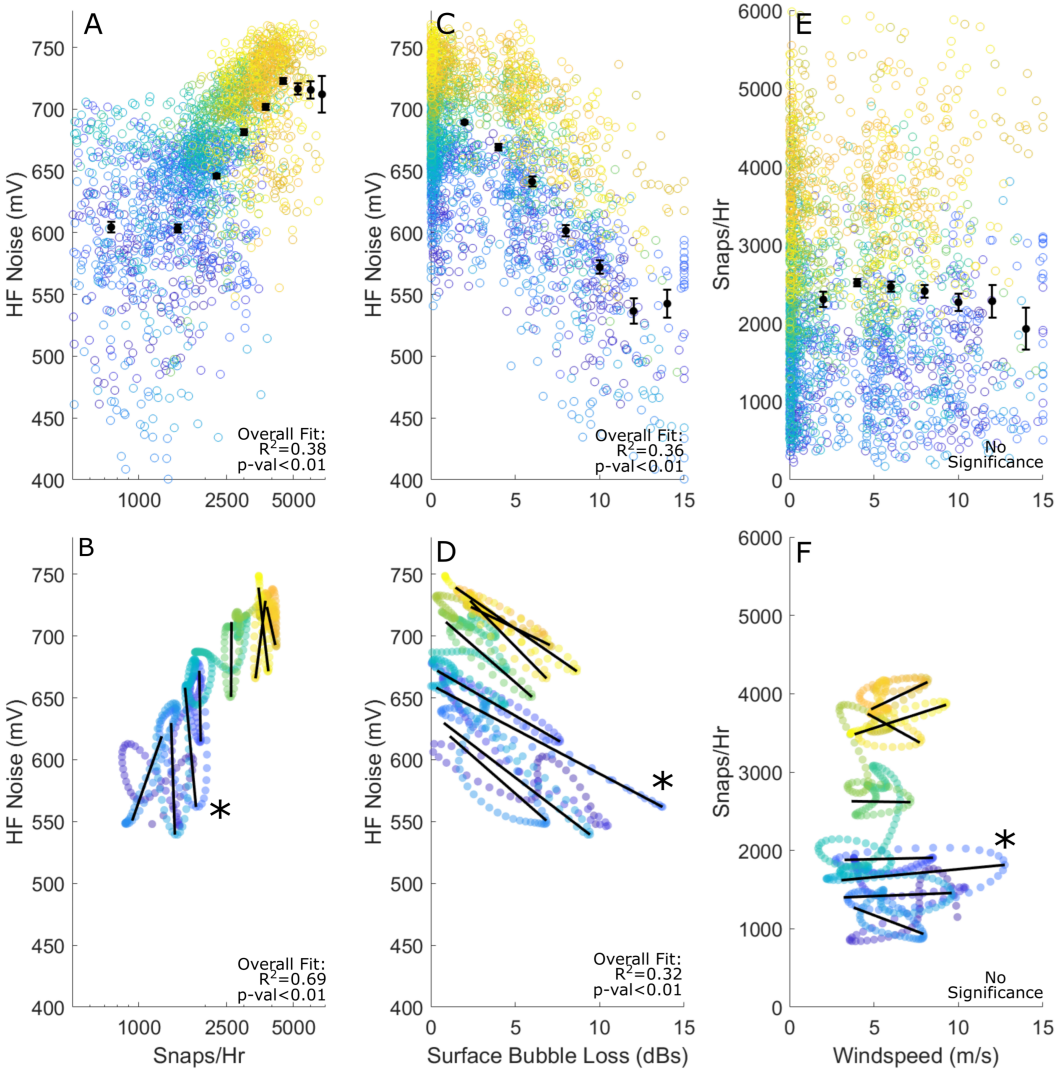


Figure 4.10: Hourly averages from spring (n=2268 hrs) of **A** raw and **B** filtered snap rate and HF noise (mV), on a log scale; **C** raw and **D** filtered SBL (dB) and HF noise (mV); **E** raw and **F** filtered snap rate and wind speed (m/s). Marker color represents the date range, January (blue) to May (yellow). Reported statistics include all plotted data; "no significance" represents p-values>0.01. Binned averages are shown over the raw data (black markers) in **A, C, E**, and significant wind events are denoted (black lines) in **B, D, F**. See Figure 4.11 for a closer examination of an isolated wind event (*).

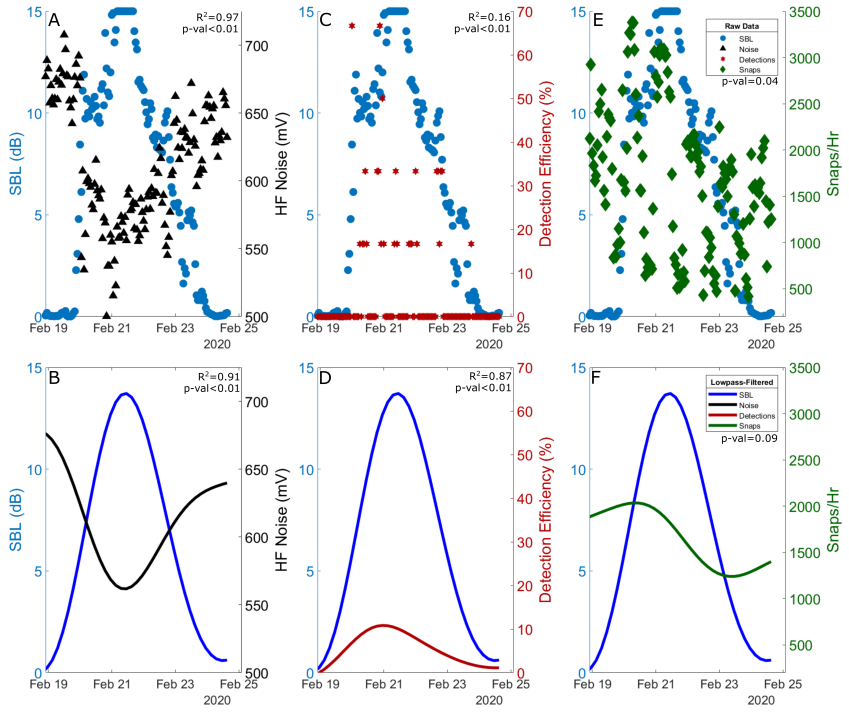


Figure 4.11: Example of a single wind event, Feb. 19th-25th 2020, with 0.3-14.3 m/s wind speed. **A** Raw and **B** low pass SBL (dB) and HF noise (mV), **C** raw and **D** low pass SBL (dB) and detections, and **E** raw and **F** low pass SBL (dB) and snap rate.

Table 4.4: Isolated wind events ranging from 3.75–6.75 days with noise (50–90 kHz) and detections measured at SURTASSTN20. Reported $R^2$ values are paired with $p < 0.01$; lack of a value (–) represents no statistical significance ($p > 0.01$).

| **Dates** | **Duration (hrs)** | **Wind Speed (m/s)** | **Snap Rate vs SBL** $R^2$ | **Noise vs SBL** $R^2$ | **Detections vs SBL** $R^2$ |
|---|---|---|---|---|---|
| Feb. 5–10 | 133 | 1.4–14.2 | – | 0.89 | – |
| Feb. 12–18 | 161 | 0.73–11.0 | – | 0.97 | 0.95 |
| Feb. 18–24 | 141 | 0.3–14.3 | – | 0.92 | 0.90 |
| Mar. 30–Apr. 3 | 109 | 0.8–12.8 | – | 0.92 | 0.76 |
| Apr. 14–18 | 90 | 2.31–10.8 | – | 0.91 | 0.98 |
| Apr. 24–28 | 93 | 0.2–11.9 | – | 0.91 | 0.47 |
| Apr. 28–May 2 | 93 | 1.3–11.3 | 0.80 | 0.91 | 0.52 |

## 4.4 Discussion

GRNMS is a considered a challenging acoustic environment for telemetry due to the magnitude of measured background noise, and the challenge in interpreting data collected there is further amplified due to large seasonal and diurnal swings in biotic background noise driven by snapping shrimp (Figures 4.5,4.6), which lead to noisier environments with fewer successful detections (Table 4.3). The results shown here demonstrate that wind events provide another layer of obfuscation in interpreting the meaning of acoustic telemetry detections, since the interfering noise of snapping shrimp can be attenuated by surface bubble layers generated during high wind events.

High winds had little to no effect on noise generation by snapping shrimp but resulted in increased high-frequency noise attenuation that appeared to improve acoustic telemetry detection rates. This analysis identifies a mechanism seen in previously observed patterns of increased detections during high wind

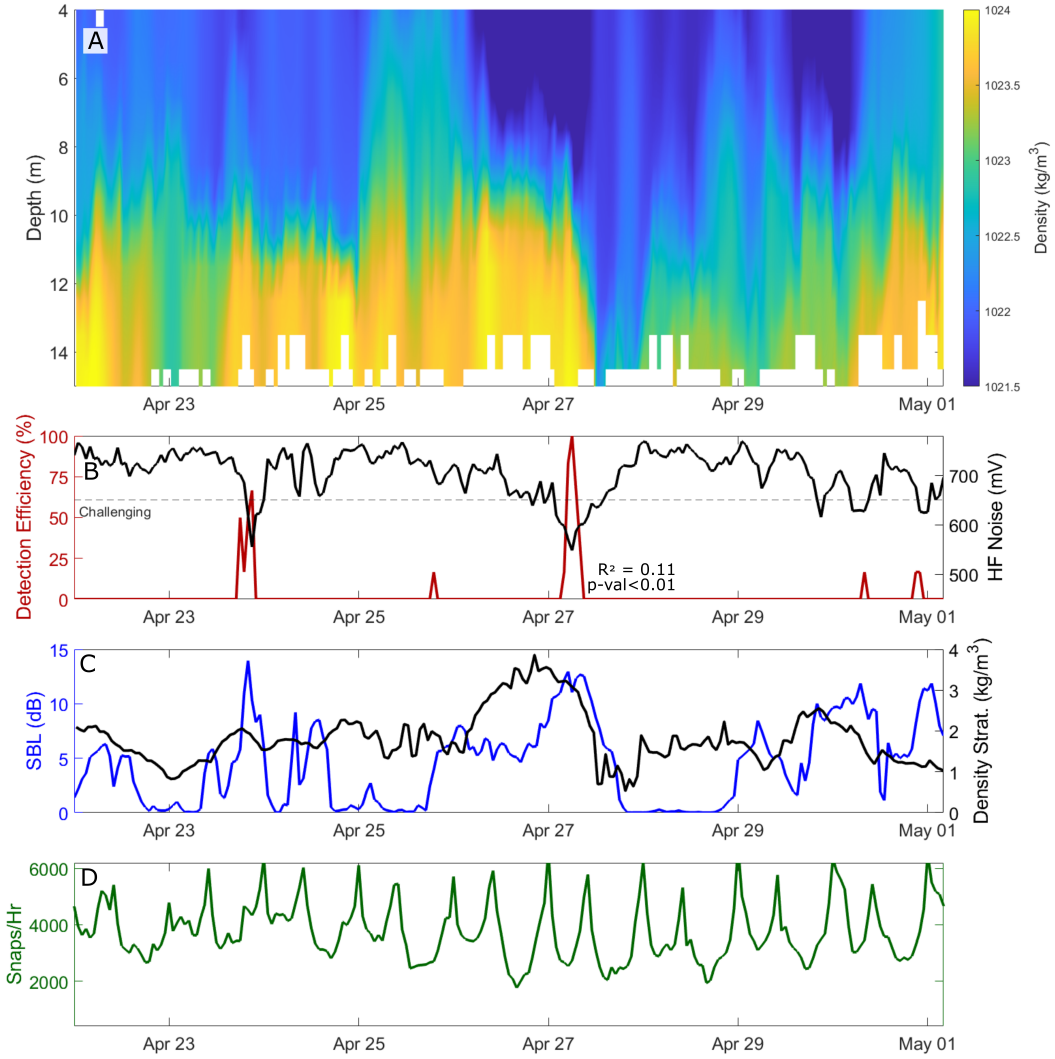


Figure 4.12: Data from SURTASSTN20, Apr. 22nd to May 4th, 2020. **A** Glider data measuring the water column's bulk density stratification (color); **B** HF noise (black) plotted against hourly detections (red) between SURTASSTN20 and STSNew1, with "challenging environment" (650 mV) denoted (–); **C** calculated SBL (blue) and AUV-measured density stratification (black); **D** Snap rate binned hourly (green). All times in UTC.

events (McQuarrie et al., 2023): a loss of high-frequency background noise, reducing interference (Figure 4.1B; Table 4.4). Most of the intermediate variability in measured HF noise was explained by the SBL in the form of sound lost at the air-sea interface (Figure 4.10; Table 4.4), while snap rate was largely unaffected by wind variability (Figure 4.11; Table 4.4).

Quantifying the snap rate with hydrophone data provides the means to determine how much noise was created (versus measured), with large spikes at dusk and dawn as shrimp behavior increases (Figure 4.5, 4.6). Warmer seasonal temperatures were correlated with increased reef activity and more noise created (Figure 4.5; Table 4.3). Previous studies that suggest that lower benthic activity may be responsible for the decreased noise levels during high wind events (Jung et al., 2012) may have incorrectly attributed measuring less noise to there being less noise created. An experiment showed that impulsive low-frequency sounds (0.05-0.6 kHz) played through an underwater speaker can affect snapping shrimp behavior (Spiga, 2022), but the low-frequency noise created by crashing waves ( 0.01-1.5 kHz) did not have the same effect. Our results suggests that noise derived from wind did not affect snap rates. There was no evidence in this study that less biotic noise is created during high winds, more noise was simply lost at the air-sea interface when attenuation is high and reflectance is low.

Calculating surface bubble loss thus appears to be an effective way to estimate noise lost at the air-sea interface and identifies the relationship between the biotic noise being created by snapping shrimp and the abiotic attenuation occurring at high frequencies due to SBL (Hildebrand et al., 2021; UWAPL, 1994). Noise attenuation also occurs coherently as a measure of distance traveled (Huang et al., 2017); this loss was not included in our calculations because we did not attempt to perfectly model sound loss but instead offer an effective explanation for the observed variability in the GRNMS soundscape. The significant correlation between measured noise and SBL was strong, especially when isolating events and removing daily and seasonal variability (Figures 4.11, 4.12; Table 4.4). Wind-driven changes in detection efficiency appeared primarily driven by increased attenuation (Figure 4.10; Table 4.4), pointing to the hypothesized abiotic relationship (Figure 4.1B) being the better explanation of the relationship between winds and detection efficiency at GRNMS. Detection efficiency in the 400-500 m range in a shallow, noisy environ-

ment like GRNMS is expected to be low (Edwards et al., 2019; McQuarrie et al., 2021), so an average of 20% efficiency during high winds (Figure 4.7) represents reasonable success averaged over Jan-May when accounting for the expected drops in efficiency due to elevated snapping activity at nighttime (Figure 4.6) and in warmer waters (Table 4.3).

In environments where HF background noise is lower and the environment is more optimal for telemetry, SBL may not have such a large effect on telemetry success, wind may even hinder the detection of high-frequency signals. SBL calculations do not consider proximity of the bubble layer to the instrumentation placement or bottom depth which may lead to reduced efficiency in shallower environments (Edwards et al., 2024; Reubens et al., 2019; Swadling et al., 2020) where the bubbles may hinder signal pathways or degrade signal strength (Chua et al., 2018). Previous research at Gray's Reef has observed that a VR2Tx transceiver in a more protected, sunken part of the reef (`FS17`) measured far less noise (McQuarrie et al., 2023). There was no hydrophone at this location, so we cannot determine if snap rate for that quieter reef area is different from the analysis above, but high-frequency noise from the telemetry transceiver was much lower than the challenging threshold (650 mV) and detections seemed unaffected by noise (McQuarrie et al., 2023). Anecdotally, detection rate decreased with higher winds over some periods in this quieter part of the reef, which may be explained by waves and bubbles hindering reflections at the air-sea interface. There was a significant slope in the bathymetry between `FS17` and the closest transmitter (`STSNew1`, 3.6 m difference) which may have limited the paths that transmissions could take between instruments. Transmissions between these moorings may reflect off the surface between transmitter and receiver while the surface is calm but attenuate and scatter when winds are high. When background noise is not the limiting factor, a decrease in possible sound pathways between instruments due to reduced surface reflectance may lower detection efficiency (McQuarrie et al., 2021), and measuring the depth of the surface bubble layer (Pelaez-Zapata et al., 2024) may explain reduced detection efficiency.

In-situ range testing may not accurately represent the effective distance of the technology if it does not correctly characterize the entire range of likely environmental conditions; users may be aware of the importance of testing transmitter and receiver pairings in their specific environment but may not fully account

for temporal variability (Payne et al., 2010). The findings presented here point to a novel relationship that, if understood, can be leveraged: wind events may attenuate interference from biotic background noise from snapping shrimp, thereby increasing the effectiveness of the telemetry in challenging acoustic environments. Snapping shrimp are found at a wide range of latitudes (Bohnenstiehl et al., 2016) and can affect acoustic telemetry; local sources of noise and attenuation need to be included as context when analyzing acoustic data collected in these environments. When measuring the amount of general high-frequency noise, users should consider whether noise interference is going to be important and what processes may help or hinder transmission detection.

## 4.5 Conclusion

Transmission power and frequency are delicate balances in complex marine environments. Transmissions with higher power can be reliably detected from farther away, but risk interfering with themselves and drain battery at a higher rate (Kessel et al., 2015). Tagging fish takes time and resources, lower power transmissions mean the tag will be effective for longer. Selecting the transmission frequency also contains trade-offs. If a transmission is closer to the 20 kHz limit, it attenuates slower but increases the sources of noise interference; if you increase transmission frequency (>100 kHz), there may be lower background noise interference but the signal attenuates quicker and will not travel as far. More experimentation should be done on how to best account for high noise environments.

The acoustic telemetry community is attempting to meet the challenge of background noise by developing sensors that better account for higher noise levels by increasing the filtering performed by the receivers, but the “high noise" environments in which these instruments have been tested have significantly less noise than the study site given here. For example, the Innovasea NexTrak R1 was tested in a 2024 technical report focused around testing in a “high noise environment" that appeared to exceed the 650 mV challenging threshold only a small percentage of the time (Pederson et al., 2024), whereas parts of GRNMS have average noise levels that exceed that threshold for almost the entirety of summer (>95% of hours) (Table

4.3). More work must be done on this type of environment to determine whether the noise levels are as detrimental (or in worst cases, prohibitive) when using newer technologies. Instrumentation with signal strength metrics, measuring not only if a detection occurred but the intensity of the signal, would help estimate transmission loss in these high noise environments and explain measured changes in effective detection range.

The next steps to understanding the acoustic environment's effect on signal transmission include modeling the signal propagation under different environmental conditions, connecting the decrease in background noise with the modeled bubble plume depth and limited reflectance/pathways between tag and receiver. Wind does not have a uniform effect on efficiency, and the next chapter will help elucidate why that is.

# Chapter 5

# Attenuation, For and Against: Modeling the Detection Efficiency of Acoustic Telemetry on a Coastal Reef

## 5.1 Introduction

Acoustic telemetry is a research tool to track animal behavior that involves tagging animals (fish, whales, sharks, etc.) with instruments that transmit high-frequency signals to be detected by receivers (Crossin et al., 2017). Unfortunately, a transmission is not always detected even when the tagged animal is close to the instrument, and the range at which a detection can reliably be detected changes both spatially (McQuarrie et al., 2021) and temporally (McQuarrie et al., 2025). When a detection occurs, users can identify the transmitting instrument but cannot be sure how far a signal traveled, so they are forced to estimate a detection range (Oliver et al., 2017; Payne et al., 2010). This variability in range makes timing and context essential for collecting and analyzing detection data in complex environments (Edwards et al.,

2019; McQuarrie et al., 2021, 2023).

Range-testing in the target environment is an important step when designing and implementing acoustic arrays to best account for variation in detection probability (Kessel et al., 2014). Changes in the physical environment affect how sound travels (Mackenzie, 1981), which may translate to predictable patterns in detection efficiency as boundaries and density gradients can refract and bend signals away from receivers (Cho et al., 2016; Edwards et al., 2019; McQuarrie et al., 2021). Tidal currents and seasonal runoff change stratification (strength of density gradients) on hourly, daily, and seasonal frequencies (Simpson et al., 1990; Weber & Blanton, 1980). These environmental changes can be magnified in shallow environments. Coastal reefs are shallow environments that are preferred habitats for many species of fish and invertebrates (ONMS, 2012). Acoustic telemetry is often used to understand animal movements on and off these reefs (Crossin et al., 2017). Coastal reefs are complex acoustic environments due to their shallow nature and abundance of marine life (Cagua et al., 2013; Stanley et al., 2021; Swadling et al., 2020); the full frequency spectrum is expected to include abiotic (winds, waves, motors) and biotic (fish, snapping shrimp, whales) sound sources (Delory et al., 2014). Background noise in the same frequency band as telemetry signals can interfere with detections and increase transmission loss (Goossens et al., 2022; McQuarrie et al., 2025; Payne et al., 2010; Reubens et al., 2019). Most acoustic telemetry instruments filter out some background noise and use the higher end (>50 kHz) of the frequency spectrum to avoid most noise interference (Innovasea, 2021), but background noise still plays an important role in detectability (Payne et al., 2010). For example, snapping shrimp are a species of benthic invertebrate that snap their claws to communicate and protect themselves. This snapping creates broadband noise (0.2-200 kHz; Bohnenstiehl et al., 2016; Stanley et al., 2021), that is capable of telemetry interference (Innovasea, 2021).

An effective way of measuring environmental interference is the signal to noise ratio (SNR). SNR is a measure of how strong a transmission is when compared to the background noise such as snapping shrimp snaps; signals that are stronger can be heard above the environmental din and can successfully be detected. Environments with high amounts of noise require a stronger signal for a detection to occur, preventing transmissions that have attenuated to near or below the background noise amplitude from being detected

(Innovasea, 2021). Telemetry users near coastal reefs where snapping shrimp are common should account for large diurnal, seasonal, and synoptic changes in background noise that may affect detection efficiency (McQuarrie et al., 2025).

Sound waves attenuate as they travel through a medium (Kuperman & Roux, 2007), with higher frequencies attenuating at a higher rate than lower frequencies (UWAPL, 1994). In addition to geometric scattering, surface bubbles created by breaking waves and strong winds provide an additional source of attenuation (referred to as surface bubble loss, SBL; McQuarrie et al., 2025). A reduction in background noise can make an environment more optimal for telemetry by lowering interference, but the same reduction attenuates the transmissions as well, lowering signal strength. This reduction makes the SNR a helpful comparison: as background noise decreases, the signal strength required for detection drops (Innovasea, 2021). Previous research has suggested that periods of high winds lead to dramatically different telemetry success outcomes: environments with high levels of background noise benefit from increased winds, but those same wind events decrease success in quieter areas (Section 3.4.3; McQuarrie et al., 2023). Figure 5.1 illustrates this juxtaposition well, comparing the detection efficiency in loud (`SURTASSTN20`) and quiet (`FS17`) environments during sustained wind events: the highest detection efficiency for transceivers in challenging acoustic environments occurred during periods with elevated winds, but the transceiver in an acoustically favorable, quieter environment had far fewer detections as the winds increased (McQuarrie et al., 2023). This work should help define the reason why this disparate effect exists. The hypothesis is that, while wind may lower signal strength through surface bubble loss (SBL) attenuation, the reduction in background noise results in higher detectability. Wind's attenuation seems to have simultaneous effects helping (lowering background noise) and hindering (lowering signal strength) telemetry efforts, and that "for and against" balance requires more scrutiny.

Previously, beam density analysis (BDA, McQuarrie et al., 2021) was developed to predict telemetry efficiency in shallow water columns: physical data (conductivity, temperature, depth) were measured or estimated, a soundspeed profile (SSP) was estimated as a measure of how sound travels through the water column (Mackenzie, 1981). Sound transmission was modeled through the estimated SSP, and the number

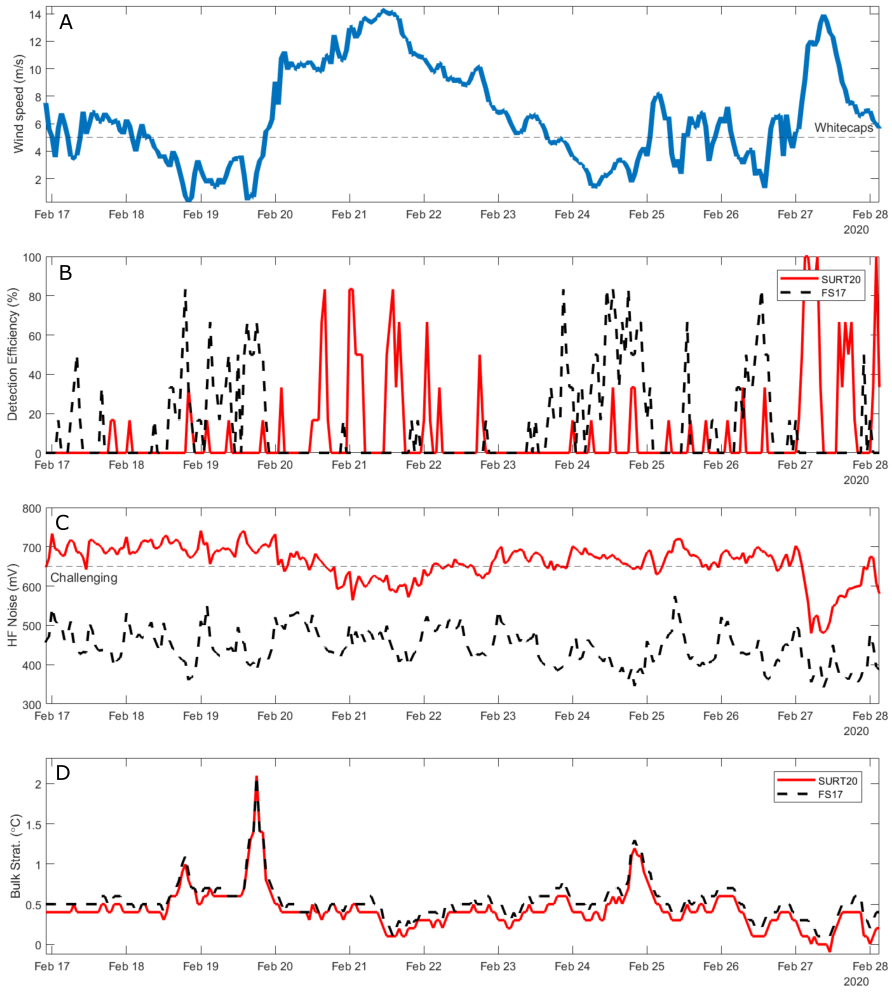


Figure 5.1: Comparison between `STSNew1` and the two nearest transceivers, `SURTASSTN20` and `FS17`: **A** wind speed (m/s) from NDBC Station 41008 buoy, with whitecap formation denoted (–); **B** hourly detection efficiency from `SURTASSTN20` (red) and `FS17` (black); **C** high-frequency (50-90 kHz) noise, with challenging environment denoted (–); **D** bulk thermal stratification between Station 41008 and the moored transceiver.

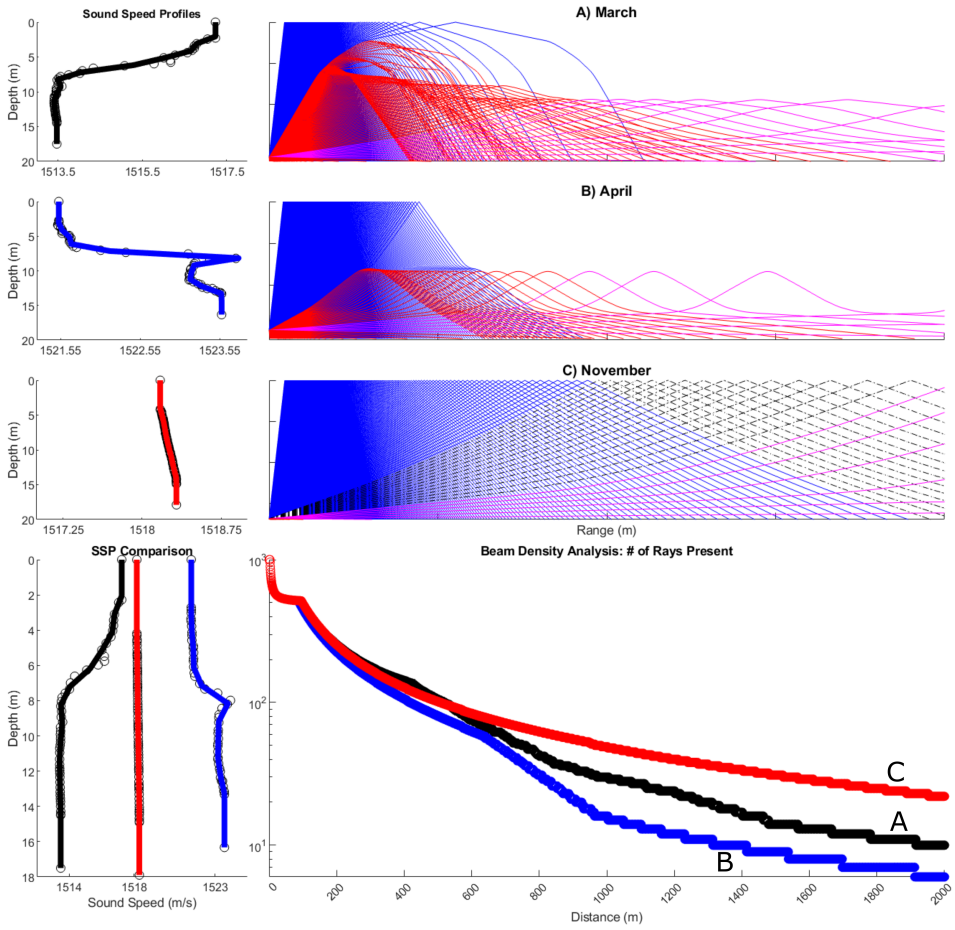


Figure 5.2: Adapted from McQuarrie et al., 2021: beam density analysis for 3 simplified scenarios from glider missions in 2019/2020.

of successful pathways between transmitter and receiver were quantified (McQuarrie et al., 2021). This method was effective for estimating detection range using an idealized environment, but did not account for variability in bathymetry, bottom composition, background noise, surface conditions, instrument location, or attenuation. This resulted in a good number of transmissions traveling and being "detected" (by BDA) 2,000 meters away in well-mixed conditions (Figure 5.2), when in reality the vast majority of those transmissions would have significantly weakened as they traveled, perhaps lowering the SNR to such a degree that the receiver fails to detect it. When a user or manufacturer reports an estimated detection range they are predicting (or have measured) sound attenuation and are attempting to account for how far a signal travels before it falls below a detection threshold. This is a metric that BDA could not capture. Without background noise or attenuation estimates, there was no way to know if the ray traced could possibly be detected.

In this chapter, additional parameters are incorporated into the acoustic model to more realistically model propagation, with the ultimate goal of predicting detection efficiency. Section 5.2.1 describes the environment, the AUV-based measurements that are used to characterize it, and the transceivers that were deployed. Section 5.2.2 builds the acoustic model that was used for this analysis. Section 5.3 analyzes the resulting metrics and Section 5.4 discusses the implications of these findings.

## 5.2 Methods

### 5.2.1 Experimental Array

Gray's Reef National Marine Sanctuary (GRNMS) is a shallow (20 m) live-bottom reef in the South Atlantic Bight (SAB), a broad section of the southeastern United States' continental shelf between the Florida Keys and Cape Hatteras, North Carolina. GRNMS is designated as a marine protected area (MPA) to protect fish and wildlife that prefer the structured environment provided by the reef (ONMS, 2012). Bathymetry at GRNMS was collected using side-scan SONAR by GRNMS staff, and surface data

was reported by National Data Buoy Center's (NDBC) Station 41008, a 3 m discus buoy that measures and reports significant wave height (m), sea surface temperature (°C, SST), and wind velocity (m/s, CW from 0° N).

Subsurface environmental data was collected by an autonomous underwater vehicle (AUV) platform (150 m Slocum glider) at GRNMS for three 4-5 week missions to measure physical properties of the water column and receive transmissions in 2019/2020. The glider comes to the surface to transmit data and localize itself every 4 hours. Salinity, temperature, and pressure data from the glider were used to calculate the sound speed profile (SSP). The AUV-collected SSPs were made monotonic for use as input for acoustic modeling, removing a small number of depth values that were not strictly decreasing during the glider's dive (often <0.1 m depth increase). An SSP from March 2020 was chosen to represent baseline stratification in spring: between 0 and 20 meters, there was a 4 m/s difference in the sound speed between the top and bottom of the water column, one of the most stratified profiles that was collected in the 2019/2020 missions. This was chosen to best test the expanded acoustic models against the past BDA findings from the previous study (Figure 5.2; McQuarrie et al., 2021).

Reported detection efficiencies were isolated to transmissions between moored VR2Tx transceivers at verified locations that were transmitting high-frequency signals to each other (6 per hour; 10 minute interval). Successful detections per hour between transceivers varied seasonally and daily (Figure 3.3), described in detail in Chapter 3.

This experiment focuses on three moorings due to their proximity to each other: `SURTASSTN20` (31°23'47" N 80°53'25" W), `STSNew1` (31°23'46" N, 80°53'45" W), and `FS17` (31°23'57" N, 80°54'08" W) (Figure 5.3; Table 5.1). `SURTASSTN20` was in a densely colonized portion of GRNMS and measured elevated high-frequency (50-90 kHz) background noise during the 2020 deployment, an average of 749+-54 mV, significantly higher than the average background noise at `STSNew1` (572 +- 107 mV) and `FS17` (532 +- 97 mV) (McQuarrie et al., 2025). For context, an environment with more than 650 mV is considered "challenging, with little to no detections" expected as defined by the manufacturer (Innovasea, 2021). `STSNew1` was the mooring closest to both `SURTASSTN20` (530 m) and `FS17` (668 m), and was the shallowest both in water

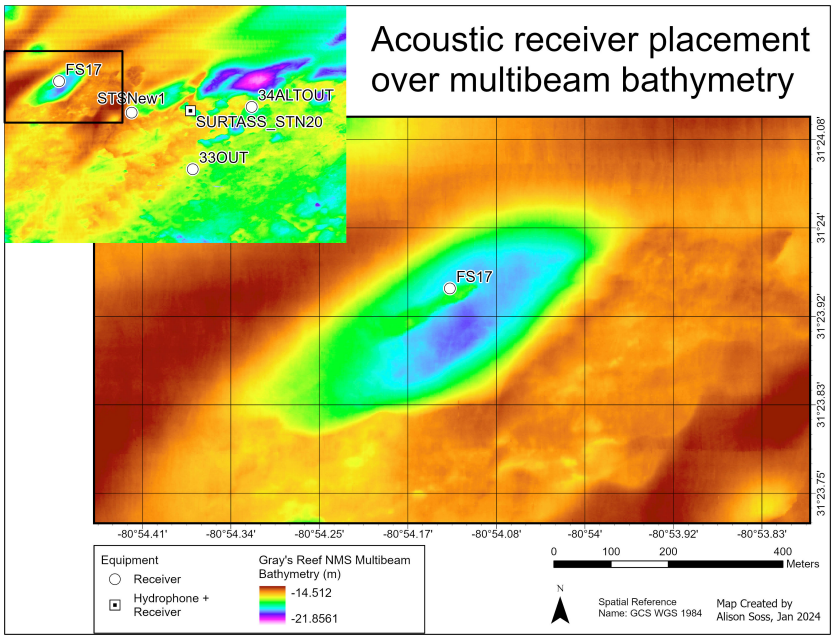


Figure 5.3: Bathymetry and transceiver placement in the Northwest region of the GRNMS acoustic array. Credit to Alison Soss with GRNMS Staff for the map and bathymetric data.

depth and instrument depth (Figure 5.4). All transceivers were assessed for collision analysis as described by Binder et al., 2016, and had a very low probability of collision interference (Chapter 3, Table 3.2).

Table 5.1: Chosen moorings at GRNMS.

| Mooring ID | Instr. Depth (m) | Bottom Depth (m) | Deployed | Last Heard |
|---|---|---|---|---|
| SURTASSTN20 | 16.8 | 20.4 | 2020-01-28 | 2020-12-18 |
| STSNew1 | 13.7 | 15.8 | 2019-11-26 | 2021-01-10 |
| FS17 | 17.8 | 19.4 | 2019-11-19 | 2021-07-31 |

### 5.2.2 Propagation Modeling

Acoustic propagation between instrument pairings was modeled in Bellhop, a research tool included in the Underwater Acoustic Propagation Modeling toolbox (Gul & Zaidi, 2017) that traces sound pathways through an environment. Combinations (n=10,000) of environmental variables were run using a Latin

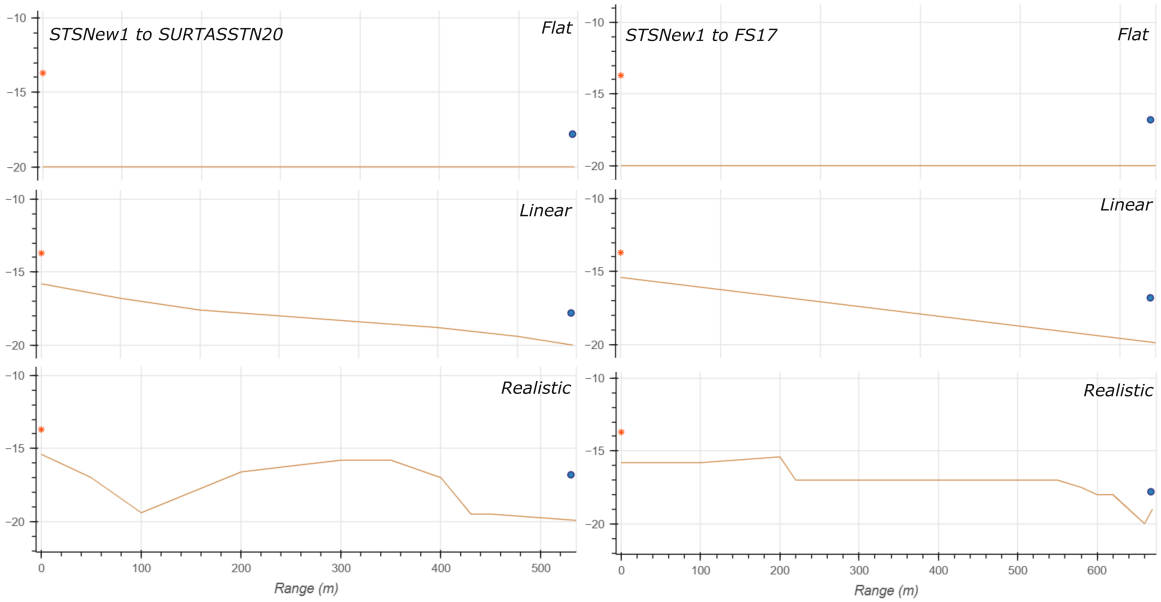


Figure 5.4: Modeled bathymetry between `STSNew1` and `SURTASSTN20`, and between `STSNew1` and `FS17`. Scenarios include the 6 shown as well as the inverse, `SURTASSTN20` and `FS17` to `STSNew1`.

Hypercube Sampling (LHS) to ensure near-random sample of scenarios and parameter values while avoiding patchiness (Stein, 1987). This sampling included combinations of sound speed profiles (strength and depth of density gradient, dominated by temp. due to relatively low variability in salinity), bathymetry, bottom absorption, surface conditions, SBL, and background noise were all varied as explained below. The model allowed the isolation of parameters that may not be physically possible (e.g., stormy days with no bubble layer, or a calm flat surface with high SBL).

Sound speed profiles (SSPs) used for the environment were estimated using a glider data profile to accurately represent the water column at Gray's Reef (Figure 5.5). Bulk change in the sound speed ($\Delta$SS), ranging from 0 (fully mixed) to 10 m/s (extremely stratified), was used to quantify stratification strength, with the 10 m/s maximum representing an approx. thermal gradient of 5°C. To assess the role of bathymetry in detectability, the sea floor is modeled as flat, a steady linear slope between instruments, or a realistic complex bottom using GRNMS data (Figure 5.4). For clarity, the transmission scenarios were renamed:

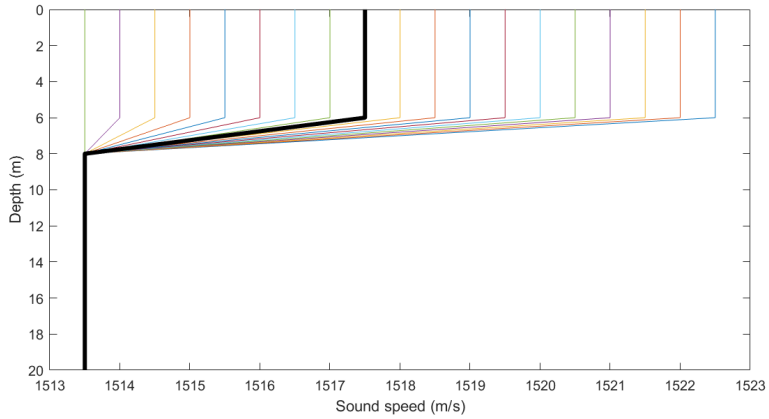


Figure 5.5: The range of sound speed profiles for modeling purposes, with baseline stratification (adapted from a March 2020 profile) bolded.

FS17 transmitting to STSNew1 as "A", STSNew1 to FS17 as "B". STSNew1 to SURTASSTN20 as "C", and SURTASSTN20 to STSNew1 as "D", with all having flat, linear, and realistic bathymetry scenarios. Three surface conditions were calculated using data from the nearby NDBC buoy but with idealized wave heights and periods: calm (flat surface), windy (1.2 m waves), and stormy (2 m waves) conditions (Table 5.2). Bottom absorption varied between 0 and 6 dB/$\lambda$ (decibel loss per wavelength) to account for differences between structured and sandy bottoms (Jackson & Richardson, 2007). The unit of bottom absorption includes the wavelength of the sound being attenuated, which results in sounds attenuating faster as frequency increases (UWAPL, 1994).

Modeled sound frequency is set to 69 kHz, the frequency used for acoustic telemetry transmissions. A full formation of 1,000 rays was traced between -60°and 60°, constraining the fan to +/- 60°to focus on forward propagation and to limit computing power needed. Rays traced through the environment were quantified and analyzed to measure the number of arriving rays and the amplitude (strength). The arrival strength (dB) reported is the amplitude expected from a low-power (142 dB) transmission at 69 kHz traveling through the modeled environment. Bellhop calculates expected coherent attenuation as a function of distance. To properly capture the effect of SBL, a new software module was created and added

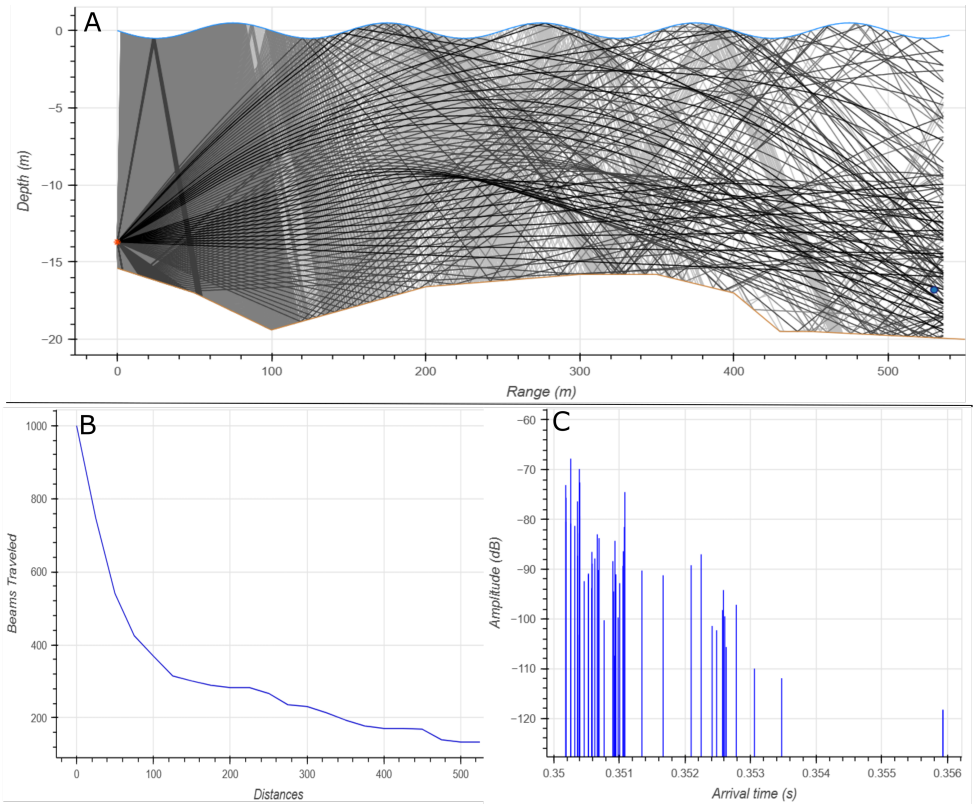


Figure 5.6: An example of the modeling process: **A** 1000 69 kHz rays are traced from `STSNew1` to `SURTASSTN20` with realistic bathymetry (scenario: C.real); **B** the number of paths reaching each distance are quantified as "beam density analysis" (McQuarrie et al., 2021); **C** attenuation is reported for each arriving beam, before originating signal power is added.

to the Bellhop workflow to calculate the attenuation described in McQuarrie et al., 2025, adapted from UWAPL, 1994. Each time a sound pathway interacts with the air-sea interface, SBL injects further attenuation, capped at 15 dB due to a previously observed insulating effect (UWAPL, 1994). This novel module combines the physical modeling strength of Bellhop with a complex surface phenomenon, effectively converting a reflective sea surface to a source of significant transmission loss.

Background noise was represented as the detection threshold, where signals below a defined noise level would be masked and/or interfered with. A range of thresholds from 30-75 dB was chosen to represent the realistic range of noise interference. All modeled rays were compared to this threshold: signals arriving

Table 5.2: Example of realistic conditions.

| Scenario | Description | Wave Amplitude (m) | Wind Speed (m/s) | Surface Bubble Loss (dB) |
|---|---|---|---|---|
| Calm | Reflective | 0.0 | 0 | 0.00 |
| Windy | Low attenuation | 1.5 | 6 | 4.42 |
| Stormy | High attenuation | 3.0 | 12 | 13.12 |

with a signal strength above the threshold had an estimated SNR greater than 1 and were defined as detectable. This distinction was applied after the propagation modeling was complete because transmission strength was added to Bellhop's outputs, then SBL attenuation was applied, and finally detectability was assessed. It is important to note that the detection threshold (SNR) itself is not changing, but a change in the level of background noise will shift the signal strength required for detection.

### 5.2.3 Statistical Analysis

A generalized additive model (GAM) was developed using the R package mgcv (v 1.9-1, Wood, 2024) to analyze the results of the acoustic models. GAMs can account for both linear and nonlinear relationships between predictors (environmental variables) and responses (signal strength, detectable pathways). All models initially used a Poisson error structure, chosen to handle the count-based data. However, model diagnostics indicated overdispersion (ratio of residual deviance to residual degrees of freedom), indicating that the variance far exceeded the mean. This phenomenon is common in data with excess zeros and temporal clustering, and was addressed by adopting a quasi-likelihood approach by adjusting the standard error but still preserving the model structure (Zuur et al., 2009).

Continuous predictors such as stratification strength, SBL, detection thresholds, and bottom absorption were smoothed using penalized regression splines to allow for sufficient flexibility (denoted with "s(...)" in formula), and used generalized cross-validation (GCV) to avoid underfitting or overfitting. Model adequacy and fit were tested using gam.check() diagnostics, which evaluated basis dimension sufficiency

(k-index) and residuals, as outlined in Wood, 2024 using R package mgcv.

## 5.3 Results

This section evaluates the outputs from the Bellhop acoustic model, followed by an analysis of the GAM outputs as a representation of all possible environmental conditions. The focus is first on the raw outputs from the propagation models, reporting the signal strength arriving at a receiver through a variety of environments and defining each signal as detectable or not detectable based on simulated background noise. The GAM outputs are then analyzed to explore detectability between transceivers and weigh the effects of parameters on that detectability metric.

### 5.3.1 Propagation Model Outputs

Rays were traced through 10,000 semi-random environments. There were more detectable rays that traveled the shorter distance between C and D (including station `SURTASSTN20`), as opposed to A and B (including station `FS17`; mean range: 29.1-34.5 vs 16.6-25.3 rays), but variance is very high as expected since these experiments include seasonal environmental variation which has been shown to be significant (McQuarrie et al., 2023). Figure 5.7 highlights the effect of SBL on both arriving signal strength and detectable pathways. A simple linear regression revealed the effects of SBL on both strength and detectability were significant (p-vals$<$0.001), with signal strength declining linearly, while detectability exhibited a more complex relationship. Detection threshold, which increases with background noise, emerged as the strongest predictor of detectability (p-val$<$0.01), with higher thresholds corresponding to markedly fewer detectable pathways.

An experiment was run using realistic wind-driven conditions for the low- and a high-noise environments representing the A-B and C-D pairs, respectively, in which SBL attenuation and surface waves

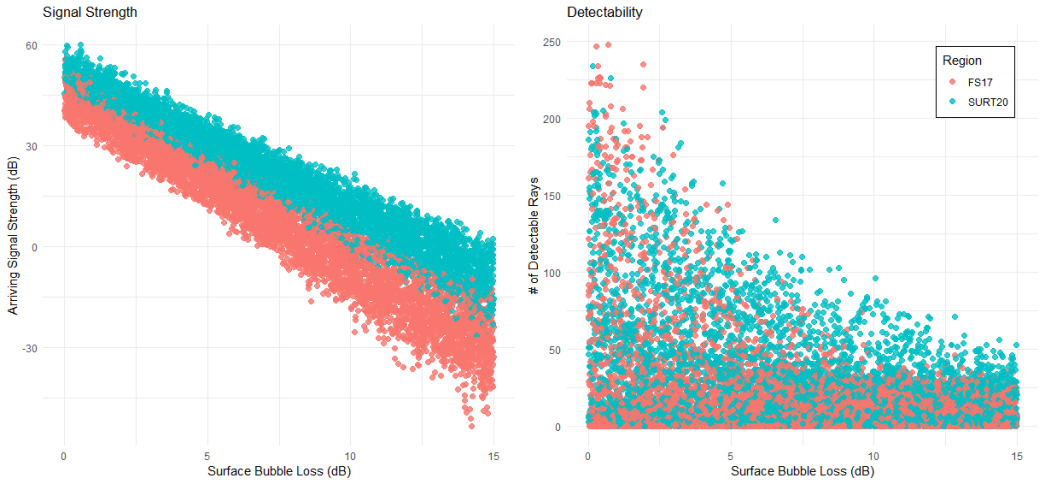


Figure 5.7: Raw model outputs plotting signal strength (dB) and detectable rays versus surface bubble loss (SBL, dB), separated by scenario.

increased with wind (Table 5.2). In a low-noise environment the background noise (and therefore the detection threshold) is considered static, while in areas with high noise the background noise change (and with it, the signal strength required for detection). There were fewer detectable rays (-32%) in the low-noise environment when wind increased (forming waves and increasing SBL attenuation), but there was a significant increase (210%) in detectable pathways in the high-noise environment for the same conditions (Figure 5.8). Signal strength alone does not fully explain the variation in detectability, and there appeared to be complex interactions between the environmental parameters that simple BDA pathways did not explain. The GAM addressed these interactions directly.

### 5.3.2 Generalized Additive Model Analysis

GAMs were used to analyze the sound propagation model outputs. An initial GAM was created, using a log link function with a quasi-Poisson distribution, to evaluate the contribution of environmental

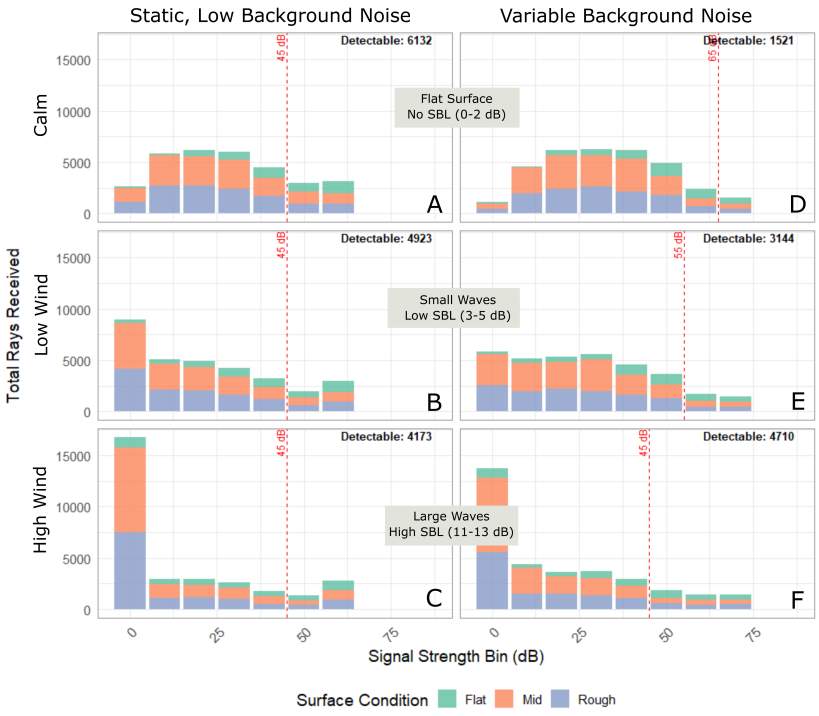


Figure 5.8: Binned arrival signal strength (dB) in comparable acoustic environments. **A**-**C** A constant low noise environment and **D**-**F** a dynamic noise environment, starting loud and dropping to quiet with SBL. The calm (0 m/s winds) category included a flat surface with no SBL; low wind (6 m/s), low waves (1.2 m waves) with moderate SBL; high wind (12 m/s), larger waves (2 m) with high SBL.

predictors as:

$$\text{Detectable} \sim \text{Scenario} + \text{Surface Waves} + s(\text{Stratification}) + s(\text{SBL, k = 12}) + s(\text{Detection Threshold, k = 28}) + s(\text{Bottom Absorption}) + s(\text{Gradient Depth, k = 11})$$

This initial global model accounted for 89.6% of the deviance ($R^2$=0.88). The smoothed, continuous variables (SBL, detection threshold, stratification strength, stratification depth, and bottom absorption) were all significant (p-val<0.001; Table 5.3), with detection threshold being the strongest predictor (Figure 5.9). Both parametric coefficients (bathymetry scenarios and surface conditions) were also significant (p-val<0.001).

Table 5.3: Initial GAM testing.

| Term | edf | F | p-value | Significance |
|---|---|---|---|---|
| Stratification Strength | 2.19 | 193.87 | 0.0002 | ** |
| Surface Bubble Loss (SBL) | 5.39 | 3497.11 | <0.0001 | *** |
| Detection Threshold | 16.11 | 1990.63 | <0.0001 | *** |
| Bottom Absorption | 2.34 | 193.87 | <0.0001 | *** |
| Gradient Depth | 8.06 | 41.43 | <0.0001 | *** |

The final version of the GAM separated the two instrument pathways, A & B (the quieter `FS17` mooring) and C & D (the louder `SURTASSTN20` mooring). Scenarios and surface conditions were subsequently combined as an interaction term to capture their combined effect on detectability, as well as combining stratification strength and gradient depth to more accurately depict their effect. These revisions resulted in a new model defined as:

$$\text{Detectable} \sim \text{Scenario} * \text{Surface Waves} + s(\text{Bottom\_Absorption}) + s(\text{Det.\_Threshold}) + te(\text{Stratification, Gradient Depth}) + te(\text{Det.\_Threshold, SBL})$$

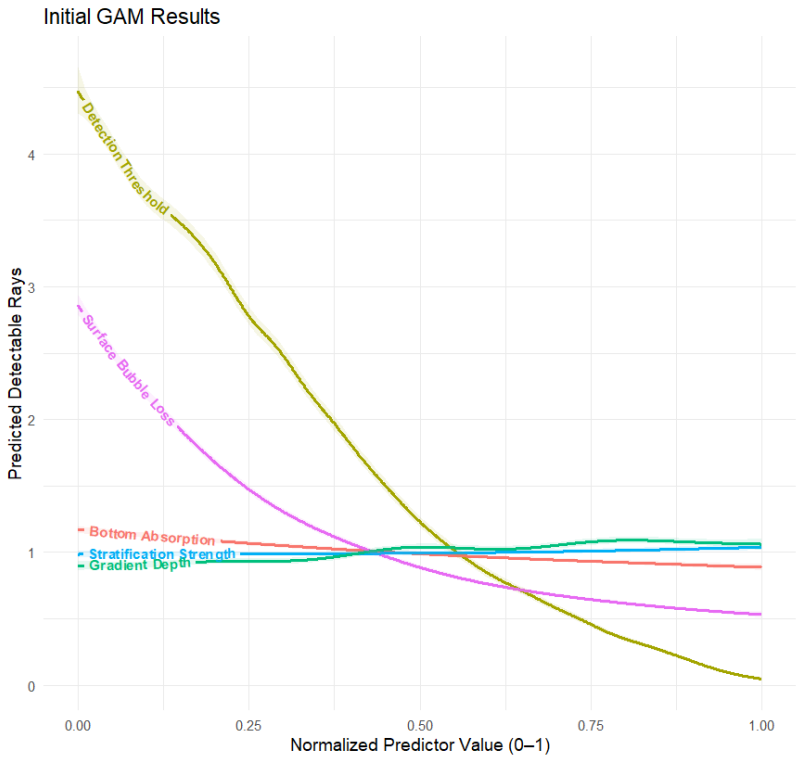


Figure 5.9: Results from the initial GAM, the detectable pathways attributed to each of the smoothed continuous predictors. All predictors were significant (p-val<0.001). Smoothing was done through thin plate regression splines (TPRS) through R package mgcv.

Both the A & B and C & D versions of the model explained more than 90% of the observed variance (adj. $R^2$=0.914 and 0.947 respectively). Increasing bottom absorption, and detection threshold reduced detectability in both models, with detection threshold having the strongest effect. The interaction between SBL and detection threshold (background noise levels) was significant (p-val<0.001) for both models (Table 5.4), but SBL alone became insignificant (p-vals=0.794, 0.0001) compared to the previous GAM, highlighting the complex interaction between SBL's attenuation and background noise (Figure 5.10). Between the two models, the most optimal environment is the low-noise environment with low SBL, a quiet scenario with no winds. Conversely, scenarios A&B and C&D had differing regions of low detectability: `FS17's` minimum was in low-noise, high wind (SBL) scenarios (Figure 5.10A), while `SURT20's` was high-noise, low wind(Figure 5.10B). The average amounts of background noise are highlighted in Figure 5.10A,B, pointing to a large difference in the typical acoustic environment between the two moorings.
The interaction effect between gradient depth and sound speed stratification strength was also stronger than the independent terms alone, since both terms affected refraction and ray tracing. Perhaps less intuitively, both models showed highest detectability in the strongest, deepest stratification scenarios (Figure 5.10C,D), but that level of gradient was not observed during the 2019/2020 glider missions (maximum of 4.8 m/s, Figure 5.10C,D). The effect of stratification was found to be significant, but the magnitude of the effect was relatively low.

## 5.4 Discussion

Modeling sound propagation through complex environments allowed for the isolation of environmental effects on detectability, including those effects that occur simultaneously with high winds. More detectable pathways exist in low-noise environments with low wind, and more in high-noise environments during high-wind conditions (Figure 5.8), echoing the measured response at Gray's Reef from March 2020 (Figure 5.1).
Previous models that relied solely on the number of pathways traveling between transmitter and receiver

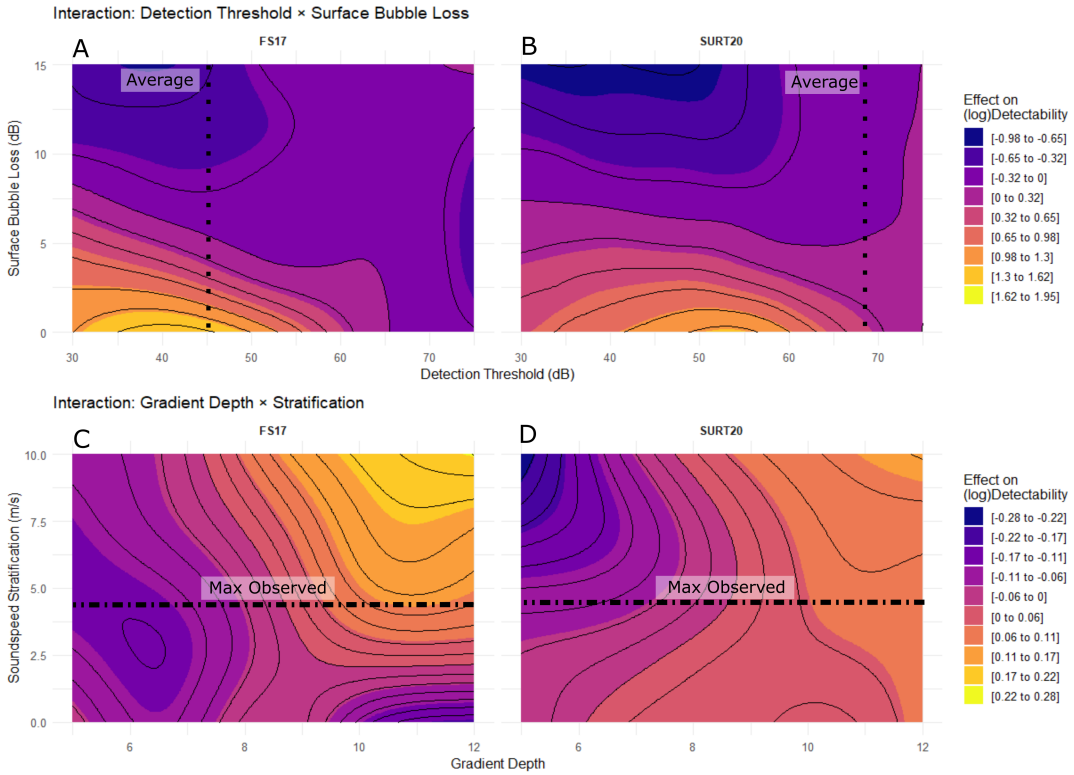


Figure 5.10: Isolation of the tensor interactions, separated by scenario, between **A,B** detection threshold and SBL with a line representing the average high-frequency noise levels in Spring 2020 at each station, and **C,D** stratification depth and strength, with color representing the partial effect on detectability and a line denoting the maximum observed sound speed stratification.

Table 5.4: Focused GAMs for Scenarios A&B and C&D, including tensor combinations to capture interactions between variables.

| Term | edf | F | p-value | Significance |
|---|---|---|---|---|
| **Scenarios A & B** | | | | |
| Bottom Absorption | 8.44 | 61.28 | <0.001 | *** |
| Surface Bubble Loss (SBL) | 2.11 | 0.34 | 0.794 | |
| Detection Threshold | 21.61 | 34.31 | <0.001 | *** |
| Detection Threshold × SBL | 15.40 | 126.47 | <0.001 | *** |
| Strat. Depth × Strat. Strength | 15.50 | 30.56 | <0.001 | *** |
| **Scenarios C & D** | | | | |
| Bottom Absorption | 1.73 | 168.71 | <0.001 | *** |
| Surface Bubble Loss (SBL) | 8.52 | 3.70 | 0.00014 | ** |
| Detection Threshold | 18.44 | 37.95 | <0.001 | *** |
| Detection Threshold × SBL | 30.95 | 30.77 | <0.001 | *** |
| Strat. Depth × Strat. Strength | 13.14 | 25.29 | <0.001 | *** |

(McQuarrie et al., 2021) were far less descriptive than the current experiment's findings; as expected, signal attenuation and background noise were both significant factors in whether or not an environment was optimal for telemetry (Figure 5.9). In environments like GRNMS that have characteristically high noise interference for much of the year (Figure 3.3; McQuarrie et al., 2023), anything that lowers noise (such as SBL) also lowers the detection threshold and allows more transmissions to be detected (Figures 5.8,5.10). This two-pronged attenuation (signal and background noise) also helps explain a difference in the effect that wind had on transceiver pairings: in quieter environments where noise is lower than the manufacturer's challenging threshold, the negative effect of SBL on signal strength resulted in fewer detections occurring, but SBL did not have a significant effect on the high-noise environment (Table 5.4).

When isolating so-called "partial effects" from the GAM, detectability appears complex. This complexity becomes apparent in Figure 5.11): high bottom absorption reduces detectability by weakening the signal strength, but in environments with low bottom absorption (such as reflective or hard substrates), stratification can marginally improve transmission detection. The bottom in these situations is more important as a path to the receiver instead of a source of signal attenuation. In realistic conditions, the

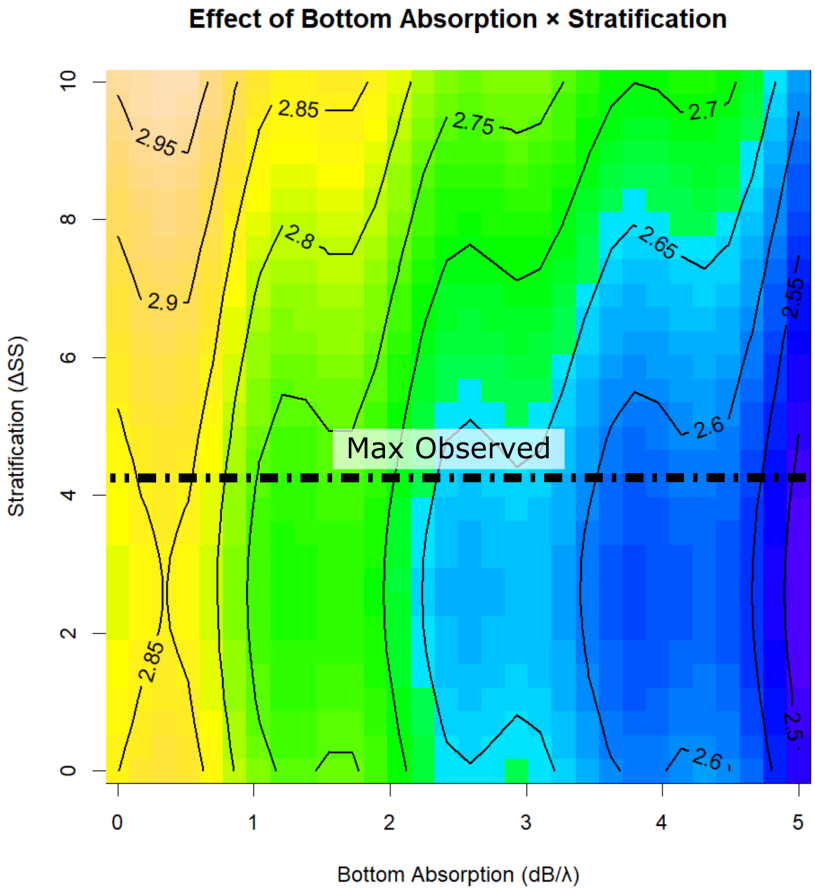


Figure 5.11: Comparison between the partial effect of sound speed stratification ($\Delta$m/s) and bottom absorption (dB/$\lambda$), with color and contours denoting predicted detectable pathways and a line denoting the maximum observed sound speed stratification.

bottom absorption has a stronger effect on detectability than stratification. Understanding these types of interactions allows telemetry users to better interpret their own findings.

Background noise levels have been shown to be one of the primary factors in detectability (Figures 3.104.6), and the sound propagation modeling results support this hypothesis (Figures 5.8,5.10; Table 5.4). The environment that a transmission propagates through controls whether a detection occurs. The surface bubble layer lowers signal strength while lowering background noise; in environments that already have a low detection threshold (<45 dB), wind may only lead to attenuated signals and lower detection

efficiency (Edwards et al., 2024). The exact detection threshold was not essential to this analysis and the SNR required for detection may be higher than 1, but the change in detectability is key to predicting detection efficiency. GRNMS is one of the most acoustically challenging environments where 50 dB of background noise is considered a "quiet" day, when in other environments that level of noise may be louder than average. Natural sources of high-frequency (>50 kHz) background noise are not as common as lower frequencies (0.2-20 kHz) sources (Delory et al., 2014), meaning that an environment that sounds noisy to the human ear or a low-frequency hydrophone may still be optimal for acoustic telemetry.

When working in environments with static detection thresholds users can set and plan for a certain level of background noise, but in areas with large amounts of benthic activity and interference users must account for the temporal swings in noise and therefore detectability. Snapping shrimp are widespread in shallow (<50 m) tropical and subtropical waters between the 35th parallels (Radford et al., 2010; Radford et al., 2008), so the background noise that hinders acoustic telemetry at GRNMS (McQuarrie et al., 2023, 2025) is not unique. The inclusion of background noise and SBL into the acoustic models is an essential step to understanding these environments.

The modeled experiment's input values were chosen from relatively large spectrum to test a wide range of environments, but many real experiments have a narrower range of expected values for bottom absorption, detection threshold, and to some degree stratification. These model results successfully explained an observed difference in detection efficiency in separate environments, and the same analysis techniques can be tuned for other environments of interest. Telemetry users can predict or measure their environmental conditions then run this same type of detectability analysis at different distances and depths, creating a locally-tuned model of detection probability as a function of range and leveraging the GAM presented here as a predictive tool for detectability.

## 5.5 Conclusion

The analysis completed in this experiment isolated the different acoustic effects of increasing wind, separating SBL, background noise reduction, and surface wave creation. Wind creates low-frequency noise and relatively little high-frequency noise (Figure 3.8), so wind does not increase high-frequency background noise. A recent paper (Radigan et al., 2025) using acoustic telemetry in shallow waters observed a negative relationship between detection efficiency and increasing winds, and attributed this relationship to wind-created noise interference. SBL can be considered a form of wind interference, but to assign direct causation to the wind-created noise as the reason for detection reduction may be overreaching. The juxtaposition between this work at GRNMS and Radigan et al., 2025's environment highlights the importance of this modeling and analysis. Even though a freshwater river is most likely a quieter environment, the users would benefit from the inclusion of SBL into their signal strength calculations.

Previous acoustic propagation modeling efforts at GRNMS (McQuarrie et al., 2021) prioritized rapid results over environmental realism or accuracy, leading to the use of highly simplified conditions. In contrast, this study incorporated detailed environmental parameters to improve the model, producing a detection efficiency predictor capable of handling a variety of local conditions rather than relying on a one-size-fits-all approach. The model's high fidelity, achieved through the incorporation of sound speed profiles, SBL, bottom absorption, surface waves, and realistic bathymetry improved its ability to mirror the physical environment, which ultimately contributes to greater predictive accuracy in estimating detection efficiency.

Collecting and understanding acoustic telemetry data requires knowledge of the environment. The propagation modeling completed in this chapter is effective at testing the wind-driven hypothesis, but the findings could be further expanded in 3-D to account for spatial differences in bottom types and horizontal stratification. The surface boundary layer: rather than using a simple attenuation value for each interaction with the surface, the depth of the bubble layer could affect how transmissions propagate (Pelaez-Zapata et al., 2024). Modeling that bubble layer would be computationally expensive but could

improve attenuation estimates. Further, representation of bottom attenuation can be improved in future models by accounting for realistic spatial variability, representing a heterogeneous reef bottom. For example, the absorption, reflection, and scattering of sound on a sandy bottom will differ significantly from that of a live-bottom structured reef. The proximity of the instruments to the bottom would be a key consideration in this case, and this model could help test that effect (Payne et al., 2010). Testing propagation in 3-dimensional space could also provide additional insights into where detections are likely to occur. Some preliminary tests of propagation through a horizontal stratification layer were completed, testing the effect of a coastal frontal zone (CFZ, Blanton et al., 1994), but the stratification seemed to have little effect on detection efficiency. More testing on a range-dependent SSP paired with a changing bathymetry would lead to a more complete understanding of the high-frequency soundscape.

# Chapter 6

# Conclusions

Binary detection data alone are not sufficient to understand if there are tags "in range", so adding environmental data as context is crucial to understanding telemetry outputs and how detection ranges change over space and time. This research can help acoustic telemetry users add context to past missions and effectively design arrays that fit their needs. The original motivation for this research was to task a fleet of robots to search an area within GRNMS for tagged fish; the Bellhop model was set up to run in real-time, using profile data to estimate the telemetry detection range to feed information to this fleet of gliders and robotic fish. The complexity of the detection efficiency was apparent while building the environment for that experiment, and the work presented here represents a significant step forward in understanding this complexity, as the environment as an acoustic medium is an important factor that can be accounted for in real-time if not largely predicted. There is uncertainty in acoustic telemetry, but this dissertation removes much of that uncertainty when working in high-noise coastal environments.

- In Chapter 3, background noise was identified as a primary factor in whether or not a detection occurs. Predictable nocturnal and seasonal patterns occurred and can be accounted for. High winds were paired with reduced noise and sharply increased detections across the reef. This chapter's findings allow users to temper their expectations when in environments with high background noise and account for the significant swings in signal to noise ratio.

Chapter 3 is a study of a complex but vitally important coastal habitat at Gray's Reef. Money is spent maintaining an acoustic telemetry array and fish-tagging efforts, and the collected data needs context. Previous research at GRNMS has focused around tidal and stratification effects on detection efficiency (Cho et al., 2016; Edwards et al., 2019), and though it was previously found that the tides affected detection efficiency (McQuarrie et al., 2023), background noise appeared to be the primary factor in whether or not a transmission was heard. On a daily scale, it was clear that detection efficiency and HF background noise (50-90 kHz) are inversely related year-round, with more noise interference occurring during crepuscular and night periods leading to less detections (Figure 3.4). If users are planning to use telemetry to study reef fidelity (daily coming and going) of tagged animals (Cagua et al., 2013; Pittman et al., 2014), it is very important to consider this variable detection probability. Seasonal changes from winter to summer resulted in warmer, noisier water columns and less detections (Figure 3.3), another reason to ensure background noise levels are quantified year round, profiling the acoustic environment for the entirety of the experiment. These findings allow users to temper their expectations when in environments with high background noise. Wind created large amounts of low-frequency (<20 kHz) noise while seeming to result in far less high-frequency (50-90 kHz) noise. This reduced noise clearly allowed more detections to occur (Figure 3.10), but the mechanism was not identified, the results were unclear whether the snapping shrimp were less active during high winds or if the increased surface attenuation was the only change that occurred.

- Chapter 4 explains a novel relationship identified in the previous chapter: high winds created a bubble layer that attenuated sound, reduced interference, and made the environment more optimal for acoustic telemetry efforts. Wind did not change snapping shrimp behavior, but it mitigated the expected noise interference and increased detectability.

Chapter 4 focused on that observed relationship between wind and noise, explaining the difference between the amount of high frequency noise created versus how much was measured. The calculated surface bubble loss accounted for the large swings in the high-frequency background noise, so even though snapping shrimp were heard throughout the wind event (Figure 4.10) the signal to noise ratio dropped

and more successful detections occurred (Figure 4.11). Reduced snapping shrimp noise during high wind events was previously observed (Jung et al., 2012), but they did not have moored hydrophone data so were unable to hear the consistent snapping throughout the high-wind events (Figure 4.12). Snapping shrimp are found in many biologically-important reefs (Bohnenstiehl et al., 2016; Stanley et al., 2021), and this work helps inform how to consider telemetry data when in proximity to these noisy invertebrates.

- The third research chapter, Chapter 5, builds the previous findings into a detectability model. Surface bubble loss and a detection threshold were added to Bellhop. These improvements and models are a useful tool; the air-sea interface is a very complex feature for acoustic signals and this work helps account for that dynamic boundary.

Chapter 5 combined knowledge from the previous chapters and modeled the environment to predict signal attenuation and detectability, isolating the different variables (bathymetry, noise, stratification, etc). Background noise was the strongest predictor of detection success (Figure 5.7). High-noise environments were found to be vastly different than low-noise environments (Figure 5.8), making one-to-one comparisons complicated. Wind has previously been shown to reduce detectability in low-noise environments (Edwards et al., 2024) and the improved models confirm that (Figure 5.10A), while also supporting the previous findings that wind dramatically increased transmission detection in noisy environments (Figure 5.10B), like most of Gray's Reef. These reasonable results explain the relationship between wind and detection efficiency, but the calculated SBL attenuation should be tested in different environments (UWAPL, 1994).

The GAM was initially created to examine detectability at GRNMS, a reef with high levels of background noise, but the outputs can be transferred to other environments. The effect of background noise as a threshold was highlighted in this work; that threshold could be held at a static, lower value in quieter environments. Levels of bottom absorption are also not expected to change rapidly and can be measured or estimated and held constant. SBL should still be considered an important factor if the environment is shallow (<30 m) or if the transmitter is close to the surface, so some type of surface data is useful. Given some basic knowledge of the environment, this same method (modeling sound propagation then creating

a GAM) can help identify what determines detectability in specific scenarios.

The surface bubble loss calculated in this work did not consider the surface bubble layer depth, or the make up of that layer. Moving forward, more insight into the structure of the SBL would be an interesting consideration. For example, using the modeling from Pelaez-Zapata et al., 2024, researchers could estimate the depth of the bubble plume rather than only calculating the expected attenuation (UWAPL, 1994). Modeling the plume would make the wind-driven bubble layer a factor in signal propagation, creating a barrier that limits pathways, in addition to being a source of attenuation. Especially in very shallow waters where the bubble layer may be a relatively large portion of the water column, the depth of this plume may have an important role in estimating detectability.

This research can be used to improve acoustic propagation models, plan future acoustic arrays, and contextualize past detection data. A mobile instrument like a glider could be an excellent tool for detection efficiency estimates as a mobile hydrophone platform. A glider spending time in different parts of the reef at different times of day/tidal cycle/year could measure hourly background noise. The data does not need to be large recordings; simple hourly averages with a water column profile would improve efficiency estimates. The noise may not be the same format as the signals but changes in relative noise levels can allow users to remotely estimate the detection threshold and SNR. Users should already know the approximate bathymetry and bottom type, but even without these variables the model would still improve detection efficiency estimates (Figure 5.9). This glider monitoring program would be especially useful when in tropical or subtropical waters that may contain snapping shrimp (Radford et al., 2008).

The first two research chapters identified, described, and explained novel relationships between detection efficiency and wind in loud and quiet environments, and the third chapter successfully models that mechanism. A follow-up experiment in a much quieter environment without snapping shrimp would be a fascinating challenge for the model because even in the "quiet" part of GRNMS, the level of background noise is considered moderate (650$>$ mV $>$325) by the manufacturer, very few hours are spent in "optimal" conditions ($<$ 325 mV). In quieter environments the SNR should be much higher and signals could be detected from farther away, this could mean that the detection threshold is relatively small, but attenua-

tion sources such as bottom absorption and SBL could have even larger effects as the effective detection range is lengthened. Deeper waters will not have the same levels of invertebrate-noise interference, and the signal's originating depth may affect the magnitude of SBL attenuation. The analysis tools created in the previous chapter can be used effectively in deeper environments with less emphasis on dynamic noise thresholds and more emphasis on the sound speed profile with depth, accounting for relatively large pressure differences.

This dissertation has presented a cohesive narrative: acoustic telemetry is a powerful tool for studying marine ecosystems, but its success depends on an understanding of the surrounding environment as a medium. While the first attempts at modeling detections were focused on simple sound speed profiles and propagation, this research shows that detectability is determined by a broad spectrum of environmental parameters. Most of the variation in detectability can be anticipated and predicted with appropriate knowledge of the environment. Advancing the field further will require not only detections but also recorded signal strength and an understanding of the levels of background noise. This data enables direct comparisons between predicted attenuation and measured transmission loss, allowing users to directly calculate the SNR. Ultimately, the more environmental information that researchers can predict or measure, the more accurately they can interpret detection data, but some context [sic] is far more important than others when estimating detection efficiency. Users can leverage these models and techniques to first understand what drives their environment's acoustic properties, then model it to set detectable ranges for their signals and choose transmission power that fits their needs.

# Bibliography


Atkinson, L. (1977). Modes of gulf stream intrustion into the south atlantic bight shelf. *Geophysical Research Letters*, *4*.

Binder, T., Holbrook, C., Hayden, T., & Krueger, C. (2016). Spatial and temporal variation in positioning probability of acoustic telemetry arrays: Fine-scale variability and complex interactions. *An. Biot*.

Blanton, B. O., Aretxabaleta, A., Werner, F. E., & Seim, H. E. (2003). Monthly climatology of the continental shelf waters of the south atlantic bight. *Journal of Geophysical Research: Oceans*, *108*. https://doi.org/10.1029/2002jc001609

Blanton, J., Werner, F., Kim, C., Atkinson, L., Lees, & Savidge, D. (1994). Transport and fate of low-density water in a coastal frontal zone. *Continental Shelf Research*.

Blanton, J., & Atkinson, L. P. (1983). Transport and fate of river discharge on the continental shelf of the southeastern united states. *Journal of Geophysical Research: Oceans*, *88*.

Bohnenstiehl, D. R., Lillis, A., & Eggleston, D. B. (2016). The curious acoustic behavior of estuarine snapping shrimp: Temporal patterns of snapping shrimp sound in sub-tidal oyster reef habitat. *PLoS ONE*, *11*. https://doi.org/10.1371/journal.pone.0143691

Bradley, D., & Stern, R. (2008, July). *Underwater sound and the marine mammal acoustic environment: A guide to fundamental principles* (tech. rep.). U.S. Marine Mammal Commission.

Brownscombe, J. W., Griffin, L. P., Chapman, J. M., Morley, D., Acosta, A., Crossin, G. T., Iverson, S. J., Adams, A. J., Cooke, S. J., & Danylchuk, A. J. (2020). A practical method to account for variation in detection range in acoustic telemetry arrays to accurately quantify the spatial ecology of aquatic animals. *Methods in Ecology and Evolution*, *11*, 82–94. https://doi.org/10.1111/2041-210X.13322

Cagua, E. F., Berumen, M. L., & Tyler, E. H. (2013). Topography and biological noise determine acoustic detectability on coral reefs. *Coral Reefs*, *32*, 1123–1134. https://doi.org/10.1007/s00338-013-1069-2

Cho, S., Zhang, F., & Edwards, C. (2016). Tidal variability of acoustic detection. *Proceedings - 2016 IEEE International Conferences on Big Data and Cloud Computing, BDCloud 2016, Social Computing and Networking, SocialCom 2016 and Sustainable Computing and Communications, SustainCom 2016*, 431–436. https://doi.org/10.1109/BDCloud-SocialCom-SustainCom.2016.70

Chua, G., Chitre, M., & Deane, G. (2018). Impact of persistent bubbles on underwater acoustic communication. *IEEE*.

Cimino, M., Cassen, M., Merrifield, S., & Terrill, E. (2018). Detection efficiency of acoustic biotelemetry sensors on wave gliders. *Animal Biotelemetry*.

Crossin, G., Heupel, M., Holbrook, C., Hussey, N., Lowerre-Barbieri, S., Nguyen, V., Raby, G., & Cooke, S. (2017). Acoustic telemetry and fisheries management. *Ecological Applications*.

Delory, E., Toma, D. M., Rio, J. D., Molina, P. R., Toma, D., Rio, J. D., Ruiz, P., Corradino, L., Brault, P., & Fiquet, F. (2014). Nexos objectives in multi-platform underwater passive acoustics. https://www.researchgate.net/publication/263768753

Edwards, C. R., Cho, S., Zhang, F., & Fangman, S. (2019). Field and numerical studies to assess performance of acoustic telemetry collected by autonomous mobile platforms , 2014. *Ser. Nat. Marine Fisheries*.

Edwards, J. E., A. D. Buijse, H. V. W., & Bijleveld, A. I. (2024). Gone with the wind: Environmental variation influences detection efficiency in a coastal acoustic telemetry array. *An. Biot.*

Ellis, R. D., Flaherty-Walia, K. E., Collins, A. B., Bickford, J. W., Boucek, R., Burnsed, S. L. W., & Lowerre-Barbieri, S. K. (2019). Acoustic telemetry array evolution: From species- and project-specific designs to large-scale, multispecies, cooperative networks. *Fisheries Research*, *209*, 186–195. https://doi.org/10.1016/j.fishres.2018.09.015

Garrison, E., Hale, J., Cameron, C., & Smith, E. (2016). The archeology, sedimentology and paleontology of gray's reef national marine sanctuary and nearby hard bottom reefs along the mid continental shelf of the georgia bight. *Journal of Archaeological Science: Reports*.

Gimbert, F., & Tsai, V. C. (2015). Predicting short-period, wind-wave-generated seismic noise in coastal regions. *Earth and Planetary Science Letters*, *426*, 280–292. https://doi.org/10.1016/j.epsl.2015.06.017

Gjelland, K., & Hedger, R. (2013). Environmental influence on transmitter detection probability in biotelemetry: Developing a general model of acoustic transmission. *Meth. in Eco. and Evo.*, *4*.

Godin, O., Zavorotny, V., Voronovich, A., & Goncharov, V. (2006). Refraction of sound in a horizontally inhomogeneous, time-dependent ocean. *IEEE Journal of Ocean Engineering*.

Goossens, J., Buyse, J., Bruneel, S., Verhelst, P., Goethals, P., Torreele, E., Moens, T., & Reubens, J. (2022). Taking the time for range testing: An approach to account for temporal resolution in acoustic telemetry detection range assessments. *Animal Biotelemetry*, *10*. https://doi.org/10.1186/s40317-022-00290-2

Gul, S., & Zaidi, S. (2017). Underwater acoustic channel modeling using bellhop ray tracing method. *14th International Bhurban Conference on Applied Sciences and Technology (IBCAST)*.

Heupel, M., Semmens, J., & Hobday, A. (2006). Automated acoustic tracking of aquatic animals: Scales, design and deployment of listening station arrays. *Marine and Freshwater Research*.

Hildebrand, J., Frasier, K., Baumann-Pickering, S., & Wiggins, S. (2021). An empirical model for wind-generated ocean noise. *The Journal of the Aoustical Society of America*.

Huang, C., Yeh, C., & Liu, K. (2024). Bubble entrainment and underwater noise caused by a single water drop falling on the surface of freshwater and saltwater. *Phys. of Fluids*.

Huang, J., Barbeau, M., Blouin, S., Hamm, C., & Taillefer, M. (2017). Simulation and modeling of hydro acoustic communication channels with wide band attenuation and ambient noise. *International Journal of Parallel, Emergent and Distributed Systems*.

Huveneers, C., Simpfendorfer, C., Kim, S., Semmens, J., Hobday, A., Pederson, H., Stieglitz, T., Vallee, R., Webber, D., Heupel, M., Peddemors, V., & Harcourt, R. (2016). The influence of environmental parameters on the performance and detection range of acoustic receivers. *Meth. in Eco. and Evo.*

Innovasea. (2021). Receiver noise measurements. www.vemco.com

Ivey, G., Winters, K., & Koseff, J. (2008). Density stratification, turbulence, but how much mixing? *Annual Review of Fluid Mechanics*.

Jackson, D., & Richardson, M. (2007). *High-frequency seafloor acoustics*. Springer.

Jung, S. K., Choi, B. K., Kim, B. C., Kim, B. N., Kim, S. H., Park, Y., & Lee, Y. K. (2012). Seawater temperature and wind speed dependences and diurnal variation of ambient noise at the snapping shrimp colony in shallow water of southern sea of korea. *Japanese Journal of Applied Physics*, *51*. https://doi.org/10.1143/JJAP.51.07GG09

K. Lisa Yang Center, C. B. a. t. C. L. o. O. (2024). Raven pro: Interactive sound analysis software (version 1.6.5). https://www.ravensoundsoftware.com/

Kendall, M. S., Williams, B. L., Ellis, R. D., Flaherty-Walia, K. E., Collins, A. B., & Roberson, K. W. (2021). Measuring and understanding receiver efficiency in your acoustic telemetry array. *Fisheries Research*, *234*. https://doi.org/10.1016/j.fishres.2020.105802

Kessel, S. T., Cooke, S. J., Heupel, M. R., Hussey, N. E., Simpfendorfer, C. A., Vagle, S., & Fisk, A. T. (2014, March). A review of detection range testing in aquatic passive acoustic telemetry studies. https://doi.org/10.1007/s11160-013-9328-4

Kessel, S. T., Hussey, N. E., Webber, D. M., Gruber, S. H., Young, J. M., Smale, M. J., & Fisk, A. T. (2015). Close proximity detection interference with acoustic telemetry: The importance of considering tag power output in low ambient noise environments. *Animal Biotelemetry*, *3*. https://doi.org/10.1186/s40317-015-0023-1

Kuperman, W., & Roux, P. (2007). Underwater acoustics. In *Springer handbooks* (pp. 149–204). Springer. https://doi.org/10.1007/978-0-387-30425-0_5

Lillis, A., & Mooney, T. A. (2018). Snapping shrimp sound production patterns on caribbean coral reefs: Relationships with celestial cycles and environmental variables. *Coral Reefs*, *37*, 597–607. https://doi.org/10.1007/s00338-018-1684-z

Loher, T., Webster, R., & Carlile, D. (2017). A test of the detection range of acoustic transmitters and receivers deployed in deep waters of southeast alaska, usa. *Animal Biotelemetry*.

Mackenzie, K. (1981). Nine-term equation for sound speed in the oceans. *Journal of the Acoustical Society of America*.

Mathies, N. H., Ogburn, M. B., McFall, G., & Fangman, S. (2014). Environmental interference factors affecting detection range in acoustic telemetry studies using fixed receiver arrays. *Marine Ecology Progress Series*, *495*, 27–38. https://doi.org/10.3354/meps10582

Matley, J., Vargas-Araya, L., Fisk, A., & Espinoza, M. (2022). Habitat-specific performance of high-frequency acoustic telemetry tags in a tropical marine environment. *Marine and Freshwater Research*.

McKenna, M. F., Baumann-Pickering, S., Kok, A. C. M., Oestreich, W. K., Adams, J. D., Barkowski, J., Fristrup, K. M., Goldbogen, J. A., Joseph, J., Kim, E. B., Kugler, A., Lammers, M. O., Margolina, T., Reeves, L. E. P., Rowell, T. J., Stanley, J. A., Stimpert, A. K., Zang, E. J., Southall, B. L., … Hatch, L. T. (2021). Advancing the interpretation of shallow water marine soundscapes. *Sec. Ocean Observation*, *8*. https://doi.org/https://doi.org/10.3389/fmars.2021.719258

McQuarrie, F., Woodson, C. B., & Edwards, C. R. (2025). A reef's high-frequency soundscape and the effect on telemetry efforts: A biotic and abiotic balance. *Journal of Marine Science and Engineering*.

McQuarrie, F., Woodson, C. B., & Edwards, C. (2021). Modeling acoustic telemetry detection ranges in a shallow coastal environment. *WUWNet 2021 - 15th ACM International Conference on Underwater Networks and Systems*. https://doi.org/10.1145/3491315.3491331

McQuarrie, F., Woodson, C. B., & Edwards, C. R. (2023). Analyzing tidal, diurnal, synoptic, and seasonal drivers of acoustic telemetry efficiency on a coastal reef. *MTS OCEANS*.

Miller, L., & Wahlberg, M. (2013). Echolocation by the harbor porpoise: Life in coastal waters. *Frontiers in Physiology*.

NOAA. (2012). *Gray's Reef CONDITION REPORT 2012 Addendum Gray's Reef* (tech. rep.). http://graysreef.noaa.gov

O'Brien, M., & Secor, D. (2021). Influence of thermal stratification and storms on acoustic telemnetry detection efficiency: A year-long test in the us southern mid-atlantic bight. *Animal Biotelemetry*.

Oliver, M., Breece, M., Haulsee, D., Cimino, M., Kohut, J., Aragon, D., & Fox, D. (2017). Factors affecting detection efficiency of mobile telemetry. *Animal Biotelemetry*.

ONMS. (2012). Gray's reef condition report 2012 addendum: Gray's reef. *Condition Report 2012*.

ONMS. (2020). *Sanctsound raw passive acoustic data* (tech. rep.). NOAA National Centers for Environmental Information. https://doi.org/https://doi.org/10.25921/saca-sp25

ONR. (Published 1999/Updated 3/2023). Ocean acoustics toolbox [Accessed: Mar 6, 2024].

Payne, N. L., Gillanders, B. M., Webber, D. M., & Semmens, J. M. (2010). Interpreting diel activity patterns from acoustic telemetry: The need for controls. *Marine Ecology Progress Series*.

Pederson, H., Bowen, E., McDonald, J., Smedbol, S., & Jaine, F. (2024). *Field testing the new nextrak r1 acoustic receiver in a high noise environment* (tech. rep.). Innovasea.

Pelaez-Zapata, D., Pakrashi, V., & Dias, F. (2024). Dynamics of bubble plumes produced by breaking waves. *J. of Phys Oc.*

Petkovic, I. (1964). Beaufort wind scale and calculated numerical values of wind speed and wind pressure curves above sea level. https://doi.org/10.3233/ISP-1964-1111701

Pincock, D. G. (2008). Understanding the performance of vemco 69 khz single frequency acoustic telemetry. www.vemco.com

Pittman, S., Monaco, M., Friedlander, A., Legare, B., Nemeth, R., Kendall, M., Poti, M., Clark, R., Wedding, L., & Caldow, C. (2014). Fish with chips: Tracking reef fish movements to evaluate size and connectivity of caribeean marine protected areas. *PLoS ONE*.

Potter, J. R., Delory, E., & Potter, J. (1999). Noise sources in the sea and the impact for those who live there. https://www.researchgate.net/publication/2634521

Prosperetti, A. (1988). Bubble-related ambient noise in the ocean. *Journal of the Acoustical Society of America*, *84*, 1042–1054. https://doi.org/10.1121/1.396740

Radford, C. A., Stanley, J. A., Tindle, C. T., Montgomery, J. C., & Jeffs, A. G. (2010). Localised coastal habitats have distinct underwater sound signatures. *Marine Ecology Progress Series*, *401*, 21–29. https://doi.org/10.3354/meps08451

Radford, C. A., Jeffs, A. G., Tindle, C. T., & Montgomery, J. C. (2008). Temporal patterns in ambient noise of biological origin from a shallow water temperate reef. *Oecologia*, *156*, 921–929. https://doi.org/10.1007/s00442-008-1041-y

Radigan, W., Engel, C., Chvala, P., Longhenry, C., & Pegg, M. (2025). Factors affecting detection probabilities of acoustic transmitters using passive receivers. *Animal Biotelemetry*.

Reubens, J., Verhelst, P., van der Knaap, I., Deneudt, K., Moens, T., & Hernandez, F. (2019). Environmental factors influence the detection probability in acoustic telemetry in a marine environment: Results from a new setup. *Hydrobiologia*.

Revathy, R., & Pillai, P. S. (2022). Effect of wind speed in undersea acoustic communications. *Oceans Conference Record (IEEE)*.

Scherrer, S., Rideout, B., Giorli, G., Nosal, E., & Weng, K. (2018). Depth-and range-dependent variation in the perfomance of aquatic telemetry systems: Understanding and predicting the susceptibility of acoustic tag-receiver pairs to close proximity detection interference. *PeerJ*.

Simpson, J., Brown, J., Matthews, J., & Allen, G. (1990). Tidal straining, density currents, and stirring in the control of estuarine stratification. *Estuaries*.

Song, Z., Ou, W., Su, Y., Li, H., Fan, W., Sun, S., Wang, T., Xu, X., & Zhang, Y. (2023). Sounds of snapping shrimp (alpheidae) as important input to the soundscape in the southeast china coastal sea. *Frontiers in Marine Science*, *10*. https://doi.org/10.3389/fmars.2023.1029003

Spiga, I. (2022). The acoustic response of snapping shrimp to synthetic impulsive acoustic stimuli between 50 and 600 hz. *Marine Pollution Bulletin*, *185*. https://doi.org/10.1016/j.marpolbul.2022.114238

Stanley, J., Parijs, S. V., Davis, G., Sullivan, M., & Hatch, L. (2021). Monitoring spatial and temporal soundscape features within ecologically significant u.s. national marine sanctuaries. *Ecological Applications*.

Stein, M. (1987). Large sample properties of simulations using latin hypercube sampling. *Technometrics*.

Stocks, J. R., Gray, C. A., & Taylor, M. D. (2014). Testing the effects of near-shore environmental variables on acoustic detections: Implications on telemetry array design and data interpretation. *Marine Technology Society Journal*, *48*, 28–35.

Stojanovic, M., & Preisig, J. (2009). Underwater acoustic communication channels: Propagation models and statistical characterization. *IEEE Comm. Mag.*

Swadling, D. S., Knott, N. A., Rees, M. J., Pederson, H., Adams, K. R., Taylor, M. D., & Davis, A. R. (2020). Seagrass canopies and the performance of acoustic telemetry: Implications for the interpretation of fish movements. *Animal Biotelemetry*, *8*, 1–13. https://doi.org/10.1186/s40317-020-00197-w

UWAPL. (1994). *High-frequency ocean environmental acoustic models handbook* (tech. rep.). University of Washington, APL.

Weber, A. H., & Blanton, J. O. (1980). Monthly mean wind fields for the south atlantic bight. *Journal of Physical Oceanography*, *10*.

Williams, B. L., Roberson, K., Young, J., & Kendall, M. S. (2019). Using acoustic telemetry to understand connectivity of gray ' s reef national marine sanctuary to the u . s . atlantic coastal ocean. *NOAA Technical Memorandum NOS NCCOS 259*, 82. https://doi.org/10.25923/r2ma-5m96

Wood, S. (2024). *Mgcv: Mixed gam computation vehicle with automatic smoothness estimation*. R Core Team.

Xiao, F., Hu, Y., Xu, X., Huang, L., Tao, Y., & Chen, Y. (2021). Transmission characteristics of high-frequency underwater acoustic channels with high-frequency marine noise in shallow sea. *IEEE/CIC Int. Conf. on communications in China*.

Zuur, A., Ieno, E., Walker, N., Saveliev, A., & Smith, G. (2009). *Mixed effects models and extensions in ecology with r*. Springer.